2015-07-21

IGF-I Producing Neural Crest Stem Cells: a Long-term DPN Treatment

Veronica R. Fortino
University of Miami, Ronnie238@aol.com

UNIVERSITY OF MIAMI

IGF-I PRODUCING NEURAL CREST STEM CELLS: A LONG-TERM DPN TREATMENT

By

Veronica Raquel Fortino

A DISSERTATION

Submitted to the Faculty
of the University of Miami
in partial fulfillment of the requirements for
the degree of Doctor of Philosophy

Coral Gables, Florida

August 2015

UNIVERSITY OF MIAMI

A dissertation submitted in partial fulfillment of
the requirements for the degree of
Doctor of Philosophy

IGF-I PRODUCING NEURAL CREST STEM CELLS: A LONG-TERM DPN TREATMENT

Veronica Raquel Fortino

Approved:

_____
Herman S. Cheung, Ph.D.
James L. Knight Professor of
Biomedical Engineering

_____
Cherie Stabler, Ph.D.
Associate Professor of
Biomedical Engineering
University of Florida

_____
Edward A. Dauer, M.D.
Research Associate Professor
of Biomedical Engineering

_____
Dean of the Graduate School

_____
Jacqueline Sagen, Ph.D.
Professor, Miami Project to Cure Paralysis

FORTINO, VERONICA RAQUEL (Ph.D., Biomedical Engineering)
IGF-I Producing Neural Crest Stem Cells: (August 2015)
A Long-term DPN Treatment

Abstract of a dissertation at the University of Miami.

Dissertation supervised by Professor Herman S. Cheung.
No. of pages in text. (151)

DPN is the most frequently observed serious and chronic complication of diabetes. Although commonly believed that hyperglycemia is the major cause of DPN, a decrease in the level of neurotrophic factors, such as IGF-I, contributes to the pathogenesis of DPN. Systemic IGF-I injections in animal models of diabetes have proven successful to ameliorate and prevent further DPN degeneration. Our laboratory recently isolated a unique pluripotent stem cell from the neural crest (NCSC). The aim of this Doctoral work was to characterize our NCSC for expression, production, secretion of IGF-I, and transplant them into an animal model of diabetes with associated DPN. Additionally, NCSC were pre-committed to a neural lineage and also characterized for IGF-I, in the event that the undifferentiated NCSC would differentiate in-vivo. Male Sprague Dawley rats were induced with diabetes using STZ. Following four weeks of diabetes induction, the animals underwent weekly behavioral tests (Von Frey, Acetone, Paw Pressure) to establish baseline results prior to transplantation. After eight weeks of STZ induction, NCSC and NCSC-derived neural progenitor cells were transplanted into the thigh muscle of male Sprague Dawley rats. Behavioral tests were continued for four weeks following transplantation. Our results indicated that our NCSC secreted quantifiable levels of IGF-I, thus making them a suitable mini-pump of IGF-I for a cellular therapy approach to DPN. Our behavioral study results suggest that our NCSC and NCSC-derived neural progenitor cells provide some

neuroprotection against further degeneration for both mechanical hyperalgesia and cold allodynia. These pilot results are encouraging to continue further work with NCSC as a cellular therapy for DPN.

This Doctoral Work and Dissertation are dedicated to my parents, whom have given me love and support throughout my entire life, and also to my Lord and Savior, Jesus Christ. It is through, with, and because of Him that I was able to reach this amazing goal.

All the honor and glory goes to Him.

Acknowledgments

There are several people that I thank for their help in making my Doctoral Work a success. First, my mentor and advisor, Dr. Herman Cheung, who taught me to not be afraid to fail, and helped me become the scientist I am today. His mentoring, teaching, and coaching have provided me with invaluable lessons that I will take with me wherever I go. A big thank you to the post-docs that taught me how to "do" science, and how to troubleshoot the science that didn't work – Dr. Daniel Pelaez, Dr. Stanislava Jergova, and Dr. Tsz Kin Ng (Michael). Thank you to all of the students that helped me collect and analyze data, not only for this Work, but also for all of the other publications I had as a Ph.D student: John Michel, Juan Andres Kochen, Matthew Penna, Deborah Hopman, Devon Pawley, Nastasja Ecker, and Yucan Zhao. An additional thank you to John, Juan, Matt, and Alexandra Lanjewar because of all of their help in editing and perfecting this Dissertation. THANK YOU!

TABLE OF CONTENTS

LIST OF FIGURES

LIST OF TABLES

SECTION I – BACKGROUND

Chapter 1 – Significance

Neuropathic pain is a chronic condition that is heterogeneous in nature and has different causes (Baron, 2006). Different from and more burdensome than nociceptive pain, neuropathic pain more severely affects quality of life (Urgellés-Lorié, 2008). Understanding the various mechanisms of the onset and progression of neuropathic pain is important in the development of an effective treatment. One of the main causes of neuropathic pain in people with diabetes is diabetic peripheral neuropathy (DPN). It is commonly known as the most frequently observed serious and chronic diabetic complication (Apfel, 1999). With a prevalence of 30-50% among patients with diabetes, over 70% of those with DPN describe it as severely painful, significantly impacting their quality of life (Geerts et al., 2008).

Although hyperglycemia is commonly attributed as the major contributor of the development of DPN, abnormalities in growth factors, such as insulin-like growth factor I (IGF-I), can also play a role in the development of nerve dysfunction and organic and structural nerve damage (Vinik et al., 1999). This is due to the fact that neurotrophic factors promote neuron development, survival, and regeneration. They also maintain functional integrity, regulate neuronal plasticity, and aid in the repairing of damaged nerves (Ossipov, 2011). Their neuroprotective and restorative functions, in combination with their abnormalities in DPN, lead to the belief that neurotrophic factors are important in the

pathogenesis and treatment of DPN. To support this claim, the loss of insulin activity produces a secondary partial decrease in IGF-I activity (Gualco et al., 2009), believed to contribute to DPN (Ishii, 1995; Thrailkill, 2000). Studies have shown that gene expression levels of both IGF-I and IGF-II are reduced in diabetic nerves with associated neuropathy (Guo et al., 1999), and that systemic IGF-I injections in animal models of diabetes with associated DPN minimize the effects of DPN (Ishii & Lupien 1995; Zhuang et al., 1996; Zhuang et al., 1997; Chu et al., 2008) as well as provide neuroprotection against apoptosis and further degeneration (Russell & Feldman, 1999). Although positive results have been seen with systemic IGF-I injections in animal models, current treatments for DPN are mainly pharmacological and have a primary indication for other, unrelated conditions such as depression and epilepsy. While some studies using pharmacological treatments have proven successful (Jensen et al., 2009), pharmacological treatments are described as "disappointing," and have been found to provide no improvement for over 35% of patients with DPN (Geerts et al., 2008).

The contribution of the proposed research is to characterize and evaluate a potential stem cell based treatment option for people with diabetes and associated DPN. As was stated above, neurotrophic factors protect and regenerate nerves. Presently, neurotrophic factors are secreted by various populations of stem cells discovered in the human body (Koh et al., 2008; Cova et al., 2010; Nesti et al., 2011; Reid et al., 2011), leading to the hypothesis that stem cells that secrete neurotrophic factors, such as IGF-I, will provide a protective and restorative microenvironment for the nerves damaged due to DPN. The

contribution of this project will be significant because it is the initial step in a continuum of research towards a long-term stem-cell based treatment designed specifically to address DPN. Once a long-term treatment designed for DPN is available, there will be a significant improvement in the quality of life of diabetics with associated DPN. Additionally to this, other researchers will have the ability to translate the information and knowledge gained to other neuropathic diseases; potentially assisting in the development of effective treatments for these painful conditions.

Chapter 2 – Neuropathic Pain[1]

Deciphering the Code-Defining Neuropathic Pain

In 2008, the International Association for the Study of Pain (IASP) formed a special interest group to redefine neuropathic pain as "pain arising as a direct consequence of a lesion or disease affecting the somatosensory system" (Treede et al., 2008). Neuropathy is heterogeneous in nature; however, neuropathic lesions may be characterized into four broad categories: focal or multifocal lesions of the peripheral nervous system; generalized lesions of the peripheral nervous system (polyneuropathies); lesions of the central nervous system (CNS); and complex neuropathic disorders (Table 1). (Baron, 2006)

Four Broad Categories of Neuropathic Lesions and Examples
Focal or multifocal lesions of the peripheral nervous system
Entrapment syndromes, Phantom limb pain, Stump pain, Post-traumatic neuralgia, Postherpetic neuralgia, *Diabetic mononeuropathy*, Ischemic neuropathy, Polyarteritis nodosa
Lesions of the CNS
Spinal cord injury, Brain infarction (especially the thalamus and brainstem), Spinal infarction, Syringomyelia, Multiple sclerosis
Generalized lesions of the peripheral nervous system (polyneuropathies)

[1]This chapter is a partial excerpt from *Fortino et al., Concise review: stem cell therapies for neuropathic pain. Stem Cells Transl Med. 2013 May;2(5):394-9.*

Diabetes mellitus, Alcohol, Amyloid, Plasmocytoma, HIV neuropathy, Hypothyroidism, Hereditary sensory neuropathies, Fabry's disease, Bannwarth's syndrome (neuroborreliosis), Vitamin B deficiency, Toxic neuropathies (arsenic, thallium, chloramphenicol, metronidazole, nitrofurantoin, isoniazid, vinca alkaloids, taxoids, gold)
Complex neuropathic disorders
Complex regional pain syndromes type I and II (reflex sympathetic dystrophy, causalgia)

Table 1: Categories of Neuropathic Lesions and Examples (reprinted with permission: Baron R. Mechanisms of disease: neuropathic pain--a clinical perspective. NAT CLIN PRACT NEUROL 2006;2:95-106.)

Although categorized as chronic pain, neuropathic pain is regarded as more severe than other types of chronic pain. This is due to the increased disruption of both physical and mental quality of life when compared to other chronic pain syndromes. People with chronic neuropathic pain report a higher severity of pain and significantly worse scores for all interference items of the Brief Pain Inventory (BPI) than non-neuropathic chronic pain patients. Also, those with chronic neuropathic pain report mean scores for the Neuropathic Pain Scale significantly higher than those with non-neuropathic chronic pain, even after adjusting for pain severity, age, and sex. (Smith et al., 2007)

Types of Pain

Neuropathic pain presents itself in many different forms. Spontaneous sensations include paroxysmal pain (shooting pain that lasts several seconds) and superficial pain (an ongoing, burning sensation). Evoked pain include mechanical allodynia (pain caused by

normally non-painful pressure), heat or cold allodynia (pain caused by normally non-painful hot/cold stimuli), hyperalgesia (increased sensitivity to a normally painful stimulus), and temporal summation (increasing pain sensation from repetitive application of identical stimuli). (Baron et al., 2010)

Neuropathic pain differs from nociceptive pain in that nociceptive pain is caused by tissue damage while neuropathic pain is produced by nerve damage. In particular, pain signaling areas of the peripheral or central nervous system are injured, causing neuropathic pain. In nociceptive pain, tissue damage causes the generation of prostaglandins that cause: vasodilation, increased blood flow, inflammatory exudates and the sensitization of nociceptive nerve endings. In neuropathic pain signals are generated by the injured nerve, sent to the brain, and interpreted as pain. Nociceptive pain is proportional to the intensity of the stimulus; neuropathic pain is not – a small stimulus may provoke increased sensations of pain. (Urgellés-Lorié, 2008)

Chapter 3 – Diabetic Peripheral Neuropathy (DPN)

Diabetes Targeting the Peripheral Nervous System

The peripheral nervous system is uniquely targeted by diabetes. The degeneration of the peripheral nerves begins at the distal terminals with sensory neurons being targeted early in the degenerative process and motor neurons being targeted later. Although controversies with the timeline of neuronal loss in diabetes exist, in most diabetic models there is one structural change that is evident: the loss of distal sensory epidermal axons. This manifestation is caused by a sub-lethal impairment of neuron function; it causes the retraction of the axon terminal within the epidermis. The loss of distal neuron branches is accompanied by a decreased capacity for regeneration. (Zochodne et al., 2008)

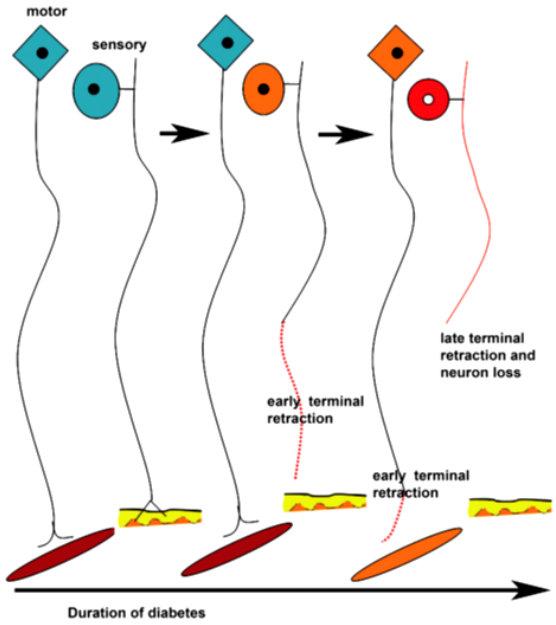

Figure 1: Diabetes targeting the Peripheral Nerves (Zochodne et al., 2008)

Distal axon targeting in diabetes may arise for several reasons. First, axonal transport of critical structural and plasticity related proteins may fall below the threshold required to maintain the viability of distal branches. This promotes a slowing down of distal conduction and an increase in the amount of axonal atrophy. Second, diabetes may trigger Wallerian degeneration, this process being more evident in the longer axons and more prominent in their distal terminals. Last, distal branches might be targeted by diabetes due to the impairment of local axonal synthesis of critical proteins. (Zochodne et al., 2008)

Associated neuropathy of the peripheral system in people with diabetes may cause debilitating and life altering pain. Painful neuropathy may be the result of DPN, and presents itself in various forms. When motor nerves are damaged, muscle weakness is the most common result. Painful cramps and fasciculations (uncontrolled muscle twitching visible under the skin) and muscle loss are other symptoms that may result from motor nerve damage. Sensory nerve damage causes a more complex range of symptoms because of their wider and highly specialized range of functions. Neuropathy of the peripheral nervous system is different than painful DPN, depending on the sensory nerves that are damaged. In fact, damage to large sensory fibers lessens the ability to feel vibrations and touch, resulting in a general sense of numbness, especially in the hands and feet. This makes it difficult to perform basic tasks such as walking and getting dressed. It may also result in the loss of reflexes and proprioception. Damage to small sensory fibers interferes with the ability to feel pain or changes in temperature. Loss of pain sensation is a serious complication as it leads to the high rate of lower limb amputations among diabetics. This

is different than when the pain receptors in the skin become damaged, which can lead to over sensitization, causing tactile allodynia (withdrawal from normally innocuous mechanical stimuli) and hyperalgesia (increased response to a painful stimuli). (NINDS, 2012)

Diabetic Peripheral Neuropathy (DPN)

Presently, the pathogenesis of DPN is not well understood. The current view of the pathogenesis of diabetic peripheral neuropathy is that it is a heterogeneous disorder. Initially, the nerve abnormalities are functional, leading to structural and degenerative changes that impair the nerve response. This is due, in part, to the decrease of important neurotrophic factors. Although it is commonly believed that hyperglycemia is the major cause of DPN, abnormalities in growth factors are also seen to play a role in the development of nerve dysfunction and organic and structural nerve damage (Vinik et al., 1999). Recently, evidence has suggested that insulin and C-peptide deficiencies are primarily responsible for the deleterious changes of neurotrophic factors in the diabetic nerve. This may be true for not only peripheral neuropathy, but also other apoptotic phenomena found in the central nervous system of diabetics. This data has led to the re-evaluation of the pathogenesis of DPN over the past years (Sima, 2003).

Chapter 4 – Insulin–like Growth Factor I (IGF-I) Abnormalities in DPN

The loss of insulin activity in people with diabetes leads to a secondary partial decrease in IGF-I activity (Gualco et al., 2009). The loss of neurotrophic IGF activity also significantly contributes to DPN (Ishii, 1995). IGF has been found to provide neuroprotection in the mature brain against different pro-apoptotic insults, and is produced locally by a large number of tissues, including the brain. The IGF-IR signaling system has garnered attention due to its multiple pro-survival and growth promoting properties, which has led to its extensive study in peripheral and central nervous system disorders. For example, IGF-IR is expressed in granular and Purkinje neurons in the cerebellar cortex and protects these neurons from apoptosis due to low potassium levels. As neuronal apoptosis is known to accompany degenerative disorders of the CNS, the IGF-I signaling system is increasingly viewed as playing an important role in neuroprotection. (Gualco et al., 2009).

There are several findings of IGF's neuroprotective properties. IGF has been shown to provide protection from: high glucose, oxidative stress, TNFα-mediated degeneration, and apoptosis induced by glutamate, nitric oxide, and N-methyl-D-aspartate. (Gualco et al., 2009). Observed in the spinal cord and brainstem of IGF-IR-/- transgenic mice (which have a marked decrease in the amount of IGF-I produced), decreased proliferation and maturation of oligodendrocytes resulted in reduced brain size and myelination, as well as altered brain structures (Liu et al., 1993). As it is known that neuropathy is disease, inflammation or damage to the nerves, it can be seen that the reduction of IGF-I is critical

to the development of neuropathy. This predicts that (i) - hyperglycemia should not be considered the main culprit of DPN, (ii) - IGF activity is reduced in diabetic neural tissue and (iii) - IGF can prevent diabetic neuropathy (Ishii, 1995).

Expressions of both the IGF-I and IGF-II genes are reduced in diabetic nerves (Guo et al., 1999). Additionally, the therapeutic potential of IGF-I has been documented in animal models and patients with diabetes mellitus. In a study by Zhuang, it was demonstrated that non-insulin dependent diabetes mellitus rats developed hyperalgesia, and the hyperalgesia was overcome by systemic IGF-II administration. Treatment with either IGF-I or IGF-II was found to arrest the progression of hyperalgesia in insulin dependent diabetes mellitus rats. Non-insulin dependent diabetes mellitus rats that demonstrated abnormal paw/pressure thresholds treated with either IGF-I or IGF-II were found to restore thresholds towards normal levels. It was also found that low doses of IGF, independently of hyperglycemia, protected against neuropathy in non-insulin dependent and insulin dependent diabetes mellitus rats (Zhuang et al., 1997).

Craner examined the expression of IGF-I and its receptor IGF-IR in dorsal root ganglia (DRG) neurons in streptozotocin-induced (STZ) painful diabetic neuropathy (Craner et al., 2002). Their findings demonstrated that IGF-I expression was significantly down-regulated in STZ rats. This reduction was found in the DRG neurons as well as in axotomized sensory DRG neurons. They concluded that the loss of IGF-I in DRG neurons

(which are mainly nociceptive) may contribute to the neuropathic pain that was observed in the models they tested.

In a study performed by Bach et al, they utilized recombinant human IGF-I (rhIGF-I) to test the hypothesis that low plasma levels of circulating IGF-I play a significant role in several aspects of the pathophysiology of diabetes mellitus, including insulin resistance and poor glycemic control. The studies examined the impact of subcutaneous rhIGF-I injections on sensitivity and metabolic parameters. In patients with type 1 and 2 diabetes mellitus, they found that insulin sensitivity was significantly improved, insulin requirements were reduced, and glycemic control of dyslipidemia generally improved (Bach et al., 1994).

Chapter 5 – Current Treatments for Neuropathic Pain

As has already been mentioned in this text, DPN is a disease that is heterogeneous in nature and has various different causes. The types of pain present in people suffering from DPN is also heterogeneous. This is one of the main reasons why treating the resulting neuropathic pain that accompanies DPN is difficult. Presently, most of the treatments for DPN are palliative, not treating the underlying neuro-degeneration resulting from diabetes. Additionally, these treatments typically have a primary indication for another, unrelated condition.

Pharmacological Agents

Most treatments for DPN have arisen from other, unrelated conditions and transferred to DPN. For example, while amitriptyline and duloxetine are commonly used for DPN, these drugs have a primary indication for depression – amitriptyline is a tricyclic anti-depressant and duloxetine (commonly known as Cymbalta) is a selective serotonin and norepinephrine reuptake inhibitor (SSNRI).

Additionally, these drugs have had conflicting reports on the effectiveness at which they can treat the neuropathic pain resulting from DPN (Boyle et al., 2012). In a randomized clinical trial, pregabalin, amitriptyline, and duloxetine were evaluated in patients with DPN for their analgesic properties, effect on polysomnographic sleep and daytime functioning, and the improvement of quality of life. When compared to placebo, all of the treatments had a significant effect, but the effect between the treatments was not

different, meaning that none was significantly higher than another. In the secondary parameters they examined, pregabalin improved sleep continuity and duloxetine negatively impacted sleep by increasing wake and reducing total sleep time. Duloxetine did, however, enhance central nervous system arousal and performance on sensory motor tasks. These reports make prescribing these drugs difficult, as the dosing required may vary greatly from patient to patient and the side effects / effects on secondary outcomes varies greatly.

Recently, pregabalin, commonly known as Lyrica (which was initially prescribed for fibromyalgia), has been prescribed for the treatment of DPN. Interestingly, in a randomized controlled clinical trial by Rauck et al (Rauck et al., 2012) in which pregabalin was used as the positive control, there was no difference observed between the pregabalin and the placebo group when it came to measuring effects on the 11-point Pain Intensity Numerical Rating Scale. Also, in the study described above (Boyle et al., 2012), a significantly higher number of adverse effects were noted in the pregabalin treatment group than in the duloxetine and amitriptyline groups. These conflicting and sometimes confusing results with pharmacological agents underscore the need for a DPN-specific treatment, one that is designed to address the neuro-degeneration commonly seen as the result of diabetes.

Topical Analgesics

Topical analgesics are mostly recommended for localized and not broad neuropathic pain – this may be pain arising from DPN and/or other neuropathic conditions. Patients with localized neuropathic pain are defined as those that are able to point to a

specific location where they have pain and that pain remains constant over time. A common topical analgesic for localized neuropathic pain is capsaicin. While a 0.025% capsaicin gel did not show improvements in comparison to placebo (Kulkantrakorn et al., 2012), capsaicin 8% patches have demonstrated improvement in pain for 34% of those studied. Something interesting to note, however, is that of those tested in this study, 31% demonstrated no improvement and 32% improved and then returned to baseline pain levels (Martini et al., 2012). Another commonly used topical agent is lidocaine – in a randomized clinical trial (Ho et al., 2008), 5% lidocaine in a pluronic-lecithin organogel demonstrated a reduction in pain intensity when compared to amitriptyline ($P < 0.05$) in 34 patients who were experiencing either DPN pain or postherpetic neuralgic pain.

Topical clonidine gel has also been used to treat painful diabetic neuropathy. The analgesic effect it produces are believed to arise from its action as an α-2 adrenergic agonist – thereby reducing the abnormal signaling from hyperactive cutaneous nociceptors. In a randomized, double-blind, placebo controlled 12 week clinical study, 0.1% topical clonidine gel was used to treat patients with painful diabetic neuropathy in the feet. Statistically significant difference was observed in comparison to placebo, demonstrating a decrease in the amount of foot pain. (Campbell et al., 2012)

Several studies have demonstrated that topical analgesics demonstrate no efficacy when compared to placebo – in a study by Lynch et al they showed that 2% amitriptyline, 1% ketamine, or 2% amitriptyline-1% ketamine combined and applied topically showed

no difference versus the placebo cream. It was later on stated that this was probably due to the dosage not being sufficient to achieve the desired analgesic response (Lynch et al., 2005). In another study, however, it was shown that a 5% ketamine cream (higher dose than the previous study) also showed no effect when compared to a placebo cream (Mahoney et al., 2012). Additionally, another study demonstrated that 5% amitriptyline (again, higher than Lynch's study) had no effect when compared to placebo (Ho et al., 2008).

The non-specificity of present DPN treatments, along with their varying degrees of efficacy, and many times unknown method of action poses a unique situation in the treatment of neuropathic pain that results from painful DPN. The additional problem of not treating the underlying nerve degeneration demonstrates the need for a DPN-specific treatment. Additionally, the pain arising from DPN is typically widespread and not limited to a small spot. A treatment that is DPN-specific and addresses the broad range of causes may be the most effective in not only treating the resulting painful effects of DPN but also the underlying cause of the pain, which is the degeneration of the peripheral nerves and typically the loss of contact of the distal branches of the peripheral nerves to the epidermal layer.

Chapter 6 – Specific Aims and Hypothesis

This project evaluated the effects of transplantation of pluripotent neural crest stem cells isolated in Dr. Cheung's laboratory, termed herein NCSC on evoked pain related behaviors in an animal model of diabetes with associated diabetic peripheral neuropathy (DPN), with the end goal of reducing or arresting the painful effects of this debilitating disease. It is well known that DPN is a chronic pain syndrome that negatively impacts quality of life and is the most frequent symptomatic complication of diabetes (Apfel, 1999). It has been proposed that the loss of insulin-like growth factor I (IGF-I) activity due to diabetes significantly contributes to neuropathy (Ishii, 1995). In support of this hypothesis, studies have shown that gene expression levels of both IGF-I and IGF-II are reduced in diabetic nerves (Zhuang et al, 1997; Guo et al., 1999). Presently, there are no effective long term treatments for this condition; therefore, efforts are needed to develop and test novel therapeutic interventions.

The long-term goal of the proposed and future research is to develop therapeutic stem cell based treatments for people experiencing DPN and other debilitating neuropathies. The overall objective of this Doctoral work, which is the initial step towards attaining the stated long-term goal, was to characterize the NCSC population and evaluate the safety of transplantation and efficacy of treatment in an animal model of diabetes with associated DPN. The central hypothesis was that transplantation of IGF-I producing NCSCs into an animal model of diabetes would minimize the painful effects of DPN. This

hypothesis was formulated on the basis that IGF-I injection in animal models of diabetes with associated DPN produce therapeutic effects (Chu et al, 2008), in addition to preliminary data stating that NCSCs express, produce, and secrete IGF-I. The rationale for the research was that a long term treatment for DPN and other neuropathic diseases may be achieved through the implantation of neurotrophic-releasing stem cells, creating a neuro-trophically rich micro-environment that will arrest or reduce the effects of this debilitating condition.

The central hypothesis was tested and, the objective of this Doctoral was attained work by pursuing the following specific aims:

Specific Aim #1

Characterize IGF-I secretion levels of NCSCs to determine dosing requirements for animal studies. Based on the preliminary data that the aforementioned unique stem cell population (neurogenic and non-neurogenic committed) expresses IGF-I, secretion levels of NCSC were compared to therapeutic levels of IGF-I and the number of cells that had to be transplanted into an animal model of diabetes with associated DPN to produce the same effect were determined.

Specific Aim #2

Evaluate the effects of transplanting neurogenic and non-neurogenic committed NCSCs into an animal model of diabetes with associated DPN. The neuroprotective effects of

NCSCs were evaluated by comparing the pain-evoked behavior of diabetic animals with associated DPN transplanted with neurogenic and non-neurogenic committed NCSCs.

The work proposed in aim 1 identified the minimum number of cells necessary for transplantation into an animal model of diabetes with associated DPN. The work proposed in aim 2 identified a potential stem cell based treatment for DPN. These outcomes have an important and positive impact because the findings and knowledge acquired provides a stepping stone for other researchers to tackle DPN using stem cells, in addition to producing data that will serve as the basis for clinical trials for DPN.

Chapter 7 – Stem Cell Therapies for Neuropathic Pain[2]

Stem Cells – Why the Hype?

Uninjured nerve fibers that intermingle with degenerating nerve fibers participate in pain signaling. Spontaneous activity in the uninjured nerve fiber produces sensitization in the area of the central nervous system responsible for development of pain. Additionally, products associated with Wallerian degeneration released near uninjured nerves might trigger changes in channel and receptor expression in the uninjured nerve, contributing to neuropathic pain. (Wu et al., 2001) It is important, therefore, that the environment surrounding uninjured nerve fibers protect them from degenerating and exacerbating neuropathic pain.

Critical in providing a protective micro-environment, neurotrophic factors are growth factors known to promote neuron development and survival. They also maintain functional integrity, promote regeneration, regulate neuronal plasticity, and aid in the repairing of damaged nerves. (Ossipov, 2011) Neurotrophic factors include various types of protective factors. The neurotrophins are: nerve growth factor (NGF), BDNF, neurotrophin 3 (NT-3), and neurotrophin 4/5 (NT-4/5). Other well characterized

[2] This chapter is a partial excerpt from *Fortino et al., Concise review: stem cell therapies for neuropathic pain. Stem Cells Transl Med. 2013 May;2(5):394-9.*

neurotrophic factors include: insulin-like growth factor I and II (IGF-I and IGF-II), glial cell line derived neurotrophic factor (GDNF), neurturin, and persephin. Ciliary neurotrophic factor (CNTF), has also been studied and shown to act upon neural crest derived sensory nerves as well as parasympathetic and motor nerves. (Apfel, 1999) The various neurotrophic factors affect different cell populations within the peripheral and central nervous system (Table 2).

Neurotrophic Factors		Peripheral Nerve Population
Neurotrophins		
	NGF	Neural crest derived – small fiber sensory Sympathetic
	BDNF, NT-4/5	Neural crest derived –medium fiber sensory Placode derived – sensory Motor
	NT-3	Neural crest derived – large fiber sensory Placode derived – sensory Sympathetic Motor
Other factors		
	IGF-I	Neural crest derived – sensory Sympathetic Motor
	IGF-II	Neural crest derived – sensory Sympathetic Motor
	GDNF	Motor Neural crest derived – sensory Nodose – sensory Sympathetic Parasympathetic
	Neurturin	Motor Neural crest derived – sensory Nodose – sensory Sympathetic
	Persephin	Motor

Table 2: Neurotrophic Factors and the Peripheral Nerve Populations They Affect (reprinted with permission – From: Apfel S. Neurotrophic factors in peripheral neuropathies: therapeutic implications. BRAIN PATHOLOGY 1999;9:393-413)

Presently, neurotrophic factors are secreted by the various populations of stem cells discovered in the human body. Human mesenchymal stem/stromal cells (hMSCs) produce a large variety of trophic factors; eighty-four trophic factors have been found in hMSC conditioned media and/or cell lysates versus basal media. Neurotrophic factors found in both conditioned media and cell lysates were: epidermal growth factor (EGF), BDNF, NT-3, CNTF, basic fibroblast growth factor (bFGF/FGF-2), hepatocyte growth factor (HGF), and vascular endothelial growth factor (VEGF). (Cova et al., 2010) Human umbilical cord derived MSCs (hUC-MSC) have also been found to secrete neurotrophic factors: VEGF, GDNF, and BDNF. Secretion of neurotrophic factors was demonstrated before, during, and after neuronal differentiation. The results of this study indicated higher production of neurotrophic factors in hUC-MSC versus bone-marrow derived stem cells; however, both cell types had measurable amounts of secreted neurotrophic factors. This study was done in-vitro, however, and in-vivo tests did not confirm the secretion of neurotrophic factors and the anti-apoptotic effects seen in-vitro. (Koh et al., 2008) Dental pulp stem cells express various neurotrophic factors, including BDNF, NGF, and GDNF (Nesti et al., 2011). Similarly, adipose derived stem cells differentiated to glial-like cells also express a range of neurotrophic factors; namely: NGF, BDNF, GDNF, and NT-4 (Reid et al., 2011). The secretion of neurotrophic factors by different populations of stem cells suggests that no matter the source of the stem cell, there is a possible use for it in treating neuropathic pain.

The secretion of neurotrophic factors by stem cells provides neuroprotection and neuroregenerative effects. When transplanted into an animal model of Parkinson's disease, hMSCs support sustained endogenous proliferation and maturation of cells in the subventricular zone of rats. Additionally, hMSCs exert a neuroprotective effect; decreasing the loss of dopaminergic neurons and increasing the levels of dopamine in animal models of Parkinson's disease. (Cova et al., 2010; Park et al., 2008) These effects were possibly accomplished through decreased caspase-3 activity. Adhesion removal tests also indicate a tendency towards lower removal times in hMSC treated mice versus mice injected with proteasome inhibitors and no hMSC transplantation. (Park et al., 2008) It is interesting to note that transplanted hMSCs did not differentiate into a neural phenotype, indicating that the mechanism of action was mediated through paracrine signaling rather than through the differentiation of the stem cells (Cova et al., 2010).When injected into the same location as a forced quinolinic acid (QA) induced cerebellar lesion site, the negative impacts of QA on rotarod learning and beam walking speed were ameliorated. Also, hMSC transplantation protected against Purkinje cell loss. (Edalatmanesh et al., 2011) Similarly, in a rat model of ischemic stroke, human umbilical cord derived MSCs (hUC-MSC) transplantation provided a significant increase in neuro-behavioral function (neuro-behavioral tests included consciousness, gait, limb tone, and pain reflex), and a significant decrease in the final infarct volume relative to the control group. (Koh et al., 2008) These studies demonstrate that MSCs not only protect against nerve damage but also help regenerate damaged nerves and restore them to their pre-injured state.

Neuroprotective effects have also been noticed with different populations of stem cells. One such population is dental pulp stem cells. When mesencephalic neurons in culture were exposed to 1-methyl-4-phenylpyridinium (MPP+) or rotenone (two neurotoxins commonly used to induce Parkinson's in animal models), a statistically significant neuroprotective effect was seen in co-cultures of the neurons with dental pulp stem cells. In particular, mesencephalic neurons challenged with MPP+ demonstrated a reduction of [3H] dopamine uptake, demonstrating a loss in dopaminergic cells. When co-cultured with dental pulp stem cells however, the decrease of [3H] dopamine uptake was significantly less. Mesencephalic neurons challenged with rotenone demonstrated similar results; those co-cultured with dental pulp stem cells demonstrated an increase in [3H] dopamine uptake, further demonstrating the neuroprotective effect of the dental pulp stem cells. (Nesti et al., 2011) Another stem cell population is derived from adipose tissue. When transplanted into an animal model of nerve injury, differentiated adipose derived stem cells were shown to decrease the expression of the pro-apoptotic genes caspase-3 and Bax, as well as significantly increase the ratio of Bcl-2:Bax (a ratio that is seemingly vital to the survival of neurons) in the dorsal root ganglia. (Reid et al., 2011) This seems to demonstrate therefore, that stem cells, regardless of source, possess the potential to be used in regenerative and therapeutic applications for neuropathy and the resulting neuropathic pain.

Do stem cells need to be in direct contact with the lesioned nerve to provide neuroprotection? Several studies have demonstrated that direct contact is not necessary to

provide neuroprotection. When bone marrow stem cells (BMSCs) were co-cultured with "ischemic" injured tissue (where BMSCs were not in direct contact with the ischemic tissue), the neuroprotective effects provided by the BMSC were found to be equal to the effects of direct transplantation onto injured tissue. Amount of cell death in the cornu ammonis (CA) of the brain significantly decreased. When assessed for the occurrence of apoptotic cells, both cytochrome c expression and activated caspase-3 positive cells were reduced in oxygen-glucose deprivation treated hippocampal organotypic slices that were co-cultured with BMSCs. Additionally, oxygen-glucose deprivation treated hippocampal organotypic slices that were co-cultured with serum-deprived BMSCs demonstrated an increase in the secretion of neurotrophic factors; significantly IGF-I, bFGF, and NGF. (Sarnowska et al., 2009) In the study by Nesti et al (described above), dental pulp stem cells were not in direct contact with mesencephalic neurons when cultured in-vitro, and were still found to provide neuroprotection from harmful toxins. (Nesti et al., 2011) It was highlighted by the researcher, however, that further in-vivo studies were required to clarify whether the transplanted stem cells still retained the ability to produce neurotrophic factors after transplantation. In another study, cortical neurons cultured with MSC conditioned media better survived trophic deprivation and nitric oxide (NO) exposure than those cultured in regular media. The cortical neurons were not co-cultured with MSCs; media from the MSC culture was applied to cortical neurons in-vitro and a protective effect was observed. This effect was shown to depend on an intact PI3kinase/Akt signaling pathway, which was activated upon application of MSC conditioned media to cortical cultures

exposed to NO. BDNF secretion by the cultured MSCs is believed to be the cause of the increased activation of this pathway. (Wilkins et al., 2009) These studies, while not completely negating the need for direct cell-to-cell contact provide for the potential to treat nerve lesions and disorders in locations where direct cell-to-cell contact would be impossible or difficult to achieve.

The neuroprotective effects of stem cells described thus far demonstrate a potential use in different pathological states. While the above-mentioned studies focus mainly on diseases in which neuropathic pain is of major concern, other equally crippling neurodegenerative diseases, such as Alzheimer's and Huntington's diseases, may benefit from the neuroprotective effects of stem cells. It is worth looking into the potential for stem cell therapies to create a neurotrophic environment conducive to the amelioration or reversal of the neurodegeneration that leads to these debilitating diseases, as well as the prevention of degeneration and degradation of uninjured nerve fibers. Additionally, the above-mentioned studies have shown that stem cells have the ability to decrease and ameliorate the negative effects on injured nerve fibers, improving the function of the injured nerve. The release of key neurotrophic factors, along with the neuroprotective and neuroregenerative effects of stem cells make them an ideal candidate for arresting and possibly reversing the incapacitating effects of neuropathic pain.

Current Uses in Neuropathic Pain

Aside from the trophically-rich environment produced by the transplantation of various types of stem cells into different animal models, continuing work is being done to determine the potential use of stem cells for the debilitating disease of neuropathic pain. Transplantation of hMSCs into a mouse model of spared nerve injury has been found to significantly reduce both mechanical allodynia and thermal hyperalgesia, as measured with paw withdrawal latency and paw withdrawal threshold tests. The mechanisms believed to be responsible for the reduction in allodynia and hyperalgesia are several – the decrease of the pro-inflammatory interleukin 1β (IL-1β) and interleukin 17 (IL-17), an increase in protein expression of the anti-inflammatory interleukin 10 (IL-10), and a reduction in the over-activation of β-galactosidase. It was also found that motor coordination was not affected by stem cell transplantation. (Siniscalco et al., 2010) Similar results have been achieved through both intra-brain injection of hMSCs and injection into the tail vein of spared nerve injury mice, indicating that the effects of hMSCs may also be achieved through a minimally invasive procedure, due to the homing effect of the cells. (Siniscalco et al., 2011)

Stem cell therapies are also currently being explored in the treatment of diabetic peripheral neuropathy. In rats that have streptozotocin induced diabetes, bone-marrow derived mesenchymal stem cell transplantation produced a significant increase in mRNA expression and protein expression of both bFGF and VEGF compared with rats receiving

saline injections. Sciatic nerve blood flow was significantly ameliorated compared to diabetes-induced rats treated with saline. Additionally, the decrease in both the capillary-to-muscle ratio and the neurofilament content was prevented in the stem cell transplanted group. (Shibata et al., 2008) Transplantation of bone-marrow derived MSCs has improved motor nerve conduction velocity in diabetic animals compared with animals simply receiving saline injections. (Shibata et al., 2008; Kim et al., 2011) Despite these benefits, however, motor nerve conduction velocity and the increase in the levels of NGF and NT-3 were found to last for only 4 weeks. (Kim et al., 2011) Interestingly, when it comes to neurotrophic factors, these two studies contradict each other. In the study by Kim, levels of neurotrophic factors, such as NGF and NT-3, but not VEGF or bFGF, were found to increase in the animals that received bone-marrow derived mesenchymal stem cell transplantation. In the study by Shibata, however, VEGF and bFGF, but not NGF and NT-3, were found to increase in the animals that received stem cell transplantation. As can be clearly seen, many more studies need to be performed to understand the effects of stem cells in these diseases.

In addition to uses in neuropathic pain with peripheral nerve injury, promising results have been seen in spinal cord injuries. In a study by Ichim, a patient with an incomplete spinal cord injury at the T12 – L1 level and a crush fracture in the L1 vertebral body (described as a type A in the ASIA scale) was administered several doses of MSC and CD34+ cells. Prior to the allogeneic transplantation of the MSCs this patient reported neuropathic pain at a level of 10/10. After several cycles of MSC and CD34+ cell

transplantation he reported a marked decrease of neuropathic pain – from daily 10/10 to once a week 3/10. No adverse effects were noted following transplantation. Muscle strength improved, various dermatome sensation increased, and urological and sexual function was recovered. While these results are positive, the study is a case report of only one patient. Therefore, caution must be taken in the interpretation of these results, particularly with regards to efficacy. (Ichim et al., 2010) A table summarizing the recent studies using stem cells to treat neuropathic pain can be found below (Table 3).

Summary of Recent Studies Using Stem Cells to Treat Neuropathic Pain			
Source of Stem Cells	**Model System**	**Mechanism of Action**	**Study / Reference**
Human bone marrow derived MSCs	Mouse model – spared nerve injury; intra-brain injection of hMSCs	↓ IL-1β, IL-17 ↑ IL-10 ↓ over-activation of β-galactosidase	Siniscalco et al., 2010
Human bone marrow derived MSCs	Mouse model – spared nerve injury; tail vein injection of hMSCs	↓ IL-1β, IL-17 ↑ IL-10 ↑ CD206	Siniscalco et al., 2011
Sprague Dawley Rat bone marrow derived MSCs	Streptozotocin induced diabetic Sprague Dawley Rats; right thigh and soleus muscle injection of MSCs	↑ Capillary number–to–muscle fiber ratio Normalization of axonal circulometry ↑ VEGF, bFGF Prevention of decrease: NF-H, NF-M, and NF-L	Shibata et al., 2008
BALB/c mice bone marrow derived MSCs	Streptozotocin induced diabetic BALB/c mice; hind limb muscle injection of MSCs	↑ NGF, NT-3	Kim et al., 2011
Human placental derived MSCs and CD34+ cells	Human: incomplete spinal cord injury at the level T12-L1, and crush fracture of the L1 vertebral body; intrathecal injection of MSCs	Unknown	Ichim et al., 2010

Table 3: Summary of Recent Studies Using Stem Cells to Treat Neuropathic Pain

Chapter 8 – Neural Crest Stem Cells[3]

The neural crest is a transient structure occurring early in embryological development. Discovered by His in 1868 (His, 1868), the neural crest is comprised of cells at the border between the neural and non-neural ectoderm during neurulation (Gammill & Bronner-Fraser, 2013). Interestingly, cells from all 3 germ layers (ectoderm, mesoderm, and endoderm) arise from the neural crest (Le Douarin & Kalcheim, 1999). This makes the neural crest an attractive source for regenerative medicine. In addition, many neural cell types arise from the neural crest, increasing the attractiveness of the neural crest as a potential cell source for neuro-regenerative medicine (Dupin et al., 2007; Dupin & Sommer, 2012) (Table 4). Recently, many stem cells have been isolated from various neural crest-derived adult human tissues. These tissues include: hair follicles (Yu et al., 2006; Krejčí & Grim, 2010; Yu et al., 2010; Yanh and Xu, 2013) the periodontal ligament (Coura et al., 2008; Huang et al., 2009), the gingiva (Fournier et al., 2013), dental pulp (Waddington et al., 2009), the olfactory mucosa (Féron et al., 2013), and the inferior turbinate (Hauser et al., 2013). These stem cells, as will be further discussed below, have been able to be differentiated into various types of neural cells.

[3] This chapter is a partial excerpt from *Fortino et al., Neurogenesis from Stem Cells. Journal of Recent Patents in Regenerative Medicine. 2014, 4:16-33*.

	CRANIAL NEURAL CREST	TRUNK NEURAL CREST
NEURONS	Sensory cranial ganglia Parasympathetic (ciliary) ganglia Enteric ganglia	Sensory ganglia in the DRG Parasympathetic ganglia Sympathetic ganglia
GLIA	Satellite glial cells in ganglia Schwann cells of the PNS Enteric glia Ensheathing olfactory cells	Satellite glial cells in ganglia Schwann cells of the PNS

Table 4: Derivatives of the Neural Crest

Although up until recently all of the stem cells derived from the neural crest have been proven to be multipotent, our lab has recently discovered a method to isolate a verifiably pluripotent population of stem cells from the periodontal ligament (Pelaez et al., 2013). These cells, when enriched by selecting for Connexin 43 and injected into immunodeficient mice, form teratomas containing all three germ layers.

Patents and Scientific Literature Highlighting Neural Crest Stem Cell Differentiation

Our patent application (Cheung et al., WO2013131012), as stated in the above publication (Pelaez et al., 2013), isolates a homogeneous population of verifiably pluripotent stem cells from the neural crest. Additionally, in this patent, we describe methods to differentiate these cells into neurogenic lineages, in order to provide a cell source for neurodegenerative diseases. While this patent has not yet been granted, the ability of isolating a homogeneous and truly pluripotent population of stem cells from the neural crest presents an exciting new source of stem cells for neurogenesis and neuro-regenerative medicine.

Additionally, there are patents on isolating and differentiating neural crest cells in animals. A patent invented by Sean J. Morrison and Eve Kruger and held by The Regents of The University of Michigan, takes post-natal stem cells from the gut and isolates the neural crest portion of these cells (Morrison & Kruger, US8043853). They isolate the $p75^{+}$ subpopulation of these cells and maintain them in standard culture conditions, where they spontaneously differentiate into neurons and glia following 14 days of culture. This suggests that cells obtained from the neural crest have the ability to spontaneously differentiate into neural cells - increasing the advantage of using neural crest stem cells for neuro-regeneration. While this is a very interesting patent - the location of the cells provides yet another stem cell source of neural crest stem cells - which we know generate many neural cells - several questions need to be answered before this can be translated to human cells. Although they state that their methods could be employed in human cells, their patent reports their data with adult rat cells.

In a patent held by Harvard College, Douglas A. Melton and Ali Hemmati-Brivanlou develop a method to differentiate stem cells into neuronal cells by inhibiting activin binding to its receptors on a cell. They accomplish this by using a follistatin protein meant to sequester the activin and/or bind directly to the activin receptors, therefore not allowing the activin to bind to its receptors on the stem cell. Additionally, they culture the cells with one or more of the following agents to induce differentiation: NGF, CNTF, schwanoma-derived growth factor, glial growth factor, striatal-derived neurotrophic factor, platelet-derived growth factor, scatter factor, a vertebrate hedgehog protein, noggin, and a

ligand for a Notch receptor. While they tested their invention in the Xenopus embryo, they state that this can be translated into other stem cells, such as neural crest stem cells (Melton & Hemmati-Brivanlou, EP0726948).

Growth Factor and Chemical Induction

The use of growth factors and chemicals is the method most employed to differentiate stem cells into neural cells. With neural crest stem cells this has proved to be no different. Our laboratory (Fortino et al., 2013) used EGF and bFGF to differentiate neural crest-derived stem cells from the periodontal ligament into neural-like cells. Our treatment demonstrated significant morphological changes under scanning electron microscopy, with the treated cells taking on both glial and neuronal phenotypes. Using gene expression there was a statistically significant difference in the gene expression of β-tubulin III and nestin; immunohistochemical studies indicated our cells positive for GFAP, β-tubulin III, and synaptophysin. Patch clamping performed on these cells demonstrated increased sodium channel and potassium channel currents following only 8 days of treatment. Our combined results suggest that our treatment of EGF and bFGF is successful in taking the neural crest stem cells towards a more neural cell type. Although this treatment was very straightforward, due to the location and formation of the neural crest it is not surprising that we would see positive results in only 8 days of treatment with EGF and bFGF.

In another protocol, neural crest stem cells were isolated from human hair follicles and were induced into neuronal cells on a collagen coated substrate with a media consisting of neuregulin 1. Following two weeks of treatment they noted a marked increase in the expression of β-tubulin III, and were able to verify this expression with positive immunostaining. Additionally, they noted positive immunostaining for Schwann cell markers (S100b) as well as GFAP (Krejčí & Grim, 2010). In another protocol to differentiate stem cells from human hair follicles, the laboratory modified a previously used protocol for differentiating mouse or rat hair follicle stem cells (Fernandes et al., 2004) and used it to differentiate human hair follicle NCSCs (Yu et al., 2010). They used a two-step differentiation protocol under adherent culture conditions: initially they employed a culture media with FGF2 - this was done for five to seven days. Afterwards, the FGF2 was removed and NGF, BDNF, and neurotrophin-3 (NT-3) were used and the cells were cultured for another five to seven days. A Schwann-cell differentiation protocol was also employed where the cells were cultured with forskolin. Using immunostaining they showed positive results for neurofilament (NF) and MAP2. Interestingly, they used gene ontology to study enrichment of neural genes following their treatment. Although they found 56 genes that they considered to be differentially expressed it is important to note that the p value stated to be significant was $p<0.1$ instead of the standard (and more stringent) $p<0.05$.

A patent invented by Maya Sieber-Blum and Milos Grim, and held by Newcastle University, describes a method to isolate and differentiate neural crest stem cells from the

bulge-region of human hair follicles (Sieber-Blum & Grim, US8030072). Following isolation, they culture the cells in adherent culture conditions where they have 70% purity of the obtained stem cells. They expand the stem cells by sub-culturing them and then use a variety of components and growth factors such as: collagen, fibronectin, alpha-modified MEM culture medium, insulin, transferrin, selenium, at least three essential fatty acids, day 11 chick embryo extract, fibroblast growth factors, epidermal growth factors and neurotrophins to differentiate these cells into neural-like cells. They verified the success of differentiation by using RT-PCR and checking for MAP2, GFAP, β-tubulin II and peripherin. Although the differentiation results were for adult mouse hair follicles, they did the isolation procedure for human hair follicles and were able to verify the presence of multipotent neural crest stem cells from the human hair follicles as well. The results from their studies suggest that there is yet another multipotent source of neural crest stem cells in adult human tissue, and provides an interesting source of neural crest stem cells that seems to be easily and readily available.

Stem cells from human exfoliated deciduous teeth (SHEDs), better known as milk teeth, are also neural crest-derived stem cells that have undergone neural differentiation. One particular study used a three-stage differentiation protocol (Jarmalavičiūtė et al., 2013). The first step involved a serum-free media for one week. Subsequently the cells were moved to a media containing bFGF and EGF for seven to ten days. Following this induction, they differentiated the SHED cells with dibutyryl cAMP, NGF, BDNF, and GDNF for 14-21 days. Their results showed morphological changes in the SHED cells -

formation of stellate or bipolar round shaped cells with expression of Brn3a and peripherin (sensory neuron markers) and myelin basic protein (a glial marker). Using PCR arrays they confirmed an upregulation of midkine, pleitrophin, tyrosine hydroxylase, Nurr1, MAF, Krox24, Krox20, and apolipoprotein E - genes related to neurogenesis and cAMP/calcium signaling. Immunocytochemistry results indicated positive staining for β-tubulin III and others positive for myelin basic protein. This demonstrated that their differentiation protocol induced cells that were a mixture of glia and neuronal subtypes.

Growth Factor and 3D Culture Differentiation

Interestingly, many recent methods for differentiating neural crest stem cells into neural cells involve initial 3D culture as "neurospheres" (either with or without treatment media) prior to using differentiation media. Although not studied yet, the use of neurosphere vs. adherent culture would be an interesting comparison to perform to determine effectiveness of neurogenic differentiation of stem cells.

While the treatment from our laboratory was aimed at inducing a non-specific neural cell, cells from the periodontal ligament have also been induced into retinal progenitor cells using a combination of Noggin and DKK-I (Dickkopf-related protein 1) along with a sequential differentiation protocol involving 3D culture (as neurospheres) and matrigel coated plates (Huang et al., 2013). Using this combination, gene expression, immunofluorescence and flow cytometry indicated positive results for several retinal markers, including photoreceptors. In particular, under neurosphere culture, these cells

showed positive gene expression for nestin, p75/nerve growth factor receptor (NGFR), Pax6, and Tuj1. Following completion of the treatment, these cells were positive for Pax6 (using flow cytometry - 94%) and expressed the photoreceptor marker rhodopsin. These results suggest that neural crest stem cells have the ability of being differentiated into specific neuronal sub-types. Additionally, these cells indicated positive response to glutamate, as demonstrated through calcium imaging techniques. It would be interesting to determine if such a long differentiation time is required (this protocol lasted more than 24 days) or if there would be a possibility of shortening the differentiation time in order to produce cells more readily available for regenerative treatments.

Similarly, 3D sphere culture was used on apical dental pulp stem cells from impacted third molar teeth (Abe et al., 2013) prior to differentiating with a neural induction media. Following seven days of sphere culture the cells were then cultured on chamber slides for seven days and then transferred to an induction media consisting of NGF, bFGF, dibutyryl cAMP, 3-isobuthyl-1-methyl xanthine and RA for seven days. Following this protocol they saw morphological changes of the apical dental pulp stem cells into neuronal cells. They also noticed a significant difference between cells cultured in the neural induction media vs the control cells; in particular, the expression of TuJ1 and MAP2 was present in the treated, but not control, cells. Interestingly, they found that the expression of the neural stem cell markers Nestin and Musahi-1 were lost following the induction into neural cells, suggesting the push from immature to a more mature neural phenotype following their treatment.

In addition to SHEDs, and cells from the periodontal ligament, another neural crest cell type - the dental follicle, has been differentiated into neural cells. In a patent invented by Özer Degistirici and Michael Thie and held by Stiftung Caesar, describes a method to differentiate neural crest stem cells into neural stem cells *in-vitro* (Degistirici & Thie, EP1705245). In this patent they isolate cells from tissue of the dental follicle or wisdom teeth, and differentiate it in various steps. First, they culture the stem cells as spheres in regular media for 8-12 days. Second, the floating spheres are transferred and placed in media containing EGF and bFGF. As the spheres proliferate and grow larger they are passaged and expanded. Third, they dissociate the spheres and re-culture them once again in sphere forming conditions with EGF and bFGF. Lastly, they isolate the neural stem cells from the spheroids that were in the media with the neurogenic factors. To determine differentiation potential, the cells were cultured under adherent conditions with NGF, bFGF, dibutryl cAMP, 3-isobutyl-1-methylxanthine, and RA. Following one to two weeks of treatment, some the cells stained positive for NF and GFAP. While their method did have some success, interpreting their results suggested that the efficiency of their differentiation protocol was not very high and it would be interesting to see if culturing for longer periods of time in the differentiation media would result in a higher population staining positive for neural markers.

Due to its location during embryological development and the tissues that arise from the neural crest, the neural crest presents a new and exciting stem cell source that may be more easily differentiated into neural cell types than stem cells from other tissues. A

summary of recent literature using various methods to differentiate human adults' neural crest stem cells can be found in Table 5.

Summary of Recent Literature for Neurogenesis from Human Adult Neural Crest Stem Cells			
Source of Stem Cells	**Method of Differentiation**	**Results**	**Study**
Periodontal Ligament	EGF, bFGF (8 days)	Gene: ↑ β-tubulin III, Nestin ↓ NOG IHC: ↑ β-tubulin III, GFAP, Synaptophysin	Fortino et al., 2013
Hair Follicle	Neuregulin 1 (14 days)	Gene: ↑ β-tubulin III IS: ↑ S100b, β-tubulin III, GFAP	Krejčí et al., 2010
Hair Follicle	FGF2 (5-7 days) NGF, BDNF, NT-3 (5-7 days)	IS: ↑ NF, MAP2	Yu et al., 2010
Exfoliated Deciduous Teeth	Serum-free (7 days) EGF, bFGF (7-10 days) dibutyryl cAMP, NGF, BDNF, GDNF (14-21 days)	Gene: ↑ Brn3a, peripherin, myelin basic protein, midkine, pleitrophin, tyrosine hydroxylase, Nurr1, MAF, Krox24, Krox20, apolipoprotein E. ICC: ↑ β-tubulin III, myelin basic protein.	Jarmalavičiūtė et al., 2013
Periodontal Ligament	Noggin, DKK-I, as neurospheres (3 days) Noggin, DKK-I, N2 on Matrigel (up to 25 days)	Gene: ↑ nestin, p75/NGFR, Pax6, Tuj1. Flow cytometry: ↑ Pax6, rhodopsin.	Huang et al., 2013

Apical Dental Pulp	Neurospheres (7 days) NGF, bFGF, dibutyryl cAMP, 3-isobuthyl-1-methyl xanthine, RA (7 days)	Gene: ↑ Tuj1, MAP2 ↓ Nestin, Musahi-1	Abe et al., 2012

Table 5: Recent Literature for Neurogenesis from Neural Crest Stem Cells

SECTION 2 – IN-VITRO RESULTS

Chapter 9 – Stem Cell Characterization for Animal Studies

As stated in the previous chapters, a population of stem cells from the periodontal ligament has been isolated in Dr. Cheung's laboratory (Huang et al., 2009). As sensory neurons and glia are also derived from the neural crest, stem cells derived from the periodontal ligament may possess several characteristics similar to sensory neurons and glia, therefore allowing them to be a viable source for transplantation. The periodontal ligament stem cell population has been further purified to obtain a neural crest remnant population, termed here NCSC for neural crest stem cell. Purification of the NCSC to a homogenous population is important because several other researchers have been able to isolate heterogeneous stem cells from various neural-crest derived tissues (as highlighted in Chapter 8). Purification for the Connexin 43 surface marker is a straightforward way to ensure consistent behavior across the various stem cell sources and cell lines obtained from different patients. Throughout this text it has been highlighted that various stem cell populations produce and secrete growth factors, and that they are helpful in ameliorating neuropathic pain (albeit the studies are on non-human stem cells). This is important because it further underscores the possibility of using NCSC to create a trophically rich micro-environment that will prevent further degeneration of the peripheral neurons. NCSC were characterized for the expression, production, and secretion of IGF-I to calculate the number of cells necessary for transplantation into an animal model of diabetes with DPN.

Commercially available mesenchymal stem cells, although by no means the gold standard, were used as the control cells for the gene expression.

Isolation of Periodontal Ligament Stem Cells and Purification Into NCSCs

Media description: High glucose-complete culture medium (HGCCM) – high glucose Dulbecco's modified eagle medium (DMEM) supplemented with 10% fetal bovine serum (FBS), 1% penicillin streptomycin (100 units/ml Penicillin and 100 µg/ml Streptomycin) and 0.1% amphotericin B (0.25 µg/ml).

Stem cells were harvested from impacted wisdom teeth following IRB approved protocols as previously described (Huang et al., 2009). Cells were cultured with HGCCM and passaged when they reached ~70% confluence. After a stable culture was established (~P3/P4) cells were selected for the neural crest remnant population (labeled NCSC – neural crest stem cells) with the Connexin 43 marker as previously described (Pelaez et al., 2013) (Figure 2). Connexin 43 was selected because it is a migrating neural crest marker present in all neural crest cells. Briefly, cells were lifted enzymatically and incubated overnight in 4°C with a primary antibody against human Cx43 (Abcam, Cambridge, MA; #ab11370) diluted 1:100 in 1% FBS-containing HG-DMEM with constant rotation. Following the overnight incubation, cells were centrifuged at 4°C at 1,000 rpm for 10 min, washed with PBS, centrifuged again, washed again with PBS, centrifuged again, and then marked for magnetic activated sorting with prewashed Dynabeads conjugated to a sheep anti-rabbit IgG secondary antibody (Invitrogen, part of Life Technologies, Grand Island,

NY; #112-03D). Following the secondary incubation, the resulting suspension was placed on a magnetic tube rack and allowed to settle, after which the supernate was removed (being careful to not remove any of the cell-bead conjugates that aggregated onto the magnet). The remaining cell-bead conjugates were washed in PBS, aggregated onto the magnet again, (the supernate was removed again being careful not to remove the cell-bead conjugates aggregated onto the magnet), and the resulting cell-bead conjugates were washed again in PBS, re-suspended with HGCCM and seeded onto T75 culture flasks (now passage 5). Cells were allowed to adhere for 7 days, media was removed, cells were washed several times with PBS to remove any excess magnetic beads, and then fresh HGCCM was added. For every subsequent media change the cells were washed multiple times to remove any excess magnetic beads. Cells were passaged once they reached ~70% confluence. Two passages were necessary to remove all of the beads.

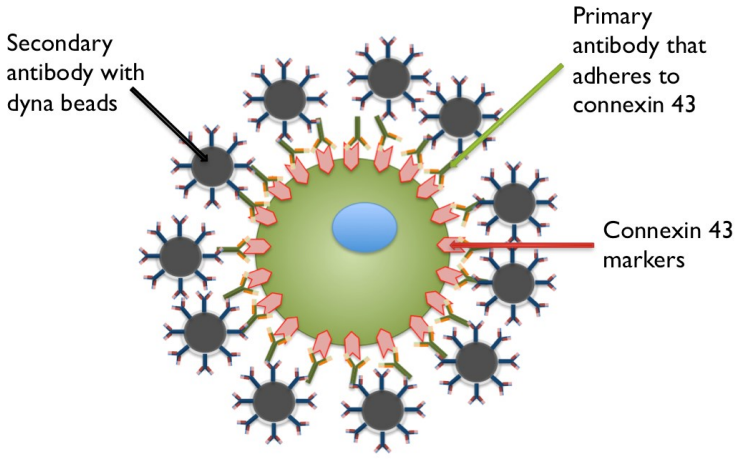

Figure 2: Selecting cells for Connexin 43 (from Pelaez, et al., 2013)

IGF-I Expression

Cell Culture and qPCR Methods

Both NCSCs and commercially available MSCs were seeded onto 6-well plates and cultured with HGCCM until they reached 90% confluence. At 90% confluence, the media was removed and cells were washed with PBS to remove any residual FBS (which contains growth factors, including IGF-I, and could cause discrepancies in the data). HG-DMEM was added to the cells. Cells were left in the serum-free condition for 7 days. Following the 7 days, the cells were washed with PBS and collected in Trizol (Life Technologies, Grand Island, NY) – two wells were considered one sample. Subsequent RNA extraction was performed using the manufacturers' instructions with the following modifications: centrifugation for phase separation and RNA precipitation was done at 14,000 rpm for 20 minutes. Centrifugation for the RNA wash was done at 7,500 rpm for 10 minutes. Total RNA yield was determined using the NanoDrop ND-1000 spectrophotometer (Thermo Scientific, Wilmington, DE). Total RNA (1µg) was converted to cDNA using the ABI High Capacity cDNA Reverse Transcription Kit (Applied Biosystems, part of Life Technologies, Grand Island, NY) and the GeneAmp PCR System 9700 (Applied Biosystems, part of Life Technologies, Grand Island, NY). Quantitative PCR (qPCR) was performed using the Stratagene Mx3005P (Agilent Technologies, Santa Clara, CA). The samples were prepared using the Sybr Green PCR master mix (Applied Biosystems, part of Life Technologies, Grand Island, NY), with 20ng cDNA per reaction. The primer

sequence for IGF-I was designed based on the corresponding human gene. Forward primer sequence 5'-3': CAATGTTCTAATCACTATGGA. Reverse primer sequence 5'-3': AACCTGTATGTCTGGAAA.

Gene Expression Results and Discussion

The data obtained (Figure 3) clearly demonstrates that the homogeneous population of NCSCs expresses a statistically significant higher level of IGF-I than the mesenchymal stem cells. The NCSC demonstrate an almost 10 fold higher gene expression for IGF-I than the commercially available MSCs.

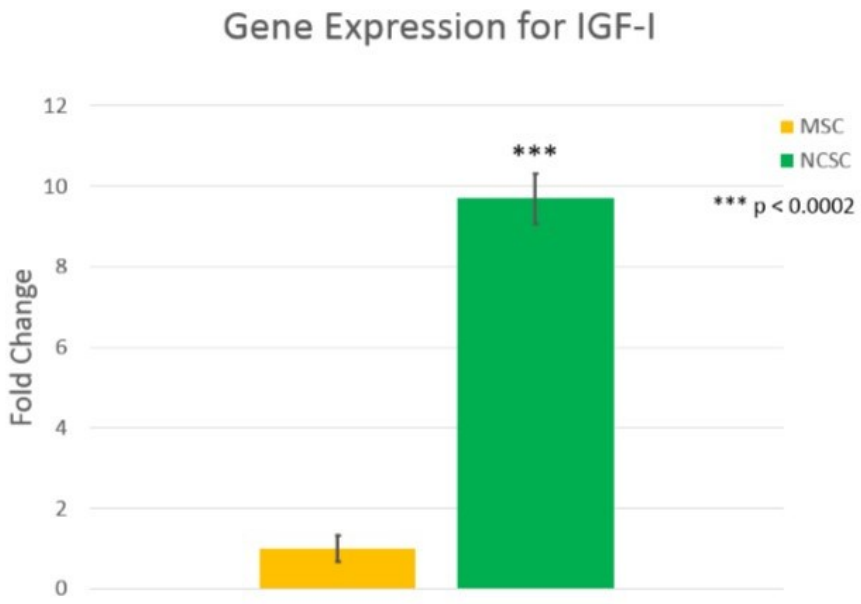

*Figure 3: Gene Expression MSCs vs. NCSCs for IGF-I. Green bar is NCSC, yellow bar is commercially available MSCs. Data presented as mean±SEM, *** p < 0.0002.*

IGF-I Production

Immunohistochemistry Methods

NCSCs were seeded onto 6-well plates and cultured with HGCCM until they reached 90% confluence. At 90% confluence, the media was removed and cells were washed with PBS to remove any residual FBS (which contains growth factors, including IGF-I, and could cause discrepancies in the data). HG-DMEM was added to the cells. Cells were left in the serum-free condition for 7 days. Following the 7 days, the cells were washed with PBS and fixed with 100% ice-cold methanol for 10 minutes at -20°C. Following the ice-cold methanol fixation, the methanol was removed and fresh PBS was added to each well. The PBS was removed and the cells were washed once again with PBS. The cells were incubated in blocking buffer (PBS + 0.05% tween 20 + 1% FBS + 20mg/mL BSA) for one hour, after which the blocking buffer was removed and the primary antibody was added. The cells were incubated in the IGF-I primary antibody (1:100 dilution in 0.5mg/mL BSA – Rb pAb to IGF-I, Abcam, Cambridge, MA; #ab9572) overnight at room temperature on a plate rocker. Following overnight incubation, the primary was removed, the cells were washed twice with PBS, and a goat anti-rabbit FITC secondary was added, (1:200 dilution in PBS – Goat pAb to Rb IgG Abcam, Cambridge, MA; #ab7050) shielded from light, and left rocking for two hours. Following the incubation with the secondary antibody, the cells were washed twice with PBS. Two drops of Vectashield hard set mounting media with DAPI (Fischer Scientific, Hampton, NH) were placed in each well.

A glass coverslip was thoroughly washed, dried, and placed in each well. The samples were shielded from light and taken to image. Immunohistochemical images were acquired using a Nikon Digital Camera DS-Qi1MC mounted to a Nikon Eclipse Ti inverted fluorescent microscope. The NIS Elements software package was used for merging images and image analysis. Quantitative image analysis was done using ImageJ.

Image Analysis and Quantification using ImageJ

ImageJ software was used to determine the number of cells which stained for DAPI and FITC. This number was then compared to produce a percentage of cells that stained positive for IGF-I. A merged picture of DAPI and FITC for each cell line was first uploaded into the program and then underwent a background reduction (rolling ball parameter was set to 50). The color scales of the images were then adjusted using the threshold feature of the system, where the appropriate brightness of an image was qualitatively determined for accurate representation of cell count. DAPI was considered any hue from 120 to 255 while FITC was considered to be any hue from 0 to 120 for all images. The cells were then counted using the analyze particle feature of ImageJ where circularity was from 0.00 to 1.00. Furthermore, the area rejection boundaries for the particles were adjusted as to represent cell count. Finally, the number of cells stained were recorded: holes and cells on the border of the image were excluded by Image J.

Production Results and Discussion

The figures below (Figure 4–6) show IGF-I production from three different established cell lines in Dr. Cheung's laboratory. Each cell line is from a different donor (age and sex). In the Figures below, ImageJ was used to quantify the number of cells that stained positive for IGF-I. In each Figure, **A** shows the merged DAPI and FITC image, **B** shows the digitized black and white image of the DAPI, **C** shows the ImageJ generated outlined drawing of the DAPI from the black and white image (used for the count), **D** shows the digitized black and white image of the FITC, and **E** shows the ImageJ generated outlined drawing of the FITC from the black and white image (used for the count).

Figure 4 shows the F17 NCSC line, which stained 94.3% positive for IGF-I (DAPI count 261, FITC count 246). In Figure 4A, we see the merged FITC and DAPI that seems to be 100% positive staining. A possible explanation for this almost 6% difference is that the ImageJ generated outline of the FITC (Figure 4E) did not take into account cells that were on the edge (in other words, cells that had part of the cell bodies cut off). This can be seen in the red outlined box of Figure 4E vs the digitized black and white image seen in Figure 4D. ImageJ did, however, take into account the nucleus of the cut off cells (the DAPI can be seen in the bottom edge of Figure 4C) when it did the count. It is believed that if the edge of Figure 4E would have been taken into account by the ImageJ software, the percentage of cells that stained positive would have been much closer to 100%. By manual counting of the cut off cells in Figure 4D, approximately 14 cells were cut off from

the bottom edge (comparing Figure 4D and 4E), which would bring the count of the FITC to 260, accounting for a new total of 99.6% of the cells staining positive for IGF-I.

Figure 5 shows the M19 NCSC line, which stained 95.9% positive for IGF-I (DAPI count 73, FITC count 70). In Figure 5A, we see the merged FITC and DAPI that seems to be 100% positive staining. A possible explanation for this almost 5% difference is that the ImageJ generated outline of the FITC (Figure 5E) did not take into account cells that were on the edges (in other words, cells that had part of the cell bodies cut off). This can be seen in the red outlined boxes of Figure 5E vs the digitized black and white image seen in Figure 5D. ImageJ did, however, take into account the nucleus of the cut off cells (the DAPI seen in the corresponding edges of Figure 5C) when it did the count. It is believed that if the edges of Figure 5E would have been taken into account by the ImageJ software, the percentage of cells that stained positive would have been much closer to 100%. By doing a manual count of the cut off edges in Figure 5D, approximately three cells were cut off from the edges (comparing Figure 5D and 5E), which would bring the count of the FITC to 73, accounting for a new total of 100% of the cells staining positive for IGF-I.

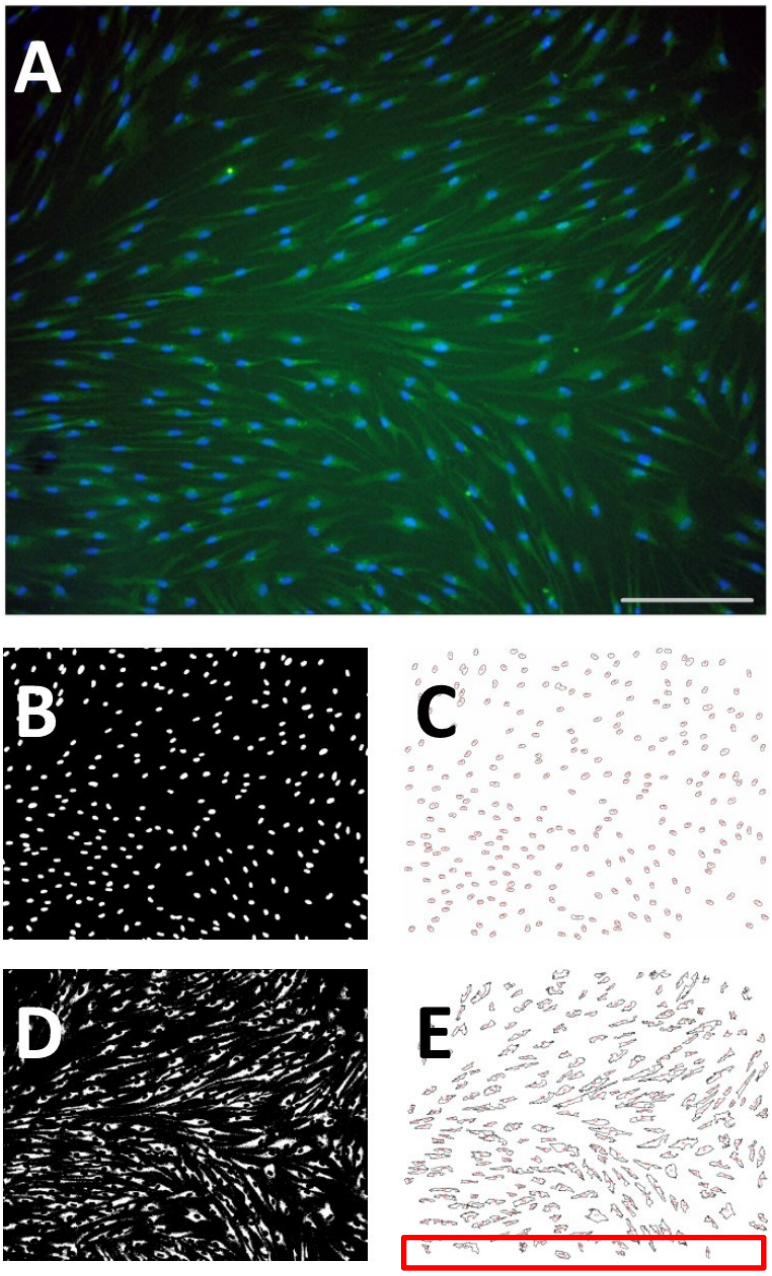

Figure 4: Immunohistochemistry for the F17 NCSC line. A) Merged DAPI and FITC image. Scale bar = 100µm. B) Digitized black and white image of the DAPI. C) ImageJ generated outline of the DAPI for the count. D) Digitized black and white image of the FITC. E) ImageJ generated outline of the FITC for the count.

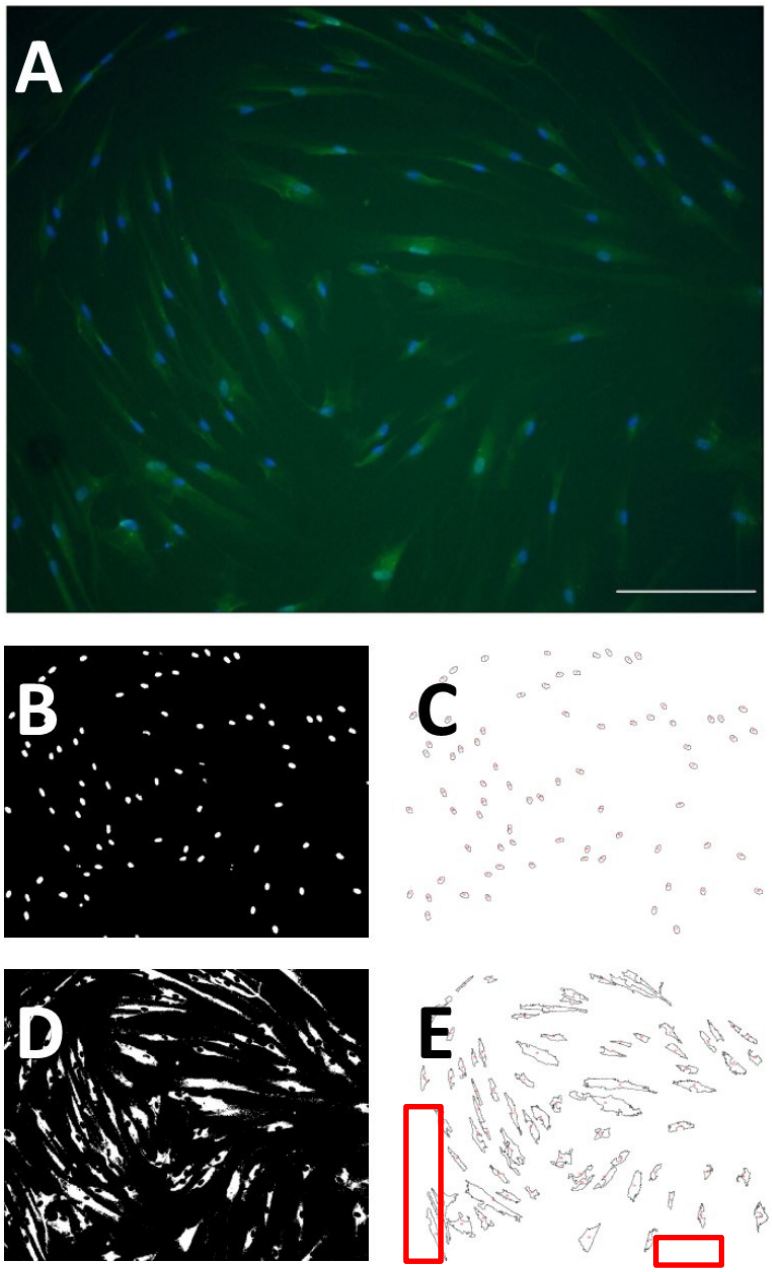

Figure 5: Immunohistochemistry for the M19 NCSC line. A) Merged DAPI and FITC image. Scale bar = 100µm. B) Digitized black and white image of the DAPI. C) ImageJ generated outline of the DAPI for the count. D) Digitized black and white image of the FITC. E) ImageJ generated outline of the FITC for the count.

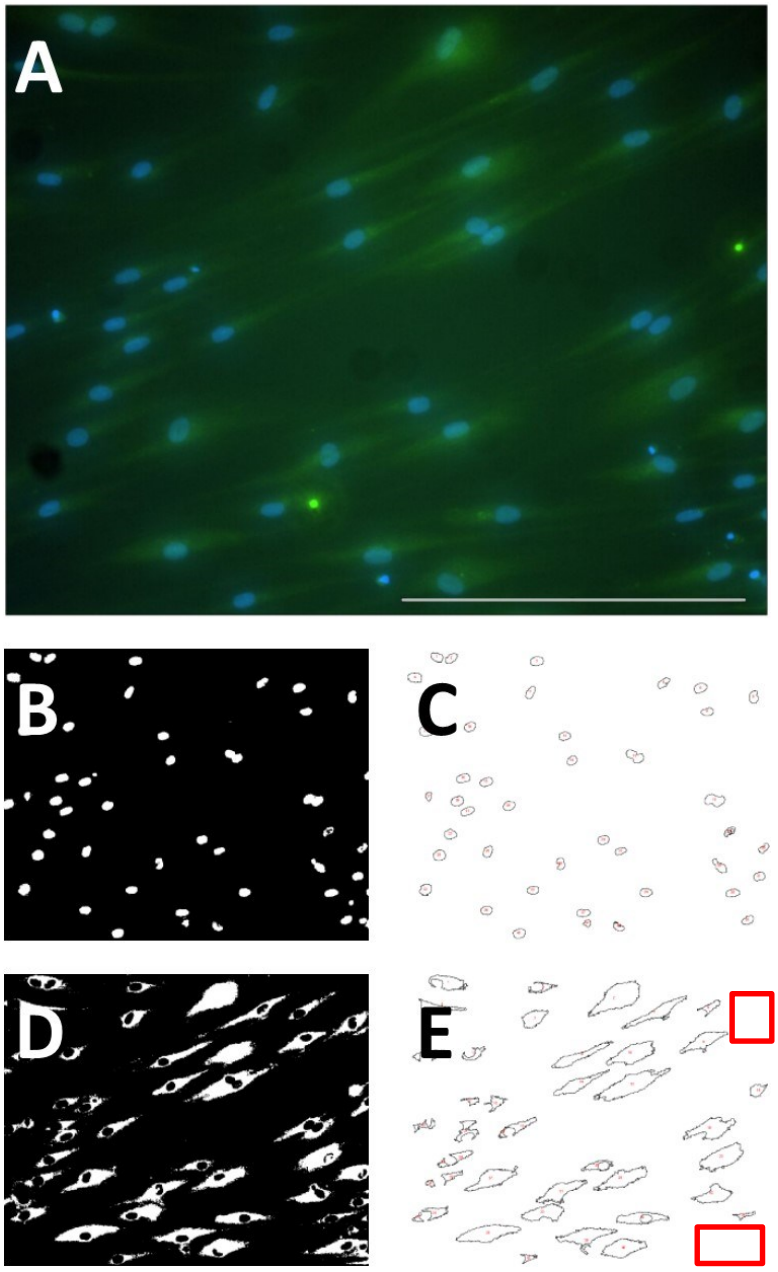

Figure 6: Immunohistochemistry for the PDL16 NCSC line. A) Merged DAPI and FITC image. Scale bar = 100μm. B) Digitized black and white image of the DAPI. C) ImageJ generated outline of the DAPI for the count. D) Digitized black and white image of the FITC. E) ImageJ generated outline of the FITC for the count.

Figure 6 shows the PDL16 cell line, which stained 95.1% positive for IGF-I (DAPI count 41, FITC count 39). In Figure 6A, we see the merged FITC and DAPI that seems to be 100% positive staining. A possible explanation for this almost 5% difference is that the ImageJ generated outline of the FITC (Figure 6E) did not take into account cells that were on the edges (in other words, cells that had part of the cell bodies cut off). This can be seen in the red outlined boxes of Figure 6E vs the digitized black and white image seen in Figure 6D. ImageJ did, however, take into account the nucleus of the cut off cells (the DAPI seen in the corresponding edges of Figure 6C) when it did the count. It is believed that if the edges in Figure 6E would have been taken into account by the ImageJ software, the percentage of cells that stained positive would have been much closer to 100%. When comparing the cut off edges, two cells were cut off (comparing Figure 6D and 6E), which would bring the count of the FITC to 41, accounting for a new total of 100% of the cells staining positive for IGF-I.

The quantitative ImageJ results indicate that any of the established NCSC lines in Dr. Cheung's laboratory may be used for transplantation.

IGF-I Secretion

Raybiotech Protein Array Methods

NCSCs were seeded onto T75 flasks and cultured with HGCCM until they reached 90% confluence. At 90% confluence, the media was removed and cells were washed with PBS to remove any residual FBS (which contains growth factors, including IGF-I, and

could cause discrepancies in the data). HG-DMEM was added to the cells. Cells were left in the serum-free condition for 7 days. Following the 7 days, the media was collected from each flask and placed in a -20°C freezer until further processing. The cells were lifted and counted for each flask and this number was recorded treating each flask as one sample. The frozen media was lyophilized overnight using the FreeZone 2.5 Plus lyophilizer (Labconco, Kansas City, MO) and re-suspended in 500µL of distilled water the following day. These samples were stored in -20°C until enough samples were collected to run a protein array. Once sufficient samples were collected, a Quantibody: Multiplex ELISA array (RayBiotech, Norcross, GA) was used to analyze the supernate for IGF-I and other growth factors. The protocol was followed according to the manufacturers' instructions. Figure 7 shows a schematic of the procedure for the Quantiplex Array. Briefly, Sample Diluent was added to each well to block the slides. Following the appropriate incubation, Sample Diluent was removed and standards or samples were added to each well. These were allowed to incubate overnight at 4°C. The following day, standards and samples were removed from each well and the wells were washed with Wash Buffer I and II. The detection antibody cocktail was added and incubated overnight at room temperature. The following day, the antibody was removed from each well and the wells were washed with Wash Buffer I and II. The Cy3 equivalent dye-conjugated streptavidin was then added to each well and incubated for one hour. The Cy3 equivalent dye-conjugated streptavidin was removed from each well and the wells were washed with Wash Buffer I. The slides were removed from their holders and washed in the slide holder tubes with Wash Buffer I and

II. The slides were shipped overnight to RayBiotech for scanning. Once the scanning service was complete, RayBiotech sent a spreadsheet with the fluorescence data. Fluorescence data was analyzed (both standards and samples) and resulting quantitative IGF-I levels were obtained.

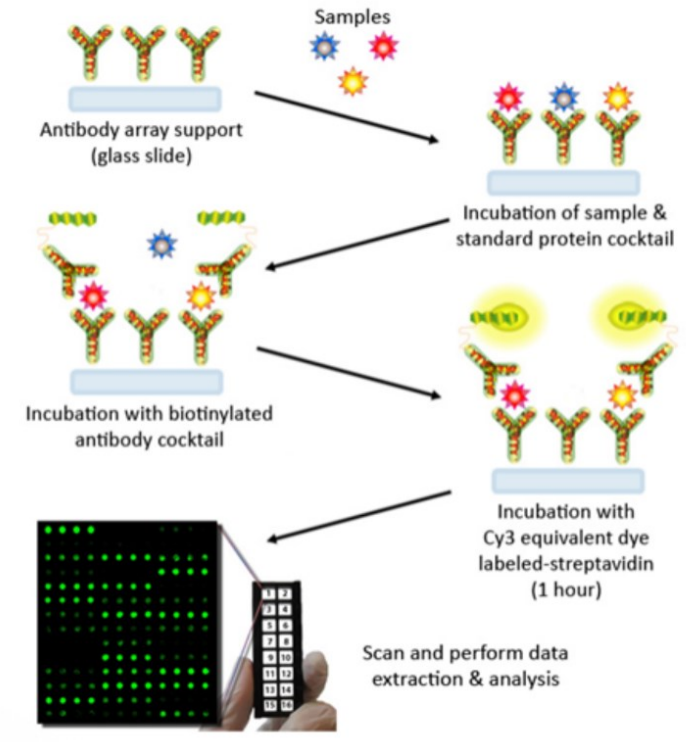

Figure 7: Schematic of Growth Factor Quantibody Array (from Raybiotech, 2015)

Secretion Results and Discussion

As can be seen in Table 6, IGF-I is secreted from two serum deprived NCSC lines. Typically when cells are under serum deprivation they become quiescent and maintain only

the functions necessary for survival. To obtain quantitative secretion data underscores the ability to use these cells as a mini-pump for IGF-I.

		NCSC Line	
		M19	***PDL19.5***
Protein (pg/mL)	***IGFBP-3***	10032.54	18212.8
	IGF-I	486.37	299
Total		10518.91	18511.8

Table 6: IGF-I Secretion for NCSCs

It is commonly known that IGF-I is typically found bound to one of its binding proteins, IGFBP-3. Up to 90% of IGF-I is found bound to IGFBP-3 in a 150-kd ternary complex along with an 80-kd acid-labile subunit, providing an increased half-life and reservoir of IGF-I (Jones and Clemmens, 1995; Ferry et al., 1999). For this reason, the quantitative values include both IGF-I and its main binding protein, IGFBP-3. In a regular IGF-I ELISA assay, an extra processing step is required to remove IGF-I from IGFBP-3 in order to obtain correct quantitative values of IGF-I. However, the Raybiotech Quantibody array used obtains quantitative values for both IGF-I and IGFBP-3, therefore quantifying total IGF-I values without the need for an extra processing/dissociating step.

Interestingly, between the two NCSC lines it can be noticed that the M19 cell line has higher levels of IGF-I and lower levels of IGFBP-3 than the PDL19.5. Conversely, the PDL19.5 has higher levels of IGFBP-3 with corresponding lower levels of IGF-I than the M19 cell line. Although the cause of this for the cell lines tested is unknown, it can be hypothesized that the higher levels of IGFBP-3 bind more of the IGF-I, thus providing less

"free" IGF-I into the media. While IGFBP-3 is known to sequester IGF-I in the vascular system, (which is typically believed to reduce its bioavailability), it is known that in some cases the binding proteins appear to enhance the activity of IGF-I (Jones and Clemmens, 1995; Ferry et al., 1999).

Stem Cell Dosing Calculations

rhIGF-I has been used therapeutically to treat patients with both type I and type II diabetes. In a study done by Thrailkill, (Thrailkill et al., 2009), they administered IGF-I twice daily in varying concentrations. They noticed that 40µg/kg administered two times per day (for a total of 80µg/kg) was well tolerated by the diabetic patients. Higher total doses, however, of 120µg/kg and 160µg/kg were found to produce edema and retinopathy in the patients. Therefore, the dose of 80µg/kg was deemed to be appropriate and was selected for the dosing calculations.

This therapeutic value for humans would need to be translated to the rat animal model that would be used in the subsequent *in-vivo* studies. There is an equation that the Food and Drug Administration recommends to translate the dosing for animal models to humans so that they may be used in clinical trials. Although there are some controversies as to its use in reverse (ie, from humans to animals), many researchers use this equation, as there is no other one available. (FDA, 2005)

$$Human\ Equivalent\ Dose = Animal\ Dose * \frac{Animal\ K_m}{Human\ K_m}$$

The equation was rearranged to calculate the Animal Dose:

$$Animal\ Dose = Human\ Equivalent\ Dose * \frac{Human\ K_m}{Animal\ K_m}$$

The corresponding Human K_m and Rat K_m were obtained from the same FDA guidance document, and are seen in the table below (Table 7):

Species	Weight (kg)	BSA (m^2)	K_m factor
Human			
Adult	60	1.6	37
Child	20	0.8	25
Baboon	12	0.6	20
Dog	10	0.5	20
Monkey	3	0.24	12
Rabbit	1.8	0.15	12
Guinea pig	0.4	0.05	8
Rat	0.15	0.025	6
Hamster	0.08	0.02	5
Mouse	0.02	0.007	3

Table 7: Km Factors (FDA, 2005)

Combining the information from Table 7 and Thrailkill's study, the required animal dose is calculated below:

$$Animal\ Dose = 80\frac{\mu g}{kg} * \frac{37}{6} = 493.3\frac{\mu g}{kg}$$

Using the secretion data and the cell line that was selected for transplantation (M19), the concentration of cells was converted into comparable units with a resulting

value of 10.52µg/kg. Using this information, along with the cell numbers obtained from the secretion studies, a proportion was used to calculate the amount of cells to be:

$$\frac{10.52\,\frac{\mu g}{kg}}{880{,}000\ cells} = \frac{493.3\,\frac{\mu g}{kg}}{X\ cells}$$

$$X = 41.26\ million\ cells$$

In the FDA guidance document for dosing translations, this resulting dose is meant to be used for drugs that have a systemic intended use. The guidance document states that the above calculated value needs to be modified for intramuscular injections (as these are not systemic) and be further normalized to the size of the therapeutic injection location.

Based on our work with the animals, it was determined that the rat thigh muscle is approximately 2.3% of the total body weight of the rat. This translates to using only 2.3% of the above calculated dose, resulting in a total amount of cells for intramuscular transplantation to be:

$$41.26\ million\ cells * 0.023 = 948{,}980\ cells$$

For ease of resuspension, this cell value was rounded up to 1 million cells. This number is comparable to other studies; for example, Shibata's study (Shibata et al., 2008) which transplanted rat stem cells into a diabetic rat animal model, used 1 million cells for transplantation.

The performed calculations for the secretion studies were done to include the total amounts of IGF-I and IGFBP-3. While this accounts for the total amount of IGF-I secreted by the cells, a potential drawback to this approach is the bioavailability of IGF-I. Will all of the IGF-I bound to the IGFBP-3 be released once it is circulating *in-vivo*? Future studies that may be performed, but were outside the scope of this Doctoral work, would be to characterize the unbinding of IGF-I from IGFBP-3 with the NCSC. This would give a better idea of the amount of available IGF-I once the cells are transplanted *in-vivo*.

Human IGF-I and rat IGF-I have a 90% homology (according to the Blast feature in the NCBI website, using accession code P05019.1). While this is a very high homology percentage, it would be interesting to see if the 10% difference has an effect on the way / amount of IGF-I binding to the rat cells. While the end goal of the research is to one day get to clinical human trials, this point could potentially have an effect on the efficacy of the human NCSC transplantation into the rat animal model, which accounts for the preliminary data for future human trials. The effect, therefore, of the 10% homology difference on the availability, binding, and action of human IGF-I in a rat animal model could be explored in future *in-vitro* co-culture work between rat cells and human NCSC.

The end goal of this project is to transplant NCSCs into an animal model of diabetes with associated DPN and determine the effects of the stem cells on evoked pain behaviors. One of the questions that arose was: will undifferentiated stem cells transplanted into the DPN animal model differentiate into neuronal cells? If they do, will they still express,

produce, and secrete IGF-I? This led to the development of protocols for neuro-induction of the NCSC in order to determine the expression and production of IGF-I. Chapter 10 describes the differentiation protocol for the NCSCs. Following the successful differentiation, the neural cells were characterized for the expression and production of IGF-I – this is highlighted in Chapter 11.

Chapter 10 - Neuro-Induction of Neural Crest Stem Cells

One of the questions that arose with regards to the transplantation of stem cells into an animal model of diabetes with associated neuropathy was whether or not the NCSC would differentiate *in-vivo* and if so, would they still secrete the desired neurotrophic factors. In order to answer the first part of this question, a neuro-induction protocol was developed for the NCSCs to drive them to a neural progenitor stage.

Methods

Culture and Differentiation Medias

High glucose-complete culture medium **(HGCCM)** – high glucose Dulbecco's modified eagle medium (DMEM) supplemented with 10% fetal bovine serum (FBS), 1% penicillin/streptomycin (100 units/ml Penicillin and 100 µg/ml Streptomycin), and 0.1% amphotericin B (0.25 µg/ml).

Neuro-induction media **(NIM)** – Dulbecco's Modified Eagle Medium/Nutrient Mixture F-12 (DMEM/F-12) supplemented with 2% FBS, 0.5% dimethyl sulfoxide (DMSO), 10ng/mL insulin-like growth factor-I (IGF-I), 10ng/mL Activin A, 150ng/mL Dickkopf-related protein 1 (Dkk1), 0.1mM β-mercapoethanol (βME), 5ng/mL neurotrophin-3 (NT-3), 50ng/mL epidermal growth factor (EGF), 50ng/mL basic fibroblast growth factor (bFGF), 1% penicillin/streptomycin (100 units/ml Penicillin and 100 µg/ml Streptomycin), and 0.1% amphotericin B (0.25 µg/ml).

Control media **(control)** – Dulbecco's Modified Eagle Medium/Nutrient Mixture F-12 (DMEM/F-12) supplemented with 2% FBS, 1% penicillin/streptomycin (100 units/ml Penicillin and 100 µg/ml Streptomycin), and 0.1% amphotericin B (0.25 µg/ml).

Culturing of Stem Cells and Connexin 43 Selection

Stem cells were harvested from impacted wisdom teeth following IRB approved protocols as previously described (Huang et al., 2009). Cells were cultured with HGCCM and passaged when they reached ~70% confluence. After a stable culture was established (~P3/P4) cells were selected for the neural crest remnant population (labeled NCSC – neural crest stem cells) with the Connexin 43 marker as previously described (Pelaez et al., 2013). Briefly, cells were lifted enzymatically and incubated overnight in 4°C with a primary antibody against human Cx43 (Abcam, Cambridge, MA; #ab11370) diluted 1:100 in 1% FBS-containing HG-DMEM with constant rotation. Following the overnight incubation, cells were centrifuged at 1,000 rpm for 10 min, washed with PBS, centrifuged again, washed again with PBS, centrifuged again, and then marked for magnetic activated sorting with prewashed Dynabeads conjugated to a sheep anti-rabbit IgG secondary antibody (Invitrogen, part of Life Technologies, Grand Island, NY; #112-03D). Following the secondary incubation, the resulting suspension was placed on a magnetic tube rack and allowed to settle, after which the supernate was removed (being careful to not remove any of the cell-bead conjugates that aggregated onto the magnet). The remaining cell-bead conjugates were washed in PBS, aggregated onto the magnet again, (the supernate was

removed again being careful not to remove the cell-bead conjugates aggregated onto the magnet), and the resulting cell-bead conjugates were washed again in PBS, re-suspended with HGCCM and seeded onto T75 culture flasks (now passage 5). Cells were allowed to adhere for 7 days, media was removed, cells were washed several times with PBS to remove any excess magnetic beads, and then fresh HGCCM was added. For every subsequent media change the cells were washed multiple times to remove any excess magnetic beads. Cells were passaged once they reached ~70% confluence. Two passages were necessary to remove all of the beads. Cells passage 7 and 8 were used for all experiments.

Cells were seeded onto different culture plates with different concentrations (depending on the subsequent processing – see "Cell Culture for Different Assays" for details). The following day, HGCCM was removed and the wells were washed once with PBS. NIM was added to each well. Media was changed every 3 days, for a total of 24 days. Several time points were tested – Day 0, Day 3, Day 6, Day 12, and Day 24.

Cell Culture for Different Assays

MicroRNA and Gene Expression – Cells were seeded in T25 flasks at a concentration of 4.5k cells/cm^2.

Immunohistochemistry – Cells were seeded in 24-well culture dishes at a concentration of 4.5k cells/cm^2.

Calcium Imaging – Cells were seeded onto 35mm^2 dishes at a concentration of 45k cells per dish.

MicroRNA Microarray and Data Analysis

The protocol for microRNA microarray analysis has been established previously by our lab (Ng, et al., 2013). Briefly, total RNA, including the miRNA fraction, in Trizol reagent was extracted according to the manufacturer's protocol (Ambion). The RNA concentration and quality were measured using the Nanodrop 2000, whereas RNA integrity was determined using the Agilent 2100 Bioanalyzer. The SurePrint G3 Human v16 miRNA Array Kit (8x60K, Release 16.0; Agilent, Foster City, CA) containing probes for 1205 human and 144 human viral miRNAs from the Sanger miRBase v16.0 was used. GeneSpring GX 11.5 software (Agilent) was used for value extraction. A 2-tailed Student's t-test was then used for the calculation of the *p*-value for each miRNA probe. Significance was defined by the fold change greater than 2 and corrected *p*-value < 0.05. Benjamini-Hochberg false discovery rate was used for the multiple testing correction. Principal component analysis and hierarchical clustering were performed to provide a visual impression of how various sample groups are related. Three samples at Day 0 and 3 neural-induced samples at Day 6 were used in the miRNA microarray experiment.

Downstream mRNA targets of the miRNAs were predicted by TargetScan (http://genes.mit.edu/targetscan/index.html) in the GeneSpring GX 11.5 software (Agilent). Context percentile of 95 was used as the criteria for target prediction. Gene

enrichment and gene ontology analysis was performed by DAVID Bioinformatics Resources 6.7 (http://david.abcc.ncifcrf.gov/) (Dennis et al., 2003). An enrichment score greater than 1.3 was considered significant.

According to a previous report (Wanet et al., 2012), miR-132 and miR-212 are miRNAs that work together and whose expression is necessary for the proper development, maturation and function of neurons. Therefore, these two miRNAs were selected for validation by TaqMan assay. In addition, based on the predicted miRNA target gene associated with neuronal differentiation, *hsa-miR-101* was also selected for validation. Total RNA (20ng) was reverse transcribed using the TaqMan MicroRNA Reverse Transcriptase kit (Applied Biosystems, Forster City, CA). The resultant products were quantified using the appropriate TaqMan MicroRNA Assays (Applied Biosystems, Forster City, CA) on a Stratagene Mx3005P Real-Time PCR Detection System (Stratagene, La Jolla, CA). Results were all normalized to U6 expression. Independent T-test was used for statistical analysis. Three samples of both neural-induced group and control group from each time-point (Day 0, 3, 6, 12 and 24) were used in the validation experiment.

Gene Expression Analysis

To validate the neural induction process on NCSCs, gene expression analysis on neuronal (*TUBB3* and *NFL*), glial (*GFAP*) and stem cell (*KLF4*) markers was performed with specific primers (see Appendix – miRNA Supplementary Table). The predicted miRNA target gene related to neuron differentiation (*GJA1*) was also examined (Santiago

et al., 2010). The gene expression analysis for the predicted miRNA target genes was performed using the Sybr green PCR master mix (Applied Biosystems) on a real-time PCR machine (Stratagene, La Jolla, CA). The housekeeping gene *GAPDH* was used for normalization. The relative expression levels were compared to that of Day 0. RNA samples used in gene expression analysis were the same as those used in miRNA validation experiment.

Statistical Analysis

All statistical analyses, except microarray analysis, were performed by commercially available software (SPSS, version 16.0; SPSS Inc., Chicago, IL). Independent T-test was used to compare the means between samples. Significance was defined as $p < 0.05$.

Immunohistochemistry

Cells were cultured in NIM for the various time points tested (Day 0, 3, 6, 12, 24). Following the differentiation protocol, the cells were gently washed with PBS and fixed with 100% ice-cold methanol for 10 minutes at -20°C to view the intracellular proteins β-tubulin III (TUBB3) and glial fibrillary acidic protein (GFAP). Following fixation, the fixative was removed and fresh PBS was gently added to each well and removed. Due to the extremely sensitive nature of the differentiated cells, the blocking step and primary incubation were done at the same time. The cells were incubated in the following primary antibodies overnight on a bench at room temperature (all in 0.5mg/mL BSA): Ms

monoclonal to TUBB3 (Abcam, Cambridge, MA; 1:100, #ab7751), Rb pAb to GFAP (Abcam, Cambridge, MA; 1:1000, #ab7260). Following overnight incubation, the primary was gently removed, and the following secondaries were added (all at 1:200 dilution in PBS): bovine anti-rabbit FITC (Santa Cruz, Dallas, TX; #sc2365), bovine anti-mouse Rhodamine (Santa Cruz, Dallas, TX; #sc2368) shielded from light, and left incubating for two hours on a bench at room temperature. Following the incubation with the secondary antibody, the secondary was gently removed, and liquid DAPI was added to each well and incubated for 20 minutes at room temperature (5µL/mL of PBS, Life Technologies, Grand Island, NY; #D1306). Following the 20 minute incubation, the cells were gently washed with PBS. The PBS was gently removed and fresh PBS was added to each sample. The samples were shielded from light and taken to image. Immunohistochemical images were acquired using a Nikon Digital Camera DS-Qi1MC mounted to a Nikon Eclipse Ti inverted fluorescent microscope. The NIS Elements software package was used for merging images and image analysis. Control and treated images were processed using the same intensity values in order to maintain consistency throughout the various images and results.

Functional Analysis – Calcium Imaging

Intracellular calcium transient following glutamate stimulation was evaluated using Fluo-4-acetoxymethyl (Fluo-4 AM) ester (Life Technologies, Grand Island, NY) on both control and NIM-treated NCSCs cultured at a confluence of 45k cells/dish. Following culture with NIM or control media, NIM and control media were removed from the treated

and control culture dishes on the time points evaluated (Day 0, 3, 6, 12, and 24). Both treated and control NCSCs were incubated in a Phosphate Buffered Saline (PBS) solution containing 20μM Fluo-4 AM and 0.1% pluronic F-127 (Life Technologies, Grand Island, NY) for 25 minutes at room temperature in the dark. After 25 minutes, the dye solution was removed from all of the dishes. Following dye loading, cells were washed once with PBS and then incubated in PBS for an additional 20 minutes at room temperature in the dark. This washing step allows for full acetoxymethyl (AM) ester cleavage.

Fluorescence videos were captured using a Nikon T2i fluorescent microscope with a 10x objective lens. As the video was recording the cells in the dish, 10μM glutamate was added to each 35mm dish. One culture dish at a time for a total of four cultures dishes per time point were recorded (two control dishes: one with glutamate and one without glutamate; two treated dishes: one with glutamate and one without glutamate). Videos were left recording for one minute after the addition of glutamate to capture any changes in fluorescence intensity. Fluorescence intensity was recorded on a total of eight cells/dish in triplicate experiments for a total of 24 cells for each of the five time points (Day 0, 3, 6, 12, 24) using Nikon Advanced Research Software. Both treated and control cells were compared with and without the addition of glutamate for calcium transient. The relative intensity of fluorescence was calculated as f1-f0 where f1 is the measured intensity and f0 is the baseline intensity of the same cells. This difference in intensity was then corrected for bleaching effects using Microsoft Excel's linear regression analysis.

Results

Neural induction in NCSCs

To evaluate the neural induction process in NCSCs, gene expression of neuronal (*TUBB3* and *NFL*), glial (*GFAP*) and stem cell (*KLF4*) markers was analyzed by quantitative PCR (Figures 8 and 9; * $p<0.05$, ** $p<0.01$, *** $p<0.001$; data presented mean±SD). Compared to the control group, KLF4 was downregulated in the neural-induced group, suggesting that NCSCs are subjected to differentiation. Moreover, upregulated expressions of *TUBB3*, *NFL* and *GFAP* in the neural-induced group along the treatment period further indicated that neuronal differentiation process is taking place in NCSCs.

The microRNA Signatures of Neural-induced NCSCs

To understand the molecular mechanism of neuronal differentiation process in NCSCs, global miRNA expression patterns (miRNome) of neural-induced NCSCs were analyzed by microarray. A total of 143 human miRNAs were differentially expressed at a two-fold difference in treated NCSCs at Day 6 compared to Day 0. The miRNA expression profiles of groups at Day 0 and Day 6 were differentially clustered and separated from each other by either hierarchical clustering (Figure 10a – the list of miRNAs is in Table 8) or principle component analysis (Figure 10b). Compared to the group at Day 0, 79 miRNAs were differentially expressed in the neural-induced group at Day 6 ($p_{corr} < 0.05$ and fold

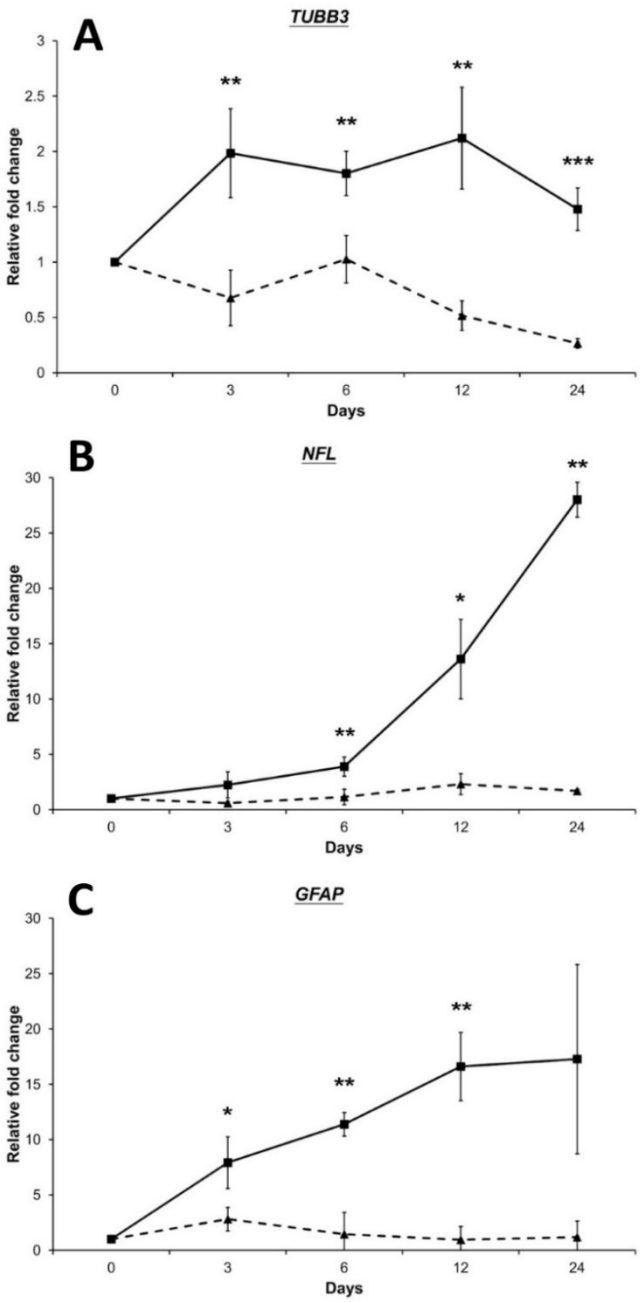

*Figure 8: Genetic Expression for Neural Genes after Neural Induction: Dashed line indicates control, Solid line indicates neural induced NCSC. A) TUBB3 B) NFL C) GFAP * p<0.05, ** p<0.01, *** p<0.001; data presented mean±SD*

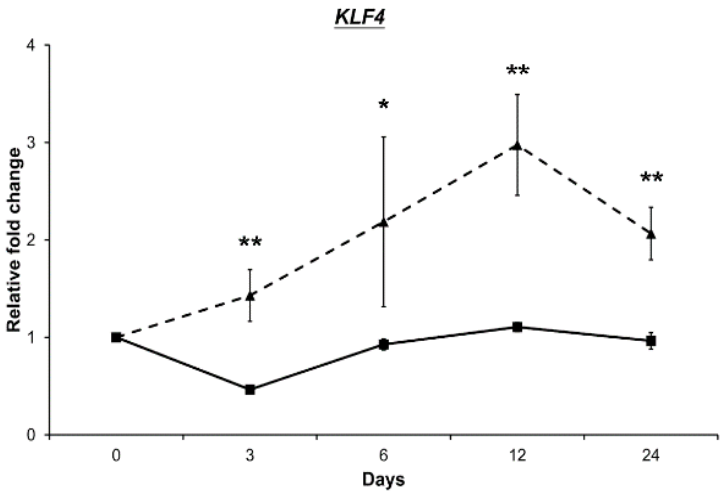

*Figure 9: Genetic Expression for KLF4 following Neural Induction: Dashed line indicates control, Solid line indicates neural induced NCSC. * p<0.05, ** p<0.01, *** p<0.001; data presented mean±SD*

change > 2; Table 8). Sixty of them were upregulated, and 19 of them were downregulated. According to a previous report and the predicted miRNA target gene associated with neuronal differentiation (Wanet et al., 2012; Santiago et al., 2010), three miRNAs (*hsa-miR-132*, *hsa-miR-212* and *hsa-miR-101*) in Table 8 were selected for validation. *hsa-miR-132* and *hsa-miR-212* (Figure 11A and B) were significantly upregulated along the neural induction treatment from Day 3 to Day 24 (Figure 11A and B). In contrast, expression of *hsa-miR-101* (Figure 11C) was significantly upregulated at Day 3 only.

Subsequently, a global target gene list of the neural-induced miRNAs (1939 genes) was generated by the TargetScan in the GeneSpring (Agilent) platform. Gene ontology of this gene list, analyzed by DAVID (1838 DAVID identities), revealed that neural-induced miRNAs might target the genes involved in neuron differentiation, neuron projection, synapse as well as synaptic transmission (Table 9).

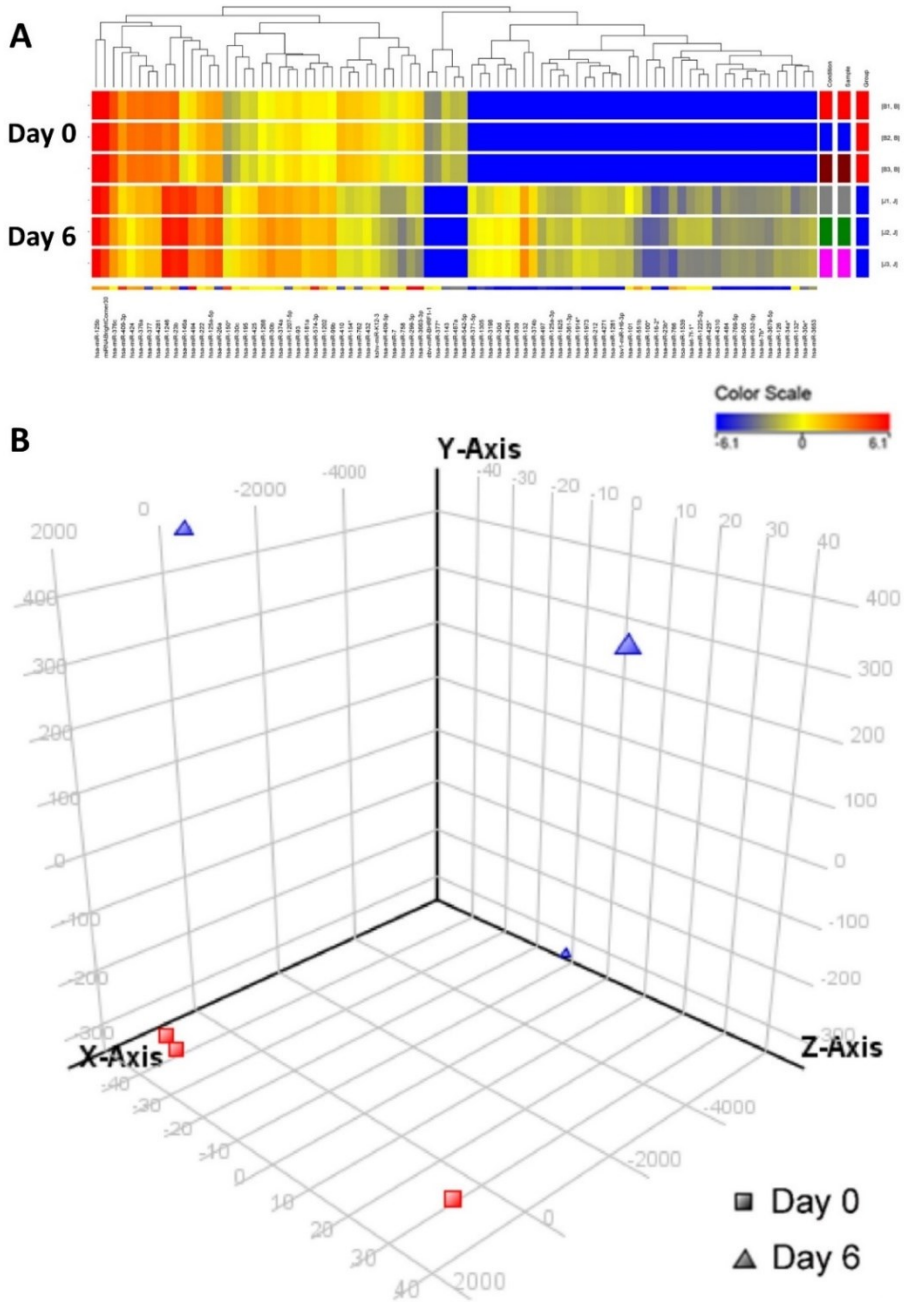

Figure 10: miRNA analysis: Hierarchical Clustering (A) and principal component analysis (B) of Neural Induced NCSC vs control. The list of all of the miRNAs in A may be found below in Table 8.

microRNAs	p_{corr}	Fold change
hsa-miR-132	1.30E-04	+ 696.99
hsa-miR-374b	1.16E-04	+ 272.33
hsa-miR-30d	3.15E-05	+ 181.96
hsa-miR-939	1.95E-04	+ 161.26
hsa-miR-4291	4.87E-05	+ 131.97
hsa-miR-3198	4.04E-04	+ 119.69
hsa-miR-371-5p	3.15E-05	+ 107.59
hsa-miR-1305	6.85E-04	+ 106.90
*hsa-miR-1914**	6.14E-04	+ 78.02
hsa-miR-1973	4.87E-05	+ 71.82
hsa-miR-212	6.10E-05	+ 69.20
hsa-miR-101	5.21E-03	+ 68.66
hsa-miR-4271	3.20E-05	+ 63.33
hsa-miR-125a-3p	2.34E-04	+ 58.78
hsa-miR-1281	3.15E-05	+ 58.44
hsa-miR-361-3p	1.19E-04	+ 50.49
hsa-miR-1825	1.53E-04	+ 49.47
hsa-miR-497	4.04E-04	+ 46.38
hsa-miR-3653	1.40E-03	+ 43.47
*hsa-miR-425**	3.64E-03	+ 40.64
*hsa-miR-34a**	3.15E-05	+ 38.60
*hsa-miR-30e**	1.05E-03	+ 37.21
hsa-miR-1225-3p	3.79E-03	+ 36.70
hsa-miR-146a	2.34E-04	+ 35.23
hsa-miR-126	1.87E-04	+ 35.09
hsa-miR-551b	1.91E-02	+ 34.86
*hsa-let-7f-1**	3.54E-03	+ 33.85
hsa-miR-769-5p	1.15E-04	+ 31.48
hsa-miR-484	3.15E-05	+ 31.46
*hsa-miR-132**	2.76E-03	+ 31.04
hsa-miR-1539	1.25E-02	+ 30.21
hsa-miR-505	1.30E-04	+ 28.43
hsa-miR-532-5p	1.30E-04	+ 28.36
*hsa-let-7b**	3.44E-05	+ 27.13
hsa-miR-3679-5p	9.11E-05	+ 26.78
hsa-miR-766	1.83E-02	+ 24.50
hsa-miR-4310	3.14E-04	+ 22.19
*hsa-miR-100**	8.68E-03	+ 16.75
*hsa-miR-23b**	1.53E-04	+ 16.41
*hsa-miR-16-2**	2.00E-04	+ 12.66
hsa-miR-494	4.96E-02	+ 6.58
hsa-miR-30b	2.81E-03	+ 6.28
hsa-miR-425	2.81E-03	+ 4.20
hsa-miR-1246	7.18E-03	+ 4.07
hsa-miR-1268	2.37E-03	+ 3.90
hsa-miR-30c	2.81E-03	+ 3.77
hsa-miR-26a	5.94E-04	+ 3.68
hsa-miR-99b	4.32E-03	+ 3.29
hsa-miR-195	7.77E-03	+ 3.08

hsa-miR-374a	4.92E-03	+ 2.81
hsa-miR-125a-5p	8.40E-03	+ 2.73
hsa-miR-1207-5p	8.38E-04	+ 2.71
hsa-miR-222	2.37E-03	+ 2.68
*hsa-miR-150**	3.48E-02	+ 2.65
hsa-miR-125b	2.00E-02	+ 2.57
hsa-miR-23b	2.45E-02	+ 2.49
hsa-miR-574-3p	4.05E-02	+ 2.44
hsa-miR-1202	1.93E-02	+ 2.25
hsa-miR-93	6.85E-03	+ 2.10
hsa-miR-181a	1.15E-02	+ 2.04
hsa-miR-143	1.04E-03	- 110.38
hsa-miR-542-5p	1.18E-03	- 88.66
hsa-miR-487a	1.18E-03	- 83.94
*hsa-miR-377**	2.25E-03	- 47.05
hsa-miR-758	4.45E-03	- 7.30
hsa-miR-3663-3p	4.67E-02	- 5.84
hsa-miR-424	1.80E-02	- 5.65
hsa-miR-299-3p	4.49E-02	- 4.70
hsa-miR-410	7.32E-04	- 4.02
hsa-miR-762	9.54E-04	- 3.99
*hsa-miR-154**	7.82E-03	- 3.80
hsa-miR-376a	1.92E-02	- 3.28
hsa-miR-377	6.88E-04	- 3.26
hsa-miR-376c	2.55E-03	- 3.02
hsa-miR-4281	1.64E-02	- 2.77
hsa-miR-7	4.77E-03	- 2.75
hsa-miR-432	8.66E-03	- 2.51
hsa-miR-409-5p	4.67E-02	- 2.35
hsa-miR-409-3p	3.70E-02	- 2.16

Table 8: The differentially expressed microRNAs in NCSC after neural induction

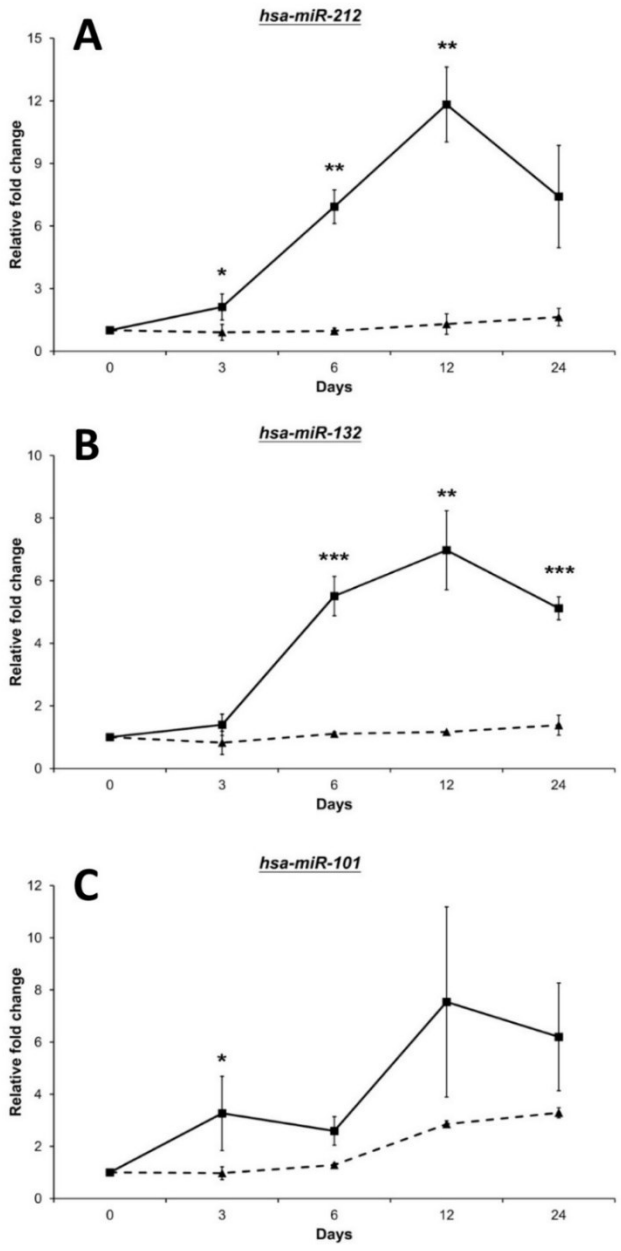

*Figure 11: miRNA validation for Neural Induced NCSC vs control. Dashed line indicates control, Solid line indicates neural induced NCSC. A) miR-212 B) miR-132 C) miR-101. * p<0.05, ** p<0.01, *** p<0.001; data presented mean±SD*

Functional Annotation	Enrichment score	Count	%	*P*
Respiratory system development	6.65	32	1.75	6.80E-08
Neuron projection	2.85	53	2.89	2.33E-04
Cytoskeleton	2.74	158	8.62	2.92E-03
Regulation of cell migration	2.54	31	1.69	1.94E-03
Microtubule cytoskeleton	2.53	79	4.31	7.74E-05
Neural tube development	2.43	15	0.82	8.20E-03
Regulation of apoptosis	2.34	114	6.22	2.70E-04
Blood vessel development	2.15	41	2.24	2.01E-03
JNK cascade	2.15	16	0.87	6.93E-04
Regulation of Ras protein signal transduction	1.82	35	1.91	4.79E-03
Tight junction	1.81	14	0.76	1.56E-02
Visual behavior	1.81	9	0.49	1.10E-02
Apoptosis	1.81	76	4.15	4.23E-02
Tube morphogenesis	1.76	25	1.36	2.26E-03
Embryonic organ development	1.75	29	1.58	9.14E-03
Regulation of synaptic transmission	1.71	24	1.31	1.10E-02
Cell division	1.7	48	2.62	1.46E-03
Gap junction	1.68	16	0.87	2.77E-02
Septin cytoskeleton	1.67	5	0.27	1.97E-02
Response to steroid hormone stimulus	1.6	31	1.69	1.26E-02
Neuron differentiation	1.57	66	3.60	1.38E-03
Synapse	1.53	47	2.57	1.21E-02
Positive regulation of mesenchymal cell proliferation	1.52	7	0.38	5.25E-03
Cell-cell junction organization	1.49	9	0.49	2.27E-02
Regulation of Rho protein signal transduction	1.47	16	0.87	7.93E-02
Cell migration	1.46	40	2.18	2.40E-02
Calmodulin binding	1.43	24	1.31	1.89E-02
Cell cortex	1.43	24	1.31	7.86E-03
Eye development	1.42	24	1.31	7.72E-03
Response to estrogen stimulus	1.34	19	1.04	2.00E-02
MAP kinase kinase kinase activity	1.34	8	0.44	2.18E-03
Adenylate kinase activity	1.31	4	0.22	4.27E-02

Table 9: The gene ontology analysis of the predicted target genes for the microRNAs differentially expressed after neural induction treatment.

Target Gene Analysis of Neural-induced NCSCs

From the predicted target gene list, *GJA1* is the target of *hsa-miR-101* and associated with neuron differentiation (see Appendix – miRNA Supplementary Table). Therefore, it was selected for subsequent gene expression analysis by qPCR. *GJA1* was significantly downregulated in the neural-induced NCSCs at Day 3 only compared to the control group (Figure 12). This suggested that *hsa-miR-101* and *GJA1* could be negatively correlated.

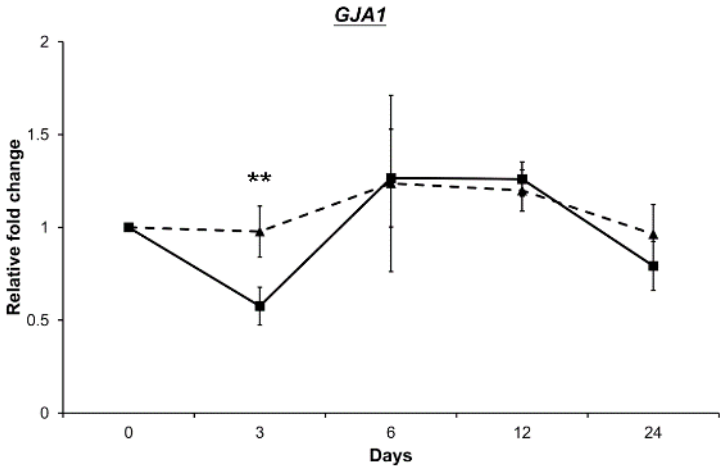

*Figure 12: Gene expression for GJA1 following Neural Induction of NCSC vs control. Dashed line indicates control, Solid line indicates neural induced NCSC. * p<0.05, ** p<0.01, *** p<0.001; data presented mean±SD*

Immunohistochemistry Results

Immunohistochemical images were taken for both β-tubulin III (a neural progenitor marker – Figure 13) and glial fibrillary acidic protein (GFAP – an astrocyte marker – Figure 14) at all of the treatment time points (Day 0, 3, 6, 12, 24). As can be seen in Figure 13 for β-tubulin III, none of the control cells at any time point exhibited this neural progenitor

marker. In the treated cells, expression increased from Day 3 to Day 12, then decreased at Day 24, suggesting that the longer differentiation time point was not advantageous to neural differentiation. Similarly, the immunohistochemical images for GFAP (Figure 14) show the same results. GFAP was not present in any of the control cells from Day 0 to 24. There was, however, an increase in GFAP from Day 3 to Day 12, with a decrease, again, at Day 24 of the presence of GFAP, suggesting that the ideal time for differentiation is somewhere between Days 6 and 12.

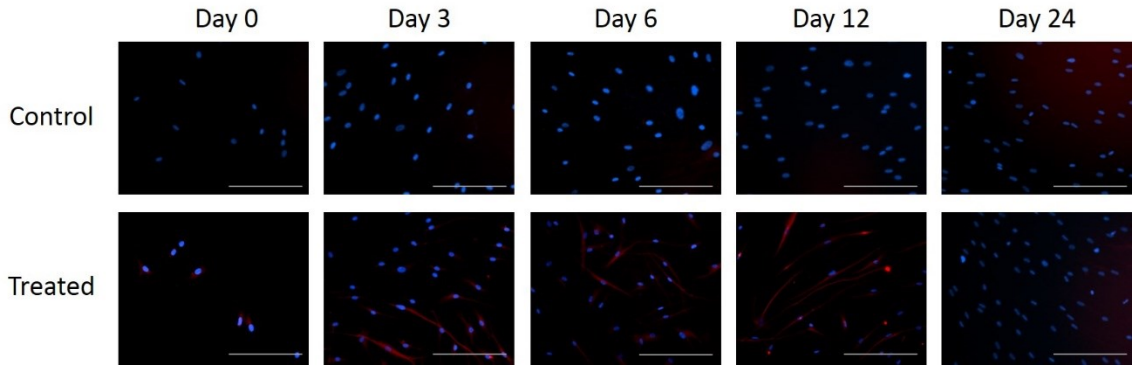

Figure 13: Immunohistochemistry for β-tubulin III for treated NCSC vs. control. Scale bars = 50μm

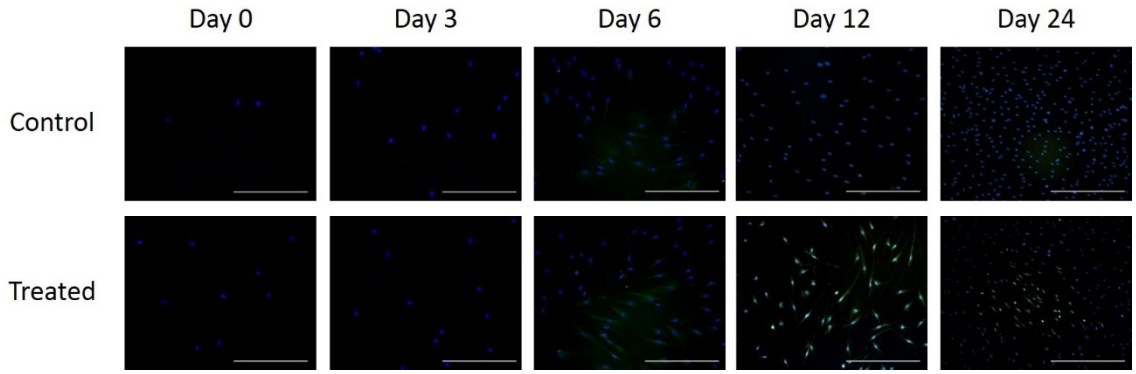

Figure 14: Immunohistochemistry for GFAP for treated NCSC vs. control. Scale bars = 50μm

Functionality of Neural-Induced NCSCs

Fluorescence videos were captured for the control cells and treated cells for five time points (Day 0, 3, 6, 12, 24) with the addition of glutamate. The culture dishes used for the images in Figure 15 were randomly selected out of three repeated trials per time point. Control and treated cell dishes not exposed to glutamate had no change in fluorescence intensity, and were used as a negative control; therefore these images are not included.

Figure 15 shows before and after the addition of glutamate to each cell culture dish. These images were taken as snapshots from fluorescence videos of control and treated cells at each time point showing the functionality of neurons based on the presence of calcium transient. There was no change in fluorescence intensity with the addition of glutamate in the control cells at any time points (Day 0, 3, 6, 12, 24). At Days 0, 3, 12, and 24, the treated cells also did not exhibit any obvious fluorescence changes with the addition of glutamate. However, at Day 6, the treated cells have an observable increase in fluorescence intensity after the addition of glutamate, indicating the neurons are functional at Day 6.

	Control Before	Control After	Treated Before	Treated After
Day 0	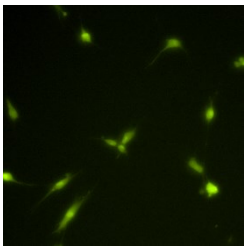	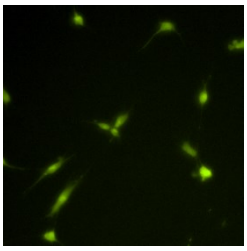	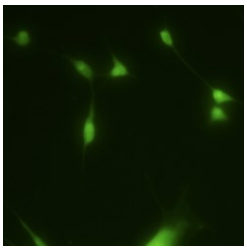	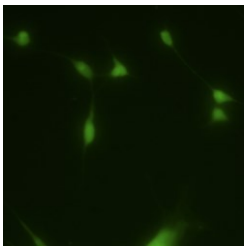

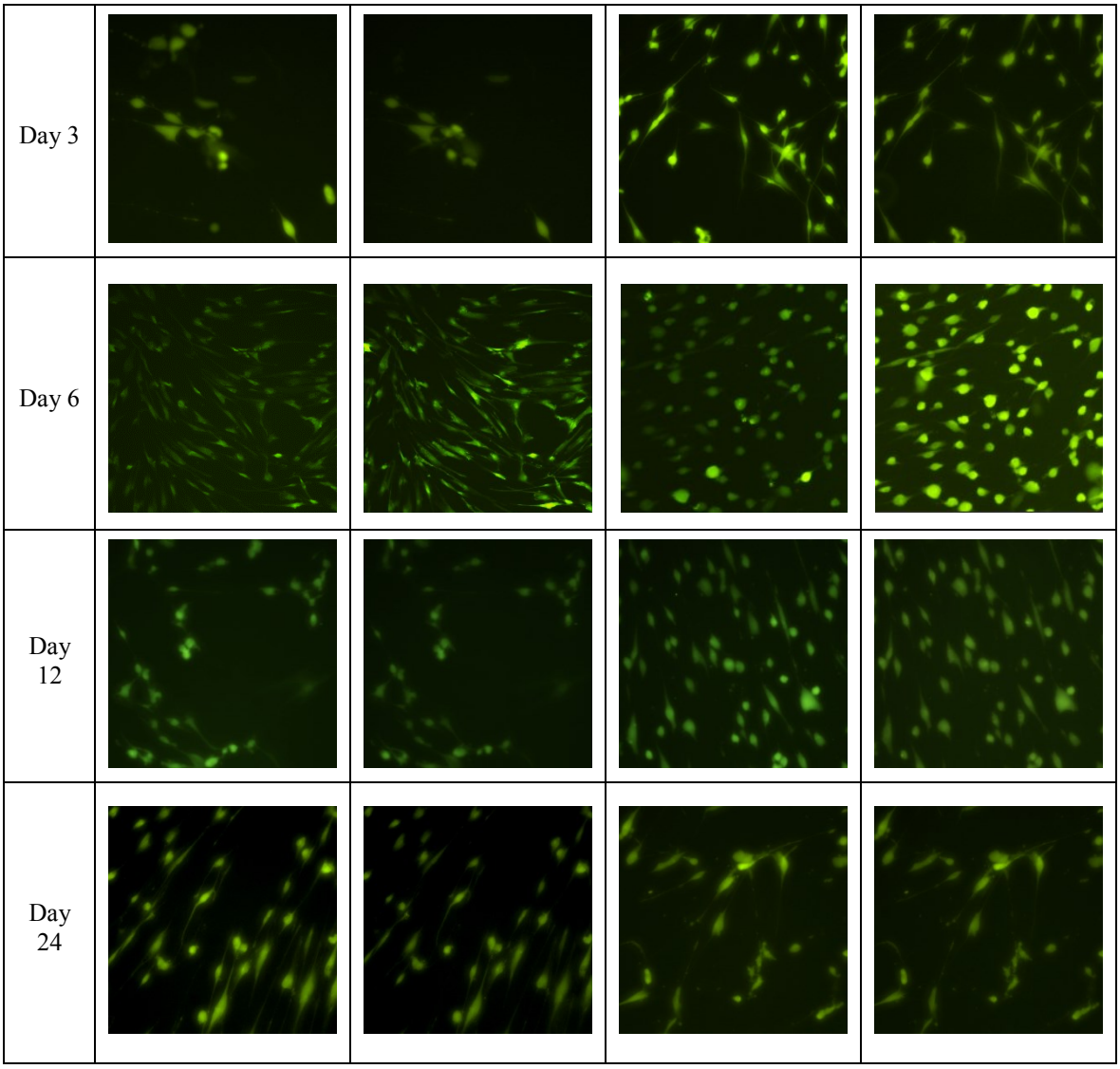

Figure 15: NCSC vs control at all of the time points demonstrating intracelullar calcium transients following glutamate stimulation. All images are snapshots from the calcium videos, taken at 10x magnification to include the largest region of cells.

Discussion

This study, for the first time, reported the miRNA signatures of neural induction in NCSCs. After 6-day neural induction treatment, 79 human miRNAs were differentially

expressed, which 60 of them were upregulated and 19 were downregulated (Table 8). Comparing to a previous miRNA profile of differentiation of MSCs into neuronal cells (Crobu et al., 2012), 2 miRNA (*hsa-miR-23b* and *hsa-miR-143*) were commonly found. Most importantly, the highest upregulated miRNA is *hsa-miR-132*. Together with *hsa-miR-212*, their upregulation in the neural-induced NCSCs verified that our miRNA profile is closely related to the neuronal differentiation processes since miR-132 and miR-212 are tandem miRNAs whose expression is necessary for the proper development, maturation, and function of neurons (Wanet et al., 2012). miR-132 regulates dendritic growth and arborization of newborn neurons in the adult hippocampus (Magill et al., 2010). Moreover, miR-132 also enhances dendritic morphogenesis, spine density, synaptic integration, and survival of newborn olfactory bulb neurons (Pathania et al., 2012). Furthermore, miR-132 is essential for visual cortex plasticity (Mellios et al., 2011). In addition, reduction or loss of miR-132 is associated with Alzheimer's disease and progressive supranuclear palsy (Lau et al., 2013; Smith et al., 2011). However, ectopic expression of miR-132 in ESCs reduced the number of differentiated TH-positive neurons without changing the total number of differentiated neurons (Yang et al., 2012). miR-132 expression has been suggested to be induced by bFGF (Numakawa et al., 2011), indicating that bFGF in the treatment medium might be responsible for the upregulation of miR-132 in the treated NCSCs. For miR-212, it is associated with neuroplasticity (Im et al., 2010). miR-212, together with miR-132, can be induced by brain-derived neurotrophic factor as well as gonadotropin-releasing hormone to generate neurite-like processes (Remenyi et al., 2010; Godoy et al., 2011).

Therefore, the upregulation of miR-132 and miR-212 further confirmed that the induction treatment directs NCSCs towards the neuronal lineage, which matches with the gene ontology analysis of the predicted miRNA target genes (Table 9).

Connexin-43 (*GJA1*) is a negative modulator of neuronal differentiation (Santiago et al,. 2010). In this study, it was found that *GJA1* could be a target gene of *hsa-miR-101* (see Appendix – miRNA Supplementary Table). The gene expression analysis confirms the prediction that *GJA1* downregulation could be correlated with *hsa-miR-101* upregulation (Figures 11C and 12). This correlation was only observed at Day 3, implying that this regulation could be related to the initiation of neuronal differentiation. Therefore, the reduced *GJA1* level, together with upregulation of *hsa-miR-101*, might be a novel mechanism for the initiation of neuronal differentiation in NCSCs. In-depth functional analyses are needed to validate this postulation.

This study revealed the altered miRNA and target gene expressions in NCSCs under neural induction treatment, further providing evidence that miRNAs are a key regulator in the neural fate determination of human adult stem cells. Results from this study provide understanding in the regulatory mechanism of human adult stem cell neuronal differentiation.

It is commonly postulated that longer differentiation times lead to better and more robust neural differentiation. In the immunohistochemical analysis, (Figures 13 and 14) we showed that there was a decrease in expression of the neural progenitor marker β-tubulin III as well as a decrease in GFAP in the longest differentiation time point. It is commonly

known that bFGF, one of the growth factors used in our NIM, maintains cells in a neural progenitor state, preventing full differentiation. Due to this, it is believed that the longer differentiation time would have been benefited by the removal of bFGF and the addition of other neural maturation factors. It would be interesting to see if a multi-step differentiation with modification of the media leads to more robust neural differentiation and maturation of the NCSCs.

It is known that using the calcium imaging method that an increase in fluorescence intensity occurs as a chemical change, or by an exchange of ions induced by the addition of glutamate. This chemical change is found in the NCSCs following neural induction at Day 6 (Figure 15), and not in the control cells at any time point. Functional neurons have this observable change in calcium transient. Treated cells at Day 6 exhibit this neuronal functionality, indicating the success of the differentiation media at this time point above the other time points.

Chapter 11 – Characterization of NCSC-Derived Neural Progenitor Cells

While the initial plan was to determine the expression, production, and secretion of IGF-I from NCSC-derived neural progenitor cells, throughout the experiments it was realized that once the cells were taken out of the induction media and placed in serum-deprived conditions, they reverted back to stem cells and lost all of their neural phenotype and genotype (data not shown). For this reason, prior to transplantation the cells were kept in the neuro-induction media to ensure the transplantation of neural progenitor cells. The expression and production of IGF-I for the NCSC-derived neural progenitor cells, however, were determined. Due to the superiority of the NCSC-derived neural progenitor cells at Day 6 (as seen by the functional studies), 6 days was selected as the ideal treatment length for the NCSCs prior to transplantation.

IGF-I Expression

Gene Expression Methods

Cells were cultured and differentiated as described in Chapter 10. Following the 6-day differentiation protocol (which was found to have the best morphological, immunohistochemical, and physiological responses), the cells were washed with PBS and collected in Trizol (Life Technologies, Grand Island, NY) – two wells were considered one sample. Subsequent RNA extraction was performed using the manufacturers' instructions with the following modifications: centrifugation for phase separation and RNA precipitation was done at 14,000 rpm for 20 minutes. Centrifugation for the RNA wash

was done at 7,500 rpm for 10 minutes. Total RNA yield was determined using the NanoDrop ND-1000 spectrophotometer (Thermo Scientific, Wilmington, DE). Total RNA (1µg) was converted to cDNA using the ABI High Capacity cDNA Reverse Transcription Kit (Applied Biosystems, part of Life Technologies, Grand Island, NY) and the GeneAmp PCR System 9700 (Applied Biosystems, part of Life Technologies, Grand Island, NY). Quantitative PCR (qPCR) was performed using the Stratagene Mx3005P (Agilent Technologies, Santa Clara, CA). The samples were prepared using the Sybr Green PCR master mix (Applied Biosystems, part of Life Technologies, Grand Island, NY), with 20ng cDNA per reaction. The primer sequence for IGF-I was designed based on the corresponding human gene. Forward primer sequence 5'-3': CAATGTTCTAATCACTATGGA. Reverse primer sequence 5'-3': AACCTGTATGTCTGGAAA.

Gene Expression Results and Discussion

Figure 16 shows the gene expression results for IGF-I for the NCSC-derived neural progenitors, compared to the same MSCs that were used in the original study with undifferentiated NCSC. As can be seen in the figure, the NCSC-derived neural progenitor cells express higher levels of IGF-I than the commercially available MSCs. These results are encouraging because it demonstrates that following 6 days of neural-induction treatment the NCSCs still express IGF-I; if differentiation were to happen *in-vivo* therefore,

the cells would still be a suitable IGF-I mini-pump. Although the expression level is not statistically significant to the stringent $p < 0.05$, the data is significant to $p < 0.1$.

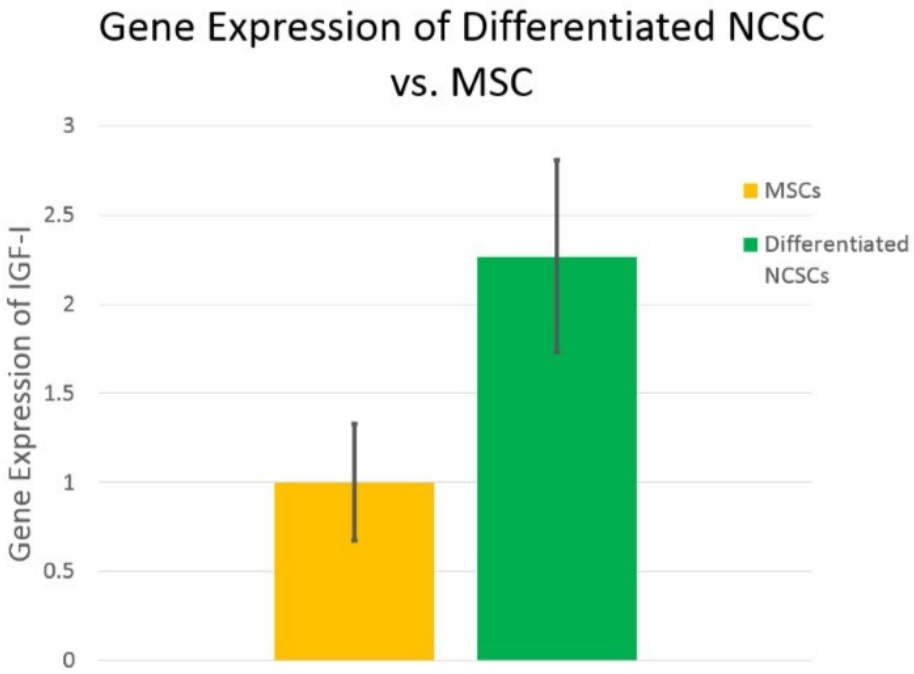

Figure 16: Gene Expression of Differentiated NCSC vs. MSC. Green bar is Differentiated NCSC and the yellow bar is commercially available MSCs. Data is shown as mean±SEM.

IGF-I Production

Immunohistochemistry Methods

Cells were cultured and differentiated as described in Chapter 10. Following the 6-day differentiation protocol (which was found to have the best morphological, immunohistochemical, and physiological responses), the cells were gently washed with PBS and fixed with 100% ice-cold methanol for 10 minutes at -20°C. Following the ice-cold methanol fixation, the methanol was removed and fresh PBS was added to each well

and removed. Due to the extremely sensitive nature of the differentiated cells, the blocking step and primary incubation were done at the same time. The cells were incubated in the IGF-I primary antibody (1:100 dilution in 0.5mg/mL BSA – Rb pAb to IGF-I, Abcam, Cambridge, MA; #ab9572) overnight on a bench at room temperature. Following overnight incubation, the primary was gently removed, and a bovine anti-rabbit FITC secondary was added, (1:200 dilution in PBS, Santa Cruz, Dallas, TX; #sc2365) shielded from light, and left incubating for two hours on a bench at room temperature. Following the incubation with the secondary antibody, the secondary was gently removed, and liquid DAPI was added to each well and incubated for 20 minutes at room temperature (5µL/mL of PBS, Life Technologies, Grand Island, NY; #D1306). Following the 20 minute incubation, the cells were gently washed with PBS. Fresh PBS was added to each sample. The samples were shielded from light and taken to image. Immunohistochemical images were acquired using a Nikon Digital Camera DS-Qi1MC mounted to a Nikon Eclipse Ti inverted fluorescent microscope. The NIS Elements software package was used for merging images and image analysis.

Image Processing

Auto-exposure was used to record all of the images since we did not use a mounting media. Random fields were taken for the IGF-I antibody, using DAPI as a guide to locate a field with a suitable amount of cells. Once the images were taken, the LUTs (look-up-table) were adjusted for DAPI and the green fluorescence of the secondary antibody. For

the DAPI, the left bar was set to the middle of the LUT peak. This was done to remove any background in the image. The right bar, used to increase the intensity, was left alone. For the color corresponding to the secondary, the left bar was set at the middle of the LUT peak. This value was recorded. The right bar was set at the recorded value + 100. Following the image processing, the DAPI and the secondary color images were merged and saved.

Image Analysis and Quantification using ImageJ

ImageJ software was used to determine the number of cells which stained for DAPI and FITC. This number was then compared to produce a percentage of cells that stained positive for IGF-I. A merged picture of DAPI and FITC for each cell line was first uploaded into the program and then underwent a background reduction (rolling ball parameter was set to 50). The color scales of the images were then adjusted using the threshold feature of the system, where the appropriate brightness of an image was qualitatively determined for accurate representation of cell count. DAPI was considered any hue from 120 to 255 while FITC was considered to be any hue from 0 to 120 for all images. The cells were then counted using the analyze particle feature of ImageJ where circularity was from 0.00 to 1.00. Furthermore, the area rejection boundaries for the particles were adjusted as to represent cell count. Finally, the number of cells stained were recorded: holes and cells on the border of the image were excluded by Image J.

Production Results and Discussion

Figure 17 shows the production of IGF-I following the 6 day neuro-induction treatment. In the Figure below, ImageJ was used to quantify the number of cells that stained positive for IGF-I. **A** shows the merged DAPI and FITC image, **B** shows the digitized black and white image of the DAPI, **C** shows the ImageJ generated outlined drawing of the DAPI from the black and white image (used for the count), **D** shows the digitized black and white image of the FITC, and **E** shows the ImageJ generated outlined drawing of the FITC from the black and white image (used for the count).

Figure 17 shows the NCSC-derived neural progenitor cells, which stained 95.2% positive for IGF-I (DAPI count 42, FITC count 40). In Figure 17A, we see the merged FITC and DAPI that seems to be 100% positive staining. A possible explanation for this almost 5% difference is that the ImageJ generated outline of the FITC (Figure 17E) did not take into account cells that were on the edges (in other words, cells that had part of the cell bodies cut off). This can be seen in the red outlined boxes of Figure 17E vs the digitized black and white image seen in Figure 17D. ImageJ did, however, take into account the nucleus of the cut off cells (the DAPI can be seen in the edges of Figure 17C) when it did the count. It is believed that if the edges of Figure 17E would have been taken into account by the ImageJ software, the percentage of cells that stained positive would have been much closer to 100%. By manual counting of the cut off cells in Figure 17D, two cells were cut

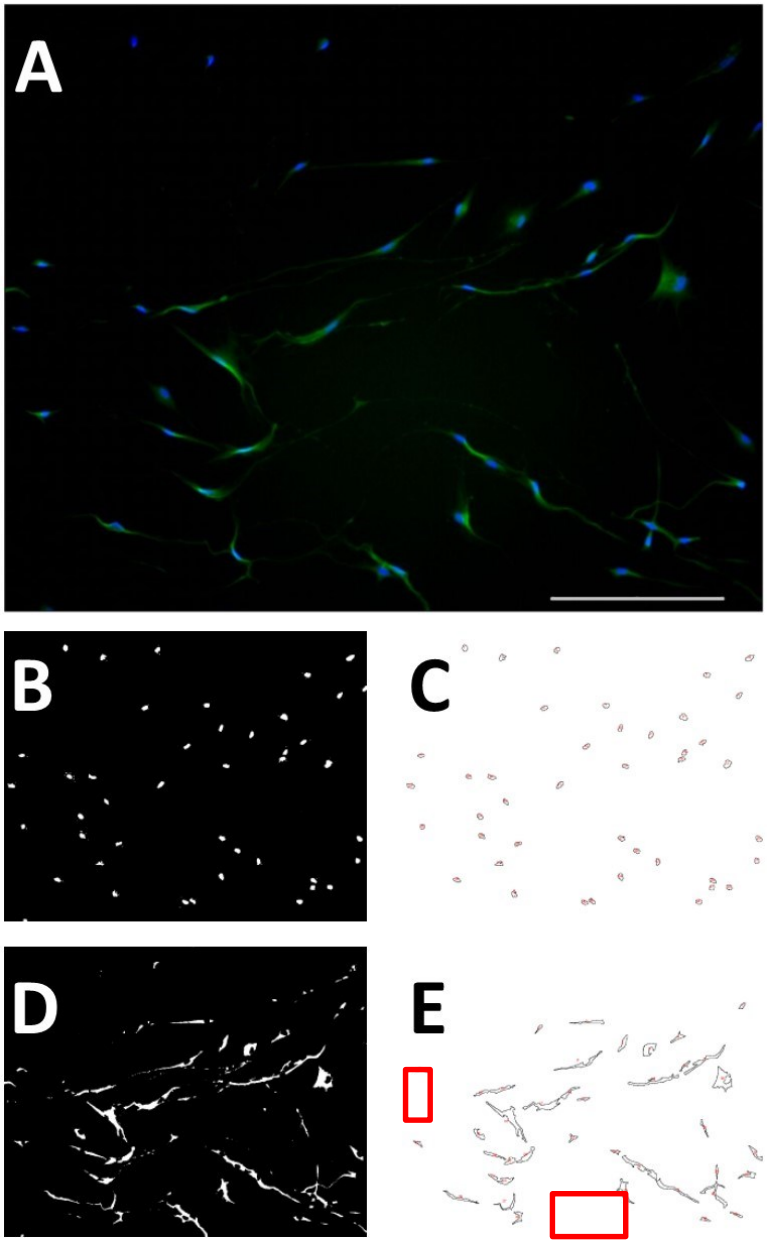

Figure 17: NCSC-derived Neural Progenitor Cells IGF-I Production. A) Merged DAPI and FITC image. Scale bar = 100µm. B) Digitized black and white image of the DAPI. C) ImageJ generated outline of the DAPI for the count. D) Digitized black and white image of the FITC. E) ImageJ generated outline of the FITC for the count.

off from the edges (comparing Figure 17D and 17E), which would bring the count of the FITC to 42, accounting for a new total of 100% of the cells staining positive for IGF-I.

This data is encouraging because it suggests that if the cells were to differentiate *in-vivo*, the NCSC-derived neural progenitor cells would still be a suitable mini-pump for IGF-I.

SECTION 3 – ANIMAL PILOT STUDIES RESULTS

Chapter 12 – Animal Pilot Studies – Feasibility

The animal studies were the necessary next step following the *in-vitro* characterization studies of the NCSC. The objective of Aim 2 was to evaluate the therapeutic potential of NCSC in an animal model of diabetes with associated DPN. To attain the objective of this aim the neuroprotective effects of transplantation of NCSC and NCSC-derived neural progenitor cells on pain evoked behaviors in a diabetic animal with associated DPN were evaluated (Chapter 13). Initially however, it was necessary to determine the feasibility of using human NCSC in the selected animal model (the rat).

Selection of Animal Model

The Sprague Dawley animal model of STZ-induced diabetes has shown reduced gene expression of IGF-I and IGF-II or IGF-IR in the peripheral nerves (Wuarin et al., 1994), the dorsal root ganglia (Craner et al., 2002), and the superior cervical ganglia (Bitar et al., 1997). Several studies have demonstrated the therapeutic potential of IGF-I and IGF-II in this animal model in reducing hyperalgesia (Zhuang et al., 1996; Zhuang et al., 1997), ameliorating impaired nerve regeneration (Ishii and Lupien, 1995), and normalizing neuroaxonal dystrophy (Schmidt et al., 1999). From the preceding citations, it can be seen that the Sprague Dawley animal model is a well-studied and widely used animal model of diabetes. Therefore, this animal model was selected for the *in-vivo* studies and for NCSC transplantation.

Stem cell transplantation into an animal model of diabetes with associated DPN has been studied by Nakamura's group (Shibata et al., 2008; Naruse et al., 2011); in their studies transplanting rat mesenchymal stem cells they also use the Sprague Dawley animal model with STZ-induced diabetes. In the Shibata study, it is interesting to note that the animals were maintained for twelve weeks as diabetic animals with no report of administration of insulin or very high mortality rates. They were able to test for four weeks following transplantation of MSCs (bringing the total time after STZ-induction to 12 weeks) without any report of animals (even saline injected STZ animals) dying mid-experiment. This further strengthened the feasibility of using this animal model for the animal studies.

Evoked pain behaviors are widely studied and well documented in the STZ-induced diabetic rat; pain on pressure, contact discomfort, pin-prick hyperalgesia, heat hyperalgesia, and cold allodynia/hyperalgesia are common tests performed to evaluate effects of treatment for DPN (Dobretsov et al., 2011). Various evoked pain behaviors were tested as assessments of efficacy of NCSC transplantation in alleviating the painful effects of DPN. (Chapter 13)

Feasibility of Using NCSC in Sprague Dawley Rat

Overview of Cell Transplantation

Human adult stem cells were injected into the right thigh of male Sprague Dawley rats, along a peripheral nerve (Shibata et al., 2008). The In-vivo Imaging System (IVIS)

available in the University of Miami Bachelor building was used to image the transplanted cells. In order to prepare the cells for imaging, the cells were transfected with a lenti-mCherry vector (Figure 18 shows the map of the vector).

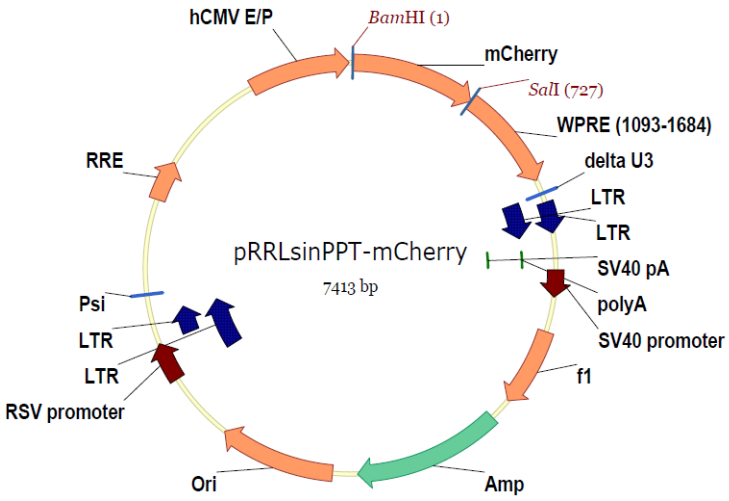

Figure 18: Lenti-map of mCherry vector

Cell Culture and Transfection

Cells were initially cultured in T75 flasks until approximately 70% confluent. Cells were then lifted, counted, and 1uL of the lenti-mCherry vector was added per one million cells. The cells were separated into aliquots of one million, added to several 1.7mL epi tubes, topped off with HGCCM, and incubated for three hours on a rotator at 37°C. Every hour the tubes were gently inverted to ensure that the cells did not form a pellet at the bottom of the tube, which would prevent the vector from reaching all of the cells. After the three hour incubation the cells were combined and then aliquoted into several flasks.

Additional media was added to each flask. Cells were allowed to adhere for two days, after which the media was changed to remove any dead cells. The cells were checked every subsequent day to determine the percentage of transfection and when media was added (approximately every other day – media was never removed after the initial removal of dead cells) more of the lenti-mCherry was added to ensure full transfection. The flasks were rocked gently back and forth every day to ensure that the vector reached all of the cells. Once a minimum of 90% of the cells were transfected, the cells were lifted, counted, separated into aliquots, put on ice, and transplanted into the right thigh muscle of male Sprague Dawley rats. Prior to transplantation, the thighs of the rats were shaved to ensure that there was no auto-fluorescence in the IVIS images. The animals were separated into groups (immunosuppressed and non-immunosuppressed) and the IVIS was used weekly for four weeks to determine the presence of the cells. (Four weeks was selected because it would be the amount of time we would perform behavioral tests on the animals following cell transplants.)

IVIS Image Analysis and Quantification

ImageJ and MATLAB were used to perform semi-quantitative analysis on the qualitative IVIS images in order to determine the percentage of a pre-defined area (maintained consistent in each animal amongst all groups) to demonstrate increased fluorescent intensity vs a threshold baseline of an area that had no cells. Initially, a baseline threshold calculation was performed doing the following: i) the control image (animal with

no cells), was converted to eight bit greyscale in ImageJ; ii) a region of interest (ROI) was designated in the shaved area in ImageJ (this designated ROI was then used in all subsequent images); iii) the average pixel intensity in this area was measured (the results obtained were 28.5, which were rounded up to 29); iv) the obtained value of 29 was used as the baseline threshold in a custom MATLAB code (MATLAB code found in Appendix 2). Additionally, a second, higher threshold of 50 was selected to determine dispersion of the cells in the tissue. (Dispersion would be able to be determined with the intensity being above the first baseline but not the second. Having cells above the second threshold of 50 would demonstrate that the cells were clumped together / located in one area.) Following the threshold baseline calculations, the image analysis was done using the following steps: i) the image of interest was converted to eight bit greyscale in ImageJ; ii) the standardized ROI area was applied onto the shaved patch; iii) a screenshot image of the IVIS image+ROI was taken to include in results below; iv) the raw pixel data was extracted to Excel; v) the pixel intensity data was run through the MATLAB code, yielding the percent of the ROI that was above the baseline threshold intensity and above the second, higher intensity. A standardized ROI was selected because the area that was shaved on each rat was different prior to transplantation and if the entire shaved area was taken into consideration it could potentially cause bias in the data (some shaved areas were much larger than others). A standard ROI, therefore, ensured a level of normalization for the different animals. The original IVIS image, along with the greyscale version with the ROI overlay, is included in the results below. Note: the raw data exported from ImageJ onto Excel which was run in

MATLAB was not included, as the raw data took up 80 pages in Excel for each animal. In the analysis of eight animals, this would have amounted to an additional 640 pages for this Dissertation.

Feasibility Experiment Results and Discussion

As stated above, the animals were separated into two groups – immunosuppressed and non-immunosuppressed. The results obtained indicated that the animals had to be immunosuppressed in order to see any cells, even one week after transplantation. Figures 19-22 show the images of the immunosuppressed rats from one week to four weeks after transplantation. Images of the non-immunosuppressed rats are not included because they had no cells following transplantation. In all of the Figures showing the animals with the IVIS images, **1** shows the original IVIS image with the red fluorescence, and **2** shows the eight bit greyscale image with the standardized ROI overlay.

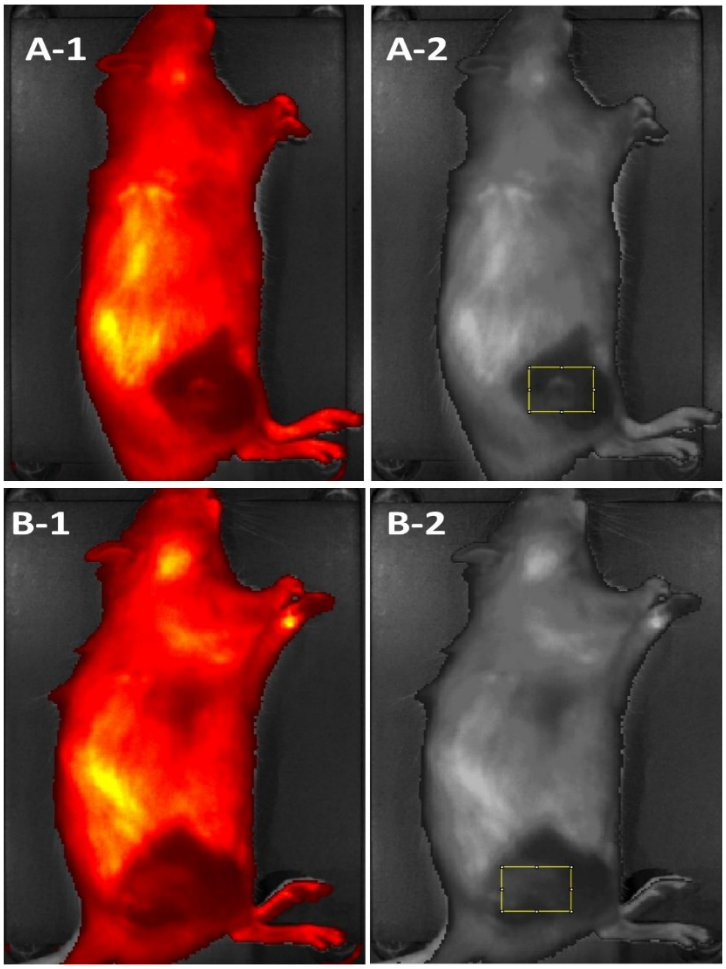

Figure 19: IVIS images showing male Sprague-Dawley rats one week after NCSC transplantation. Animal one) A-1 and A-2; Animal two) B-1 and B-2. 1 shows the original IVIS image, 2 shows the eight bit greyscale image generated with ImageJ with the standardized ROI overlay.

In Figure 19, which shows animals with immunosuppression following one week of transplantation, the values for the animals were as follows: for the first animal, depicted in Figure 19 A-1 and A-2, the percent of the ROI above the baseline threshold intensity was 81.02% and the percent of the ROI above the second, higher threshold was 0.93%. For the second animal, depicted in Figure 19 B-1 and B-2, the percent of the ROI above the

baseline threshold intensity was 97.52% and the percent of the ROI above the second, higher threshold was 7.69%.

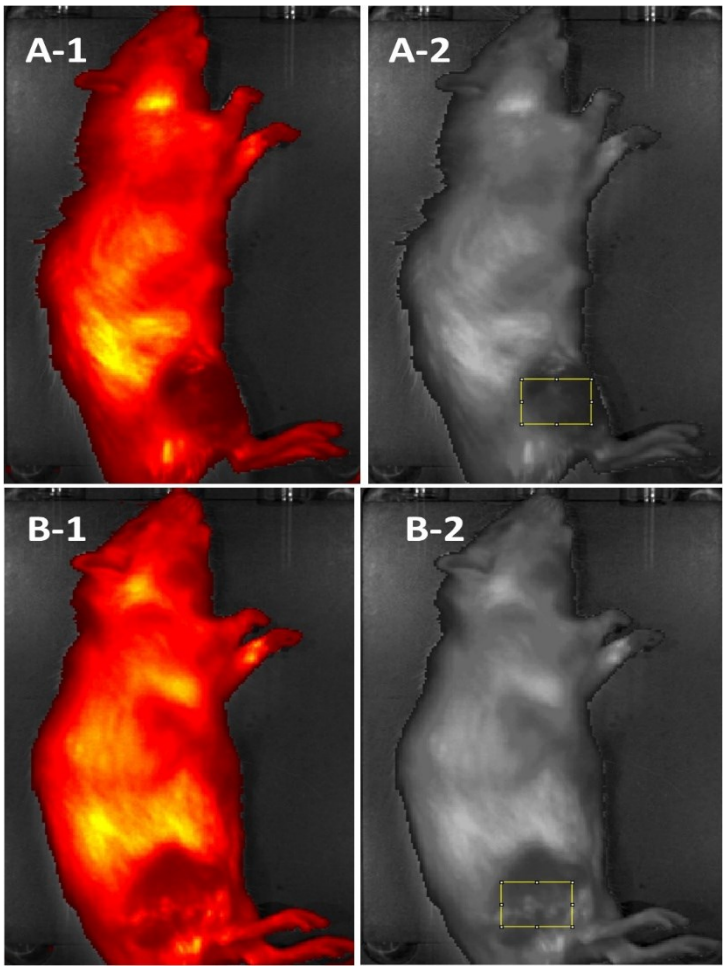

Figure 20: IVIS images showing male Sprague-Dawley rats two weeks after NCSC transplantation. Animal one) A-1 and A-2; Animal two) B-1 and B-2. 1 shows the original IVIS image, 2 shows the eight bit greyscale image generated with ImageJ with the standardized ROI overlay.

In Figure 20, which shows animals with immunosuppression following two weeks of transplantation, the values for the animals were as follows: for the first animal, depicted in Figure 20 A-1 and A-2, the percent of the ROI above the baseline threshold intensity

was 87.50% and the percent of the ROI above the second, higher threshold was 11.81%. For the second animal, depicted in Figure 20 B-1 and B-2, the percent of the ROI above the baseline threshold intensity was 100% and the percent of the ROI above the second, higher threshold was 74.97%. This second value is interesting because it demonstrates that the cells clumped together and now have a higher overall intensity. In this animal, the theory of the cells dispersing did not happen in the second week.

In Figure 21, which shows animals with immunosuppression following three weeks of transplantation, the values for the animals were as follows: for the first animal, depicted in Figure 21 A-1 and A-2, the percent of the ROI above the baseline threshold intensity was 74.81% and the percent of the ROI above the second, higher threshold was 0.45%. The decrease in the amount of cells that pass the first threshold level may indicate the death of some of the cells. For the second animal, depicted in Figure 21 B-1 and B-2, the percent of the ROI above the baseline threshold intensity was 100% and the percent of the ROI above the second, higher threshold was 0.59%. The fact that the first threshold level was 100% and the second was less than 1% indicates that the cells are spread out throughout the tissue.

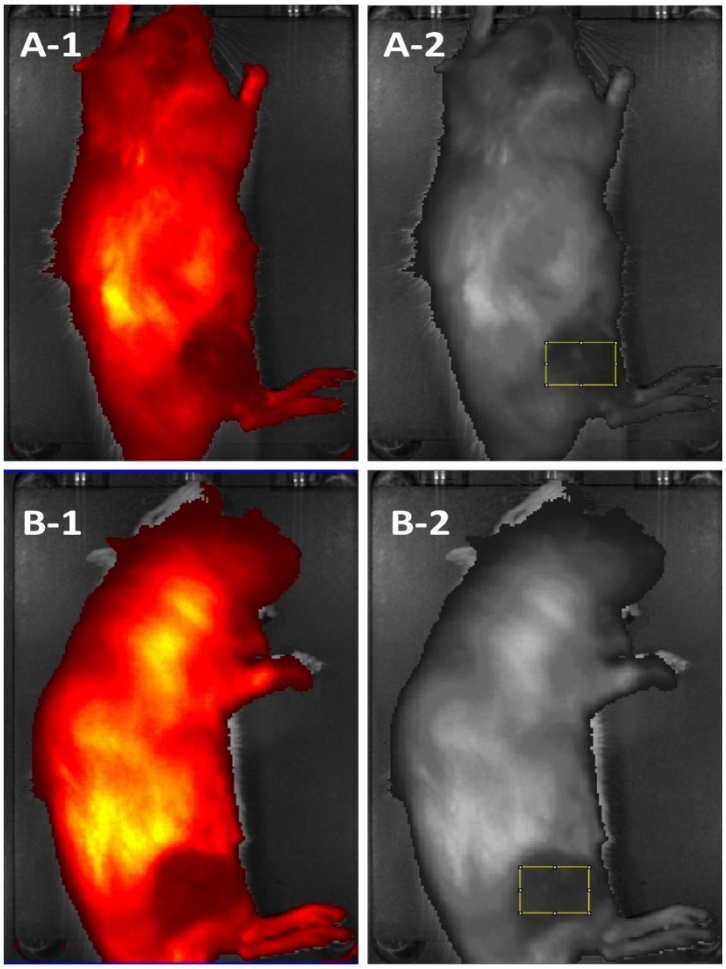

Figure 21: IVIS images showing male Sprague-Dawley rats three weeks after NCSC transplantation. Animal one) A-1 and A-2; Animal two) B-1 and B-2. 1 shows the original IVIS image, 2 shows the eight bit greyscale image generated with ImageJ with the standardized ROI overlay.

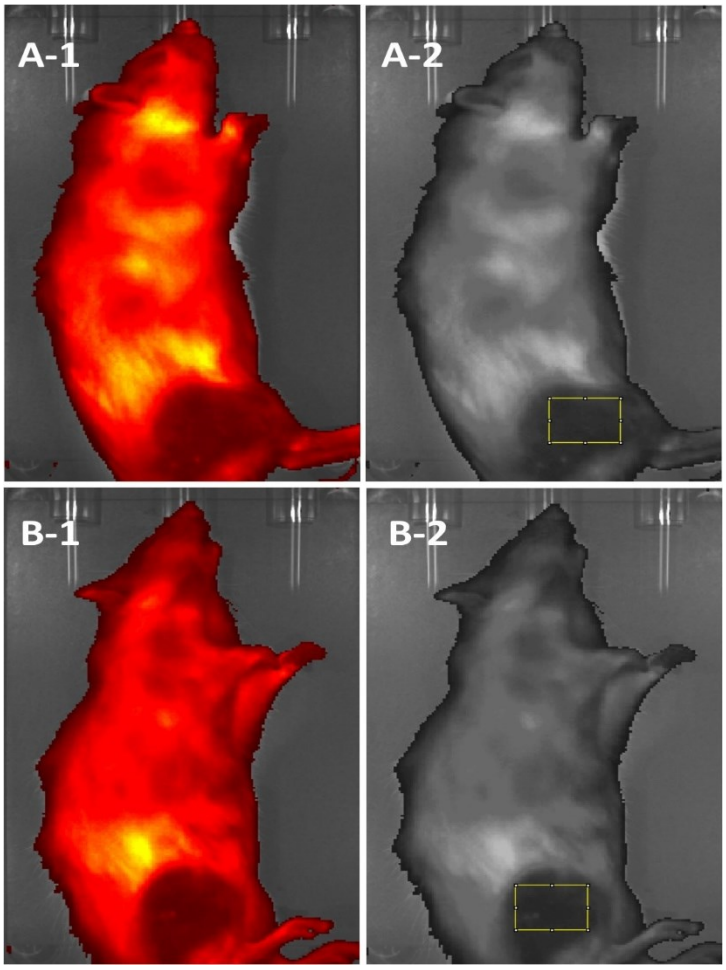

Figure 22: IVIS images showing male Sprague-Dawley rats four weeks after NCSC transplantation. Animal one) A-1 and A-2; Animal two) B-1 and B-2. 1 shows the original IVIS image, 2 shows the eight bit greyscale image generated with ImageJ with the standardized ROI overlay.

In Figure 22, which shows animals with immunosuppression after four weeks of transplantation, the values for the animals were as follows: for the first animal, depicted in Figure 22 A-1 and A-2, the percent of the ROI above the baseline threshold intensity was 100% and the percent of the ROI above the second, higher threshold was 0%. This indicates that the cells were completely spread out throughout the tissue. For the second animal, depicted in Figure 22 B-1 and B-2, the percent of the ROI above the baseline threshold

intensity was 100% and the percent of the ROI above the second, higher threshold was 0.24%. Again, the extremely low values (less than 1%) for the second threshold indicate that the cells have dispersed throughout the tissue.

As was quantified in Figures 19-22, the cells are present in the immunosuppressed rats even several weeks after transplantation. It is, however, difficult to see the cells following the second week due to what seems to be their spreading out in the tissue. This perceived dispersion was also observed in the MATLAB results, where the amount of cells that were above the second intensity threshold decreased after the second week. This suggests that now the cells are not localized in one particular spot but are more spread out (as could be seen with having a large percentage of the cells above the lower baseline threshold). Even accounting for the cell dispersion, these results are encouraging because it demonstrates that human NCSC can survive in the rat after several weeks with immunosuppression. In future studies, it would be interesting to evaluate what effect the cell dispersal has on the NCSC and their ability to be an IGF-I mini pump. If the dispersal of the cells reduces the effect that the NCSC exert on the animals, the cells could be encapsulated to ensure that the cells remain in the desired location.

Chapter 13 – Animal Pilot Studies – Behavioral Studies

Following the successful feasibility studies, the effect of human NCSC and NCSC-derived neural progenitor cells in the male Sprague Dawley diabetic animal model on evoked pain behaviors were determined.

Animal Experimental Protocol

Diabetes Induction and Monitoring

Upon arrival at the Lois Pope Life Center and prior to diabetes induction, baseline behavioral tests (Von Frey, Acetone, and Paw Pressure) were performed on male Sprague Dawley rats (125-150g). Animals considered to be hypersensitive were not included in the studies and/or results, due to potential biasing of the data. After baseline testing, male Sprague Dawley rats (weight between 150-200g) were injected twice, 2-3 days apart, with 65mg/kg STZ. This protocol was previously established by Dr. Stabler's laboratory, and was proven successful in the induction of diabetes in the rat animal model. Animals were fasted overnight prior to the first induction and those with normal glucose levels (below and/or around 100mg/dL) before the second induction were also fasted overnight prior to the second induction. Selection of diabetic animals (those with a glucose level of >350mg/dL after two consecutive measurements on different days) was performed following one week of STZ injection. Animals were allowed to develop diabetes for four weeks. Animal glucose levels were monitored twice weekly for the duration of the experiment. Animals that demonstrated signs of distress (hair raised, brown/dark red

around the eyes, weight loss, and decrease in grooming/activity) were given 2mL of saline intraperitoneally following glucose monitoring. After eight weeks of diabetes induction, all animals were supplemented with 2mL saline intraperitoneally a minimum of three times per week.

Behavioral Testing

Four weeks after the confirmation of diabetes and selection of diabetic animals, the following behavioral tests were performed once a week – Paw Pressure Test (to measure mechanical hyperalgesia), Von Frey Test (to measure tactile allodynia), and Acetone Test (to measure cold allodynia). Each test was performed on a different day to ensure that the animals had time to recover between tests. Each test was performed by the same operator, to ensure consistency in the testing method. Beginning at and including week four and continuing until the 11^{th} week, these tests were performed for the duration of the experiment (t=4-11 weeks inclusive; four time points prior to injection/transplantation and four time points following injection/transplantation).

Paw Pressure Test Procedure

The paw pressure test (using the analgesiometer by UGO Basile, Italy, type 37215) was used to test mechanical hyperalgesia in the male Sprague Dawley rats. Rats were wrapped in a towel and an increasing force (48g/s) was applied to the plantar surface of the hind paw until the rat reacted with either struggle, flight response, and/or vocalization. The test was repeated three times with an interval of approximately 2-3 minutes between each

test. The apparatus terminated at 480g (12 in scale units) in the absence of a response. The test was performed on both the right and left hind paw.

Von Frey Test Procedure

Male Sprague Dawley rats were placed in elevated mesh cages and were allowed to acclimate to their environment for at least ten minutes. Using a series of Von Frey filaments, each with a characteristic weight corresponding to thickness, the rats were tested for tactile allodynia. The first test began at a weight of 4.31g and the filament was gently pressed against the center of the rats' hind foot until bending occurred. The filament was held in this position for four seconds or until the rat withdrew its foot. A withdrawal was considered a positive response and was followed by testing with a thinner filament; conversely, testing with a thicker filament followed a negative response. Left and right feet were tested independently and every rat was given at least 20 seconds before re-testing. Testing was considered complete if any of the following four criteria were met: i) animal had a positive response at the thinnest filament; ii) animal had a negative response for the thickest filament; iii) sixth test had been performed with the first test yielding a positive responsive; iv) the current test was five tests after the first positive response with the first positive response not occurring on the first test. Once testing was completed, the series of positive and negative responses for each foot were plugged into a computer algorithm based on Dixon and Moods "up and down" test (Dixon and Mood, 1948), which produced a relative weighted response value.

Acetone Test Procedure

Male Sprague Dawley rats were placed in elevated mesh cages and were allowed to acclimate to their environment for at least ten minutes. Using room temperature acetone, the animals were tested for cold allodynia. Using a syringe filled with acetone, approximately one drop of acetone was placed in the bottom of the hind paw. Time to wait for a response was five seconds. A positive response was taken to be any of the following: shaking of the paw, moving to the other side of the cage, licking of the paw, startled/anxious behavior. All of the right paws were tested, then followed by the left paws, which concluded one cycle. The cycle was repeated five times. Animals were allowed to completely calm down in between cycles. The number of positive and negative responses and the results were given in terms of positive responses.

NCSC and NCSC-derived Neural Progenitor Cell Transplantation

Following the stem cell dosing calculations and the feasibility studies, it was determined that the most appropriate location for NCSC and NCSC-derived neural progenitor cell transplantation was the thigh muscle, and the animals needed immunosuppression. The immunosuppression regimen can be found in Table 10. The immunosuppression regimen was started one day before cell transplantation and continued until the end of the experiment. Initially, the immunosuppression regimen used was daily injections of Cyclosporin A. However, it was found that to protect the xenogenic tissue a stronger immunosuppression cocktail was required, as following Cyclosporin injection

there were no cells in the animal model (IHC data not shown). In a data club session in the Miami Project another team presented their findings showing the immunosuppression cocktail in Table 10 as being protective of human cells in an animal model. For this reason, the immunosuppression cocktail in Table 10 was selected.

Day of exp.	Week 1	Week 2	Week 3 +
Day -1	Depo 10mg/kg, i.m.	2x Prograf 1mg/kg, s.c.	2x Prograf 1mg/kg, s.c.
		CellCept 30mg/kg, s.c.	
Day 0	TRANSPLANT		
	Depo 1mg/kg, i.m.	Depo 1mg/kg, i.m.	Depo 1mg/kg, i.m.
	2x Prograf 1mg/kg, s.c.	2x Prograf 1mg/kg, s.c.	2x Prograf 1mg/kg, s.c.
	CellCept 30mg/kg, s.c.	CellCept 30mg/kg, s.c.	
Day 1	2x Prograf 1mg/kg, s.c.	2x Prograf 1mg/kg, s.c.	2x Prograf 1mg/kg, s.c.
	CellCept 30mg/kg, s.c.	CellCept 30mg/kg, s.c.	
Day 2	Depo 1mg/kg, i.m.	Depo 1mg/kg, i.m.	Depo 1mg/kg, i.m.
	2x Prograf 1mg/kg, s.c.	2x Prograf 1mg/kg, s.c.	2x Prograf 1mg/kg, s.c.
	CellCept 30mg/kg, s.c.	CellCept 30mg/kg, s.c.	
Day 3	2x Prograf 1mg/kg, s.c.	2x Prograf 1mg/kg, s.c.	2x Prograf 1mg/kg, s.c.
	CellCept 30mg/kg, s.c.	CellCept 30mg/kg, s.c.	
Day 4	2x Prograf 1mg/kg, s.c.	2x Prograf 1mg/kg, s.c.	2x Prograf 1mg/kg, s.c.
	CellCept 30mg/kg, s.c.		
Day 5	Depo 1mg/kg, i.m.	Depo 1mg/kg, i.m.	Depo 1mg/kg, i.m.
	2x Prograf 1mg/kg, s.c.	2x Prograf 1mg/kg, s.c.	2x Prograf 1mg/kg, s.c.
	CellCept 30mg/kg, s.c.		

Table 10: Immunosuppression regimen for Sprague Dawley rats with NCSC and NCSC-derived neural progenitor cells

NCSCs or NCSC-derived neural progenitor cells were transplanted into the right thigh muscle of the male Sprague-Dawley rats eight weeks after diabetes induction. This time point was selected because it is when impairment of nerve conduction becomes difficult to reverse and degenerative nerve changes take place (8 weeks in rats and 5 years in humans) (Oltman et al., 2008; Ziegler et al., 1988). After four weeks of NCSC or NCSC-derived neural progenitor cell transplantation, the animals were euthanized.

For cellular transplantation, the experiment was separated into 4 groups, each group containing animals that underwent STZ injection: i) STZ-induced diabetic rats with saline injections, ii) STZ-induced diabetic rats with NCSC, iii) STZ-induced diabetic rats with NCSC-derived neural progenitor cell transplantation, and iv) STZ-induced diabetic rats with IGF-I injection. The animals in group iv served as the positive control.

Statistical Analysis

The analysis for the behavioral tests were done using a two-way ANOVA with repeated measures, determining the effects of time and treatment within and between each group. In the figures presented below, the statistical significance on the graph denotes significant differences amongst the various treatment groups compared to the saline group. Significant differences within the same group (whether for time or treatment) are discussed in the text and not shown on the graphs to avoid confusion. The table below denotes the significance values seen in the graphs. In all of the behavioral study figures below, the black arrow represents the time of injection.

Significance Values vs. Saline Injections			
	Significance Levels		
Treatment Groups	$p < 0.05$	$p < 0.01$	$p < 0.001$
NCSC - denoted "Stem Cells"	*	**	***
Neural Progenitors	+	++	+++
bolus IGF-I - denoted "IGF-I"	ǂ	ǂǂ	ǂǂǂ

Table 11: Description of significance values for the various treatment groups vs. the saline group shown in the behavioral studies graphs.

Behavioral Studies Results

Paw Pressure Test (Mechanical Hyperalgesia) Results

Figures 23 and 24 show the results for the Paw Pressure tests (Figure 23 shows the left paw results and Figure 24 shows the right paw results) performed on all of the diabetic animals. Note: for the Paw Pressure Test higher values indicate a lower sensitivity level (good) and lower values indicate that the animals have a quicker response to pain (indicating that their threshold for pain is lower – bad). The black arrow represents the time of injection.

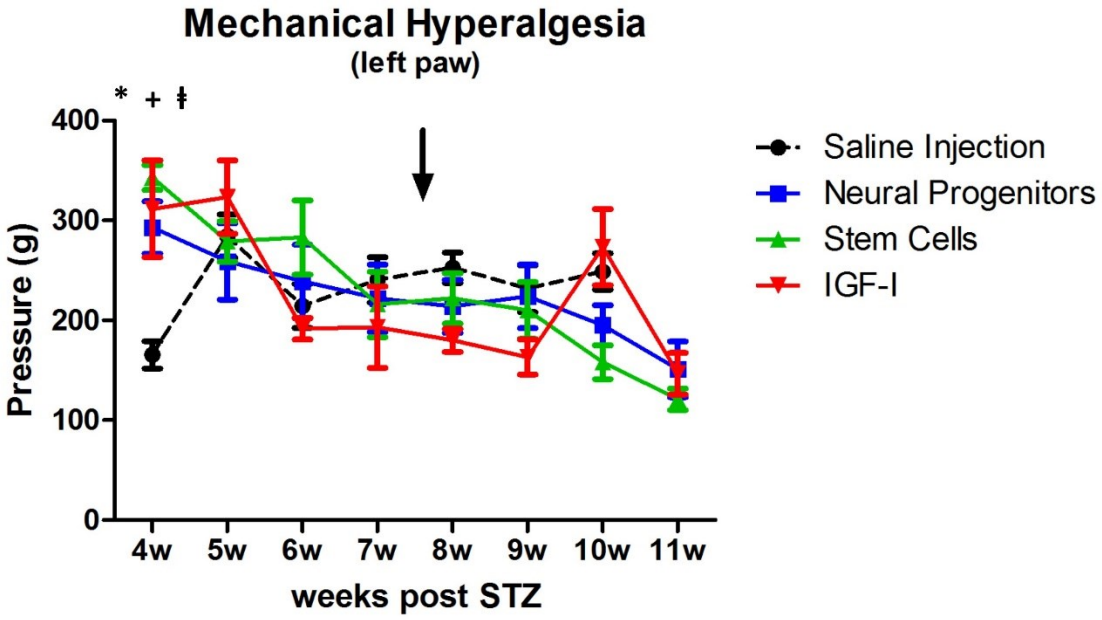

Figure 23: Paw Pressure Test Results for Left Paw. Data presented mean±SEM. Saline Injection n=9; Neural Progenitors n=5, Stem Cells n=5, IGF-I n=3.

The left sides of the diabetic animals received no injection. Therefore, the black arrow, which represents the time of injection, corresponds to the injection in the right thigh. As can be seen in Figure 23, in the first time point (week 4) all of the groups were significantly different from the control group. This difference, however, is not maintained throughout the rest of the testing. Within each group, however, as time progressed, significant differences were observed. For the Neural Progenitor group, the Stem Cell group, and the IGF-I group, the animals got significantly worse as time went on and the testing progressed. This is not surprising, as the left side received no injection/transplantation. Table 12 shows the significant differences within the groups as the testing progressed. Interestingly, for the saline (control) group, the initial testing point was very low and then the values increased, indicating that the animals were not as sensitive to this test as the weeks went on.

Within Group Difference - Paw Pressure Test Left Paw								
		Weeks post STZ						
Treatment Groups		5	6	7	8	9	10	11
Saline	Significant difference to week 4?	Y	N	Y	Y	Y	Y	N/A
NCSC - denoted “Stem Cells”		N	N	Y	Y	Y	Y	N
Neural Progenitors		N	N	N	N	N	Y	N
bolus IGF-I - denoted “IGF-I”		N	Y	Y	Y	Y	N	N

Table 12: Table showing differences within the same group as the testing progressed. Differences shown are for the group as compared to its starting week (week 4). Significant difference denotes $p < 0.05$.

In addition to the significant differences from their starting weeks, several of the groups also had significant differences throughout (in between) weeks, getting worse from one week to the next. This was seen in the Stem Cell group, which had significant

differences between weeks 5 and 11, as well as 6 and 11. The IGF-I group had significant differences between all weeks and week 5, in addition to what was shown in Table 12 above. This indicates that the animals were progressively getting worse from week to week.

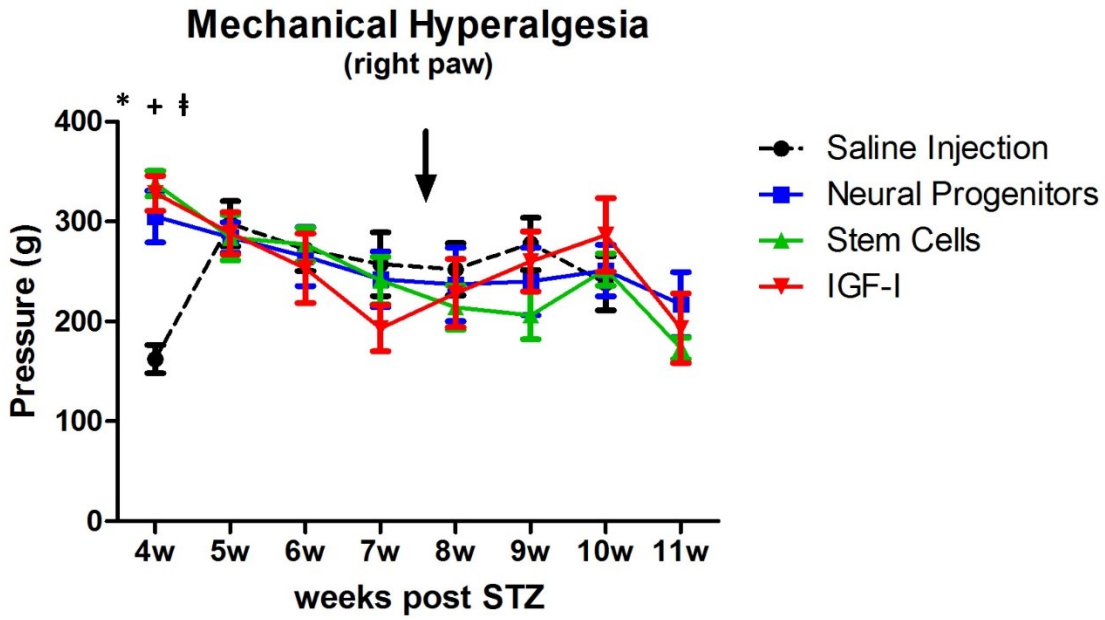

Figure 24: Paw Pressure Test Results for Right Paw. The overall F(Df 3,6) = < 0.001. Data presented mean±SEM. Saline Injection n=9, Neural Progenitors n=5, Stem Cells n=5, IGF-I n=3.

In Figure 24, which shows the Paw Pressure Test results for the right paw (the right side is the one that received the injection/transplantation), there was no significant difference between the treatments compared to the saline injected group, aside from the first time point (week 4), which was before any of the injections took place. Interestingly, however, within each group there are once again significant differences; in particular in the Saline Injection group and the Stem Cell group (Table 13). There was no significant difference, however, between the Neural Progenitor group and the IGF-I group pre and

post injection, unlike in the left paw, where there was significant difference because the animals worsened as time went on. This suggests that the animals that received bolus IGF-I injections as well as the ones that received the neural progenitor cells remained stable as time progressed. This data suggests that the neural progenitor cell transplant provided some level of protection for the animals.

Within Group Difference – Paw Pressure Test Right Paw								
		Weeks post STZ						
Treatment Groups		5	6	7	8	9	10	11
Saline	Significant difference to week 4?	Y	Y	Y	Y	Y	Y	N/A
NCSC - denoted "Stem Cells"		N	N	Y	Y	Y	Y	N
Neural Progenitors		N	N	N	N	N	N	N
bolus IGF-I - denoted "IGF-I"		N	N	Y	N	N	N	N

Table 13: Table showing differences within the same group as the testing progressed. Differences shown are for the group as compared to its starting week (week 4). Significant difference denotes $p < 0.05$.

Von Frey Test (Tactile Allodynia) Results

Figures 25 and 26 show the results for the Von Frey tests performed on all of the diabetic animals (Figure 25 shows the left paw results and Figure 26 shows the right paw results). Note: for the Von Frey Test higher values indicate that the non-noxious stimuli does not provoke a response (good) and lower values indicate that the animals have a strong response to a non-noxious stimuli (bad). The black arrow represents the time of injection. Although the statistical analysis was able to be performed on the data obtained for the Von Frey Test, the data failed the Shapiro-Wilk test for normality. It is believed that this was due to the extremely low sample size, as well as the large amount of variability that was seen with this test.

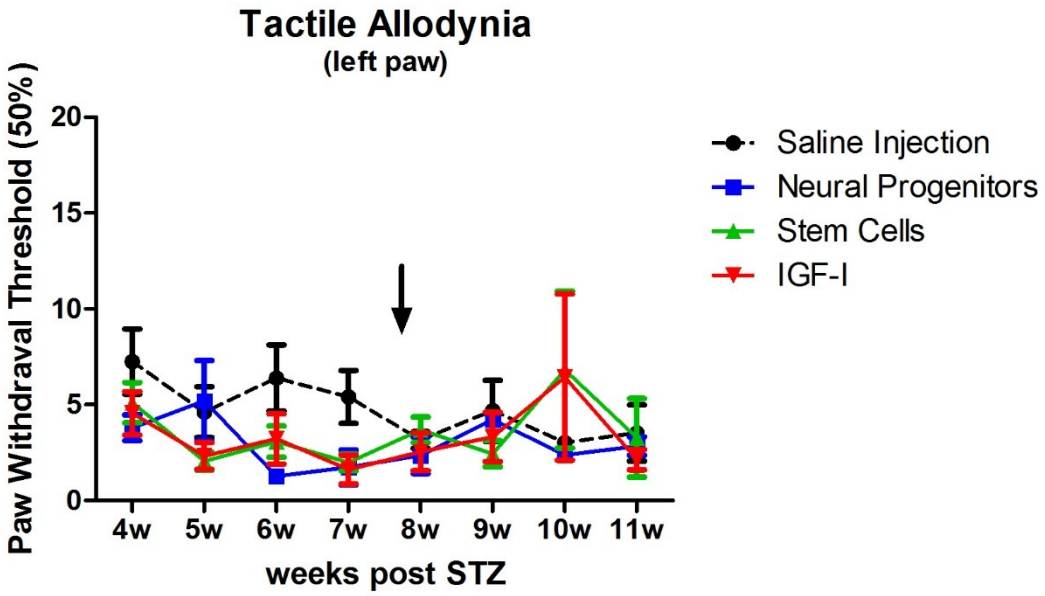

Figure 25: Von Frey Test Results for the Left Paw. Overall F(Df 3,7) = 0.449. Data presented mean±SEM. Saline Injection n=9, Neural Progenitors n=2, Stem Cells n=3, IGF-I n=3.

The left sides of the diabetic animals received no injection. Therefore, the black arrow shown in Figure 25, which represents the time of injection, corresponds to the injection in the right thigh. There was no significant difference seen between the treatment and the saline for the left paw (which is not surprising because the left side receives no injection) and there was also no difference seen within the groups in any of the time points (Table 14).

Within Group Difference – Von Frey Test Left Paw								
		Weeks post STZ						
Treatment Groups		5	6	7	8	9	10	11
Saline	Significant difference to week 4?	N	N	N	N	N	N	N
NCSC - denoted "Stem Cells"		N	N	N	N	N	N	N
Neural Progenitors		N	N	N	N	N	N	N
bolus IGF-I - denoted "IGF-I"		N	N	N	N	N	N	N

Table 14: Table showing differences within the same group as the testing progressed. Differences shown are for the group as compared to its starting week (week 4). Significant difference denotes $p < 0.05$.

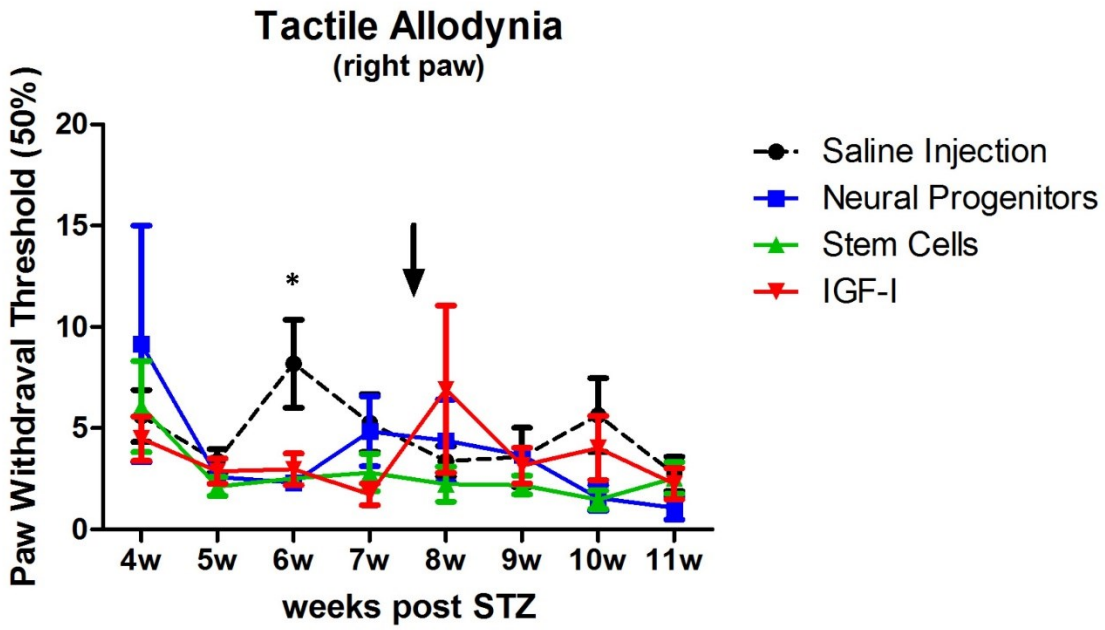

Figure 26: Von Frey Test Results for the Right Paw. Overall F(Df 3,7) = 0.347. Data presented mean±SEM. Saline Injection n=9, Neural Progenitors n=2, Stem Cells n=5, IGF-I n=3.

In Figure 26, which shows the Von Frey Test results for the right paw (the right side is the one that received the injection/transplantation), there was no significant difference between the treatments compared to the Saline Injection group, aside from the third time point (week 6), which was before any of the injections took place. Additionally,

there were no differences between any of the treatment groups pre and post injection (Table 15). While this would suggest that there was some level of protection provided by the injection/transplant, as there was no significant difference seen in the left paw of the saline injected animals within their groups (Table 14), or for the right paws of the saline injected animals within their groups (Table 15), the injection/transplant cannot be credited for the animals remaining stable as the testing progressed.

Within Group Difference – Von Frey Test Right Paw								
		Weeks post STZ						
Treatment Groups		5	6	7	8	9	10	11
Saline	Significant difference to week 4?	N	N	N	N	N	N	N
NCSC - denoted "Stem Cells"		N	N	N	N	N	N	N
Neural Progenitors		N	N	N	N	N	N	N
bolus IGF-I - denoted "IGF-I"		N	N	N	N	N	N	N

Table 15: Table showing differences within the same group as the testing progressed. Differences shown are for the group as compared to its starting week (week 4). Significant difference denotes $p < 0.05$.

While there was no significant difference within the groups as compared to the first time point (week 4), the saline group did have a significant difference between weeks 5 and 6, 5 and 8, and 5 and 11.

As stated above, the results for the Von Frey Test failed the Shapiro-Wilk test for normality. Due to the low amount of samples for this test, analysis of this data would need a larger sample size to provide a robust analysis. This sample size was small due to the number of animals that had to be excluded due to the hypersensitive baseline results.

Acetone Test (Cold Allodynia) Results

Figures 27 and 28 show the results for the Acetone tests performed on all of the diabetic animals (Figure 27 shows the left paw results and Figure 28 shows the right paw results). Note: for the Acetone Test, a higher value indicates that the animal is more sensitive to the room temperature acetone (bad), while the lower values indicate that they are less responsive to this non-noxious stimuli (good). The black arrow represents the time of injection.

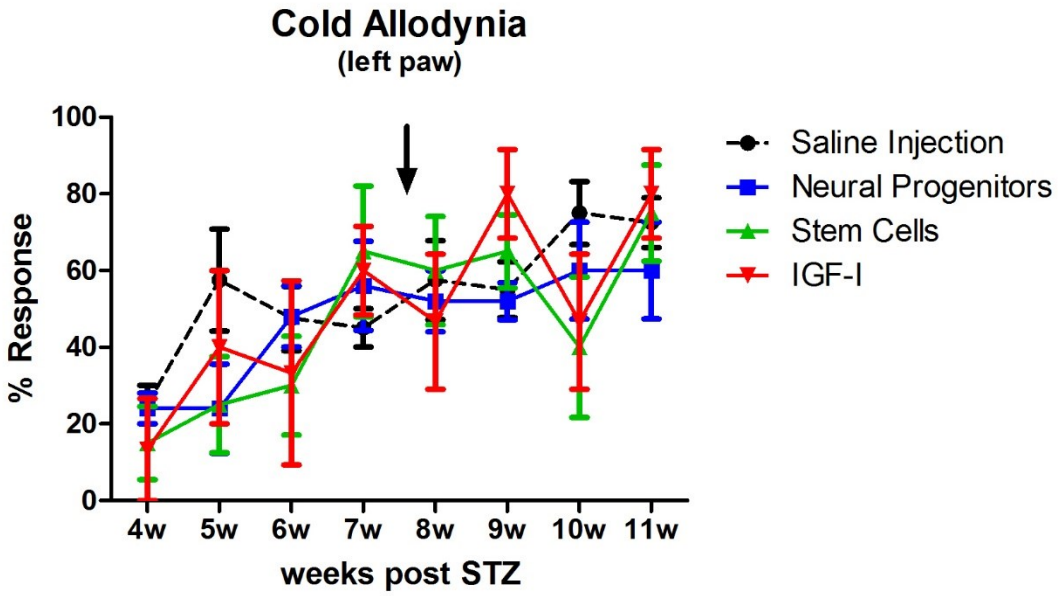

Figure 27: Acetone Test Results for the Left Paw. Overall F(Df 3,7) = 0.194. Data presented mean±SEM. Saline Injection n=8, Neural Progenitors n=5, Stem Cells n=4, IGF-I n=3.

The left sides of the diabetic animals received no injection. Therefore, the black arrow, which represents the time of injection, corresponds to the injection in the right thigh. As can be seen in Figure 27, there was no significant difference seen between the treatment

and the saline for the left paw (which is not surprising because the left side received no injection). Within each group, however, as time progressed, significant differences were observed. These differences were seen in the Saline Injection group, the Stem Cell group, and the IGF-I group, where the animals got significantly worse as time went on and the testing progressed. Table 16 shows the significant differences within the groups as the testing progressed.

Within Group Difference – Acetone Test Left Paw								
		Weeks post STZ						
Treatment Groups		5	6	7	8	9	10	11
Saline	Significant difference to week 4?	N	N	N	N	N	Y	Y
NCSC - denoted "Stem Cells"		N	N	Y	N	Y	N	Y
Neural Progenitors		N	N	N	N	N	N	N
bolus IGF-I - denoted "IGF-I"		N	N	N	N	Y	N	Y

Table 16: Table showing differences within the same group as the testing progressed. Differences shown are for the group as compared to its starting week (week 4). Significant difference denotes $p < 0.05$.

In addition to the significant differences from their starting weeks, the Stem Cell group also had significant differences between weeks 5 and 11.

Figure 28 shows the results for the Acetone Test for the right paw. There are significant differences between the Saline Injection group and the IGF-I group the week after the bolus injection of IGF-I. Additionally, there was a significant difference between the Stem Cell group and the Saline Injection group three weeks post injection, as well as the IGF-I group and the Saline Injection group also three weeks post injection. This suggests that the stem cell injection had a positive effect on the acetone response of the

animals. Additionally, there were significant changes in the Saline Injection group throughout the time points tested, in particular, after the saline injection at the fifth time

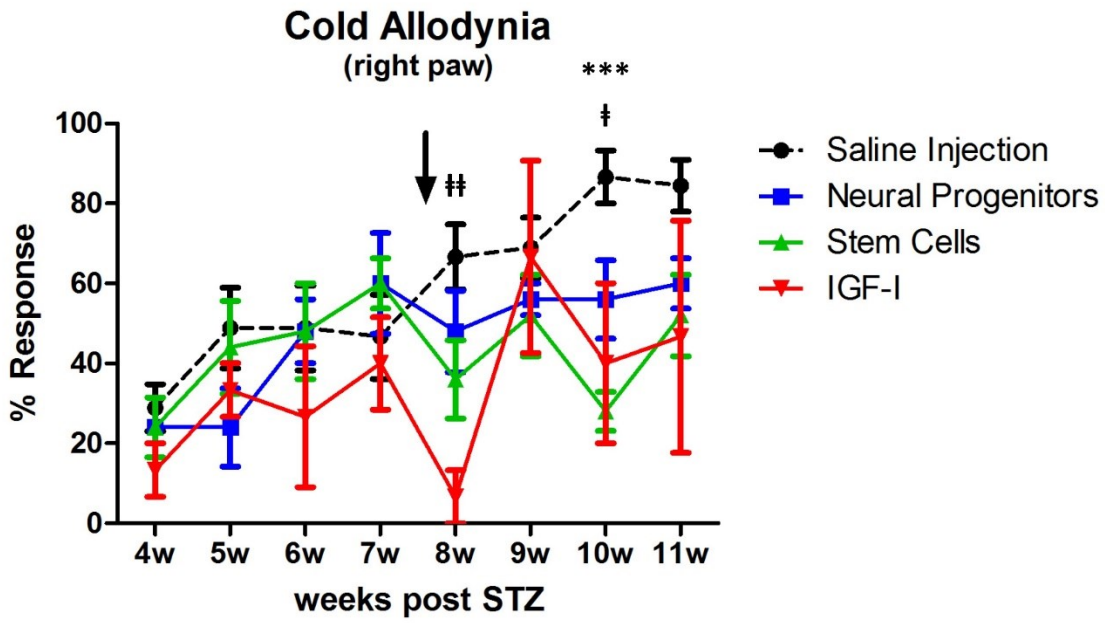

Figure 28: Acetone Test Results for the Right Paw. Overall F(Df 3,7) = 0.058. Data presented mean±SEM. Saline Injection n=9, Neural Progenitors n=5, Stem Cells n=5, IGF-I n=3.

point, indicating that the animals were getting worse as time progressed. In contrast, there were no significant changes in any of the treatment groups, suggesting that the injections/transplants provided a level of protection for the animals from getting significantly worse as time progressed (Table 17).

Within Group Difference – Acetone Test Right Paw								
		Weeks post STZ						
Treatment Groups		5	6	7	8	9	10	11
Saline	Significant difference to week 4?	N	N	N	Y	Y	Y	Y
NCSC - denoted "Stem Cells"		N	N	N	N	N	N	N
Neural Progenitors		N	N	N	N	N	N	N
bolus IGF-I - denoted "IGF-I"		N	N	N	N	N	N	N

Table 17: Table showing differences within the same group as the testing progressed. Differences shown are for the group as compared to its starting week (week 4). Significant difference denotes $p < 0.05$.

In addition to the significant differences in the Saline Injection group in comparison to its starting week, there were also significant differences between the following weeks: 5 and 10, 5 and 11, 6 and 10, 6 and 11, 7 and 10, and 7 and 11. These significant differences indicated that the animals were in fact getting worse as time progressed. This also further indicates the protective effect that the stem cell and neural progenitor cell transplantation had on the animals' ability to remain stable as time progressed.

Behavioral Studies Discussion

The behavioral studies, while being a pilot study, gave some interesting results. Due to the small sample size and variability of the data in the Von Frey Test, significant differences were not observed in any of the treatments. In the Paw Pressure Test, although there was no restoring of the response, in the Neural Progenitor group some protection was seen post injection in that the animals remained stable throughout the testing and did not get significantly worse as time progressed. This same phenomena was observed in the IGF-I group. This was in contrast to the Saline Injection group, which got significantly worse from week to week. In the Acetone Test, although there was no restoration of the response

(which could have been observed if there was a significant difference in the positive direction as compared to the Saline Injection group), there was some level of protection observed post injection in the Neural Progenitor group, the Stem Cell group, and the IGF-I group. The animals in all three groups remained stable throughout the various time points; this was in contrast to the Saline Injection group, which got significantly worse as time progressed.

While these results are encouraging, the sample size needs to be greatly increased in order to reduce the variability and add robustness to the data analysis.

Chapter 14 –Discussion and Future Work

This Doctoral work evaluated the potential of using human NCSC in an animal model of diabetes with associated DPN. Although some discussion was given in their respective sections (when the data was initially presented), the following presents an overall conclusion of this Doctoral work, along with future studies.

In-Vitro Work

The *in-vitro* experiments done through this Doctoral work demonstrated that purified periodontal ligament stem cells (known as NCSC throughout the text), express, produce, and secrete quantifiable levels of IGF-I, a growth factor known for its anti-apoptotic and neuroprotective properties. While IGF-I has shown to be a potent mediator of the reduction of DPN in animal studies (Liu et al,. 1993; Gualco et al., 2009), there are several other neurotrophic factors that would be of interest to study. Continuing work will be on expanding the studies into other growth factors in addition to IGF-I for DPN. There are several other neurotrophic factors (as stated in Chapter 7) that are neuroprotective, and it would be of interest to see the effects that these other neurotrophic factors have on DPN. Additionally, it would be interesting to see if there are combinatory effects of IGF-I plus other neurotrophic factors or if they are antagonistic to each other. In the *in-vitro* area, this can be done by using a rat primary nerve culture and adding different combinations of growth factors and evaluating their neuroprotective effects.

For further study on the effect of IGF-I on the rat peripheral nerve, a co-culture experiment of human NCSC on rat nerves can be done as was discussed in Chapter 9. This could potentially elucidate the effect of human NCSC on the rat peripheral nerves, and take into account how human IGF-I interacts with the rat nerve. Genetic expression for apoptotic genes, such as the caspase family, as well as staining for mitotic activity will provide information as to the effects of the NCSC on the rat nerve prior to transplantation. Although the data from the secretion studies was used to determine amount of cells for transplantation, the abovementioned co-culture studies will help in optimizing the amount of cells that should be transplanted in the animal model of diabetes with associated DPN.

This Doctoral work focused on using NCSC from established cell lines in Dr. Cheung's laboratory. In translating this work to clinical trials, autologous vs allogeneic transplantation of NCSC will have to be taken into consideration. In order to begin to evaluate these differences, a sub-project evaluating the neuroprotective potential of stem cells from diabetic patients will be established. NCSC may be obtained from diabetic patients and evaluated for their expression, production, and secretion of IGF-I and other neurotrophic factors compared to non-diabetic NCSC. These differences will be very important to establish the potential use of autologous stem cell transplants for diabetic patients.

Work was presented here on the miRNA profile of NCSC-derived neural progenitor cells. Although not a part of the DPN study, a potential avenue for future research is the

study of the upregulated miRNA on the differentiation of NCSC into neural progenitor cells. Over-expression and inhibition of the miRNA that were differentially upregulated would help to better understand the mechanisms of NCSC differentiation.

The neuro-induction protocol performed on the NCSC prior to transplantation was a single step induction protocol. As was demonstrated in Chapter 10, six days of differentiation was selected as the optimal time point for differentiation prior to transplantation. One of the ways that differentiation prior to transplantation could be improved is to focus the differentiation to create more sensory neurons and not a mixed population of neural cells. Different chemical cocktails could be employed, in the same method that was used to optimize the current differentiation protocol, and use the one that produces the highest amount of sensory neurons. This could be done using either a single step or a multi-step protocol.

With the optimization of the neuro-induction protocol, reversal of the differentiation of the NCSC was seen after 12 days. A possible reason for this is that the single-step protocol, while allowing the NCSC to go to a neural progenitor lineage, did not allow full maturation of the neural progenitor cells. This may be due to the bFGF in the induction media, known to maintain neural cells in a neural progenitor state. A multi-step protocol may be needed to ensure full maturation of the neural progenitor cells. Another potential reason for the decrease/decline of the neural markers observed in Figures 14 and 15 could be that while many of the NCSC differentiated within the first six to twelve days,

there were NCSC that did not differentiate. The NCSC that did not differentiate continued to be mitotically active, while the cells that were differentiating decreased their mitotic activity. The non-differentiated NCSC, therefore, could have potentially overrun the culture by day 24. This could be determined using a BrdU assay in future studies. Another, technically related reason for the decrease/decline of the differentiated cells in the immunohistochemistry images seen in Figures 14 and 15, could be that as the neural cells became more mature, they were more sensitive to the processing performed during the immunohistochemistry preparation and were washed/removed during preparation. This could account for the differences between the increased gene expression of TUBB3 and GFAP and the decreased IHC presence of TUBB3 and GFAP. If this is the case, further optimization of the IHC procedures would be necessary to ensure that the more mature NCSC-derived neural cells remain intact during IHC preparation.

During the differentiation protocol, it was noticed that the NCSC had to be maintained in the differentiation media up until transplantation, otherwise they would revert back to NCSC. Although not studied in this Doctoral work, it would be interesting to determine the effects of the muscular microenvironment on the differentiated NCSC. Would this microenvironment contribute to the maturation of the NCSC-derived neural progenitor cells? Would the cells, now that they are not in the differentiation media, revert back to their stem-like state? Based on the studies presented in Chapter 9 (Stem Cell

Characterization for Animal Studies), even if the NCSC were to de-differentiate in the muscular environment the NCSC would still be able to secrete quantifiable levels of IGF-I.

Pilot Animal Studies

The focus of this Doctoral work was to establish this animal model in our hands, determine the possibility of transplanting human NCSC into a rat (which is known to be highly xenogenic), and run pilot behavioral studies on the cellular transplantations.

Cellular transplantation was performed eight weeks following diabetes induction, where it was believed that impairment of nerve conduction becomes difficult to reverse and degenerative nerve changes take place (8 weeks in rats and 5 years in humans) (Oltman et al., 2008; Ziegler et al., 1988). In doing so, the neuro-regenerative potential of these cells was being tested. However, the studies brought up an interesting question: could potentially the eight week waiting time be too long, ie – translated to human/clinical studies this would indicate that the majority of the peripheral nerves would be destroyed – indicating a high level of DPN. In human studies, stem cells would ideally be transplanted in the early stages of DPN to create a microenvironment that *prevents* further degeneration and protects the existing neurons. For this reason, continuing work will be to assess the effects of transplantation earlier in the diabetic induction process, to determine whether or not cellular transplantation can prevent the increased responsiveness of the animals to the various behavioral tests.

NCSC and NCSC-derived neural progenitor cell transplantation was seen to provide some level of protection from further degeneration for the Acetone Test, which tests cold allodynia. Additionally, while the effect was not significant, it appears to be that NCSC-derived neural progenitor cell transplantation also provided some protection from sensitization in the Paw Pressure test. The Von Frey test demonstrated no significant or transient improvements in the animals tested. A potential reason for the cells not having significant effects as compared to the Saline Injection group could be the death/dispersal of the cells in the thigh muscle. As was noted in the IVIS images in Chapter 12, following two weeks after cellular transplantation it seemed to be that the cells were dispersing/diffusing from the initial injection site. This could potentially have an impact on the cells' ability to act as an IGF-I pump.

Additionally, it seems that in order to have a more potent effect on the animals the cell number transplanted would need to increase. A potential avenue for future studies is having different groups of animals with different numbers of cells transplanted and determining which cell number produces the best effect. Another potential action to improve the efficacy of the transplanted cells would be to inject cells more frequently (ie weekly or every two weeks). This could be combined with the study above as another way to optimize the cell transplants.

Behavioral studies, although known to be one of the standards for animal testing, are subjective tests. It is impossible to determine with 100% accuracy if the movement of

the animals indicates pain/discomfort based on the stimulus that is applied, or if the movement was for other another reason. There are several objective measurements that can be performed once cellular transplantation occurs to further validate the effectiveness of transplantation. These objective measurements will constitute the starting point of the independent research following this Doctoral work. One of the questions that may be answered with objective measurements is whether or not the transplantation of human NCSC into a rat model of diabetes with associated DPN increases the systemic IGF-I levels in the rat. This may be determined by evaluating the gene expression of the injection sites for IGF-I and measuring the quantitative levels of IGF-I in the blood serum of the animals. The IGF-I quantification may be done for both human and rat IGF-I in order to determine if the increase in IGF-I is due to the production/secretion of IGF-I from the human NCSC or if NCSC transplantation induces the rat to increase its own production of IGF-I. Additionally, a quantitative test that can be performed on the animals is motor nerve conduction velocity. Although the exact methodology of this test is presently unknown and has not been performed/learned throughout this project, it is part of the continuing and future work on NCSC transplantation into the Sprague Dawley rat model with diabetes and associated DPN.

The behavioral tests performed in this Doctoral work assessed the increased tactile allodynia (Von Frey Test), mechanical hyperalgesia (Paw Pressure Test), and cold allodynia (Acetone Test). While all of these tests determine the response to pain-evoked behaviors, as was discussed in Chapter 3, the result of DPN is not always an increase in

the pain response. Depending on the sensory nerve fibers that are affected, (for example, the large diameter sensory nerves) DPN may cause a *decrease* in the pain response, where diabetic patients *lose* responsiveness to different stimuli. This, in fact, is the most common cause for foot amputations amongst diabetic patients. While evoked pain behaviors were studied in this Doctoral work, another avenue for future research would be to evaluate the effects of DPN on hypoalgesia, and the restorative/regenerative effect of NCSC transplantation on preventing the loss of sensation. Weak responses were observed with the transplantation of NCSC and NCSC-derived neural progenitor cells in all of the behavioral studies performed. Several potential reasons for this exist. i) The total amount of cells transplanted was not enough to produce the desired effect. This may be due, in part, to the numbers calculated consisting of both IGF-I and IGFBP-3. It is possible that in the case of the NCSC, the IGFBP-3 was still bound to the IGF-I *in-vivo*, decreasing the amount of IGF-I available for therapeutic use. ii) The cells diffusing/spreading out in the tissue, thus affecting their ability to act as an IGF-I mini-pump. This could be tested by creating a small scaffold/encapsulating the cells so that they remain together and transplanting them into the rat and observing the differences compared to what was established in this work. iii) Some cells may be dying, decreasing the total amount of cells and the amount of IGF-I available. Although the immunosuppression regimen that was employed in the animal studies was tested by another group (Chapter 13), it is possible that there were still cells that were dying in the rat as the weeks progressed. Additionally, the dying cells could have been secreting apoptotic factors, further decreasing the other cells' effectiveness as a

treatment. iv) The cells were secreting "competing" factors. In the overall characterization of the NCSC, it was found that our cells express and secrete other factors in addition to IGF-I (data not shown – part of continuing work). While some of these factors could act in conjunction with IGF-I to produce anti-nociceptive effects, some factors may produce nociceptive effects. As stated in the discussion above, the effect of various factors on the rat peripheral nerves will be evaluated as part of a sub-project in future studies. v) Undifferentiated NCSC are differentiating *in-vivo* into unwanted cell types, thus reducing their effectiveness in the animals. It was noticed in both the Acetone Test and the Paw Pressure Test that the transplantation of the neural progenitor cells, while not producing a significant effect, did prevent the cells from becoming significantly worse throughout the various time points tested. In order to have a positive effect, it may be necessary to always pre-commit the NCSC prior to transplantation.

One of the items that will need to be addressed in the future, as the studies move from animals to humans, is the ideal injection/transplant site. While DPN is a widespread disease that targets all of the peripheral nerves in people with diabetes, the present work was done only in the thigh muscle of the rats for ease of testing and injection (the amount of cells that had to be transplanted could not be injected into the spinal cord but could be easily injected into the rat thigh muscle). Ideally, the site of injection in the human would be the spinal cord, in the dorsal root ganglia. As these animal studies progress and the amount of cells necessary to produce the desired effect is optimized, it will be clearer as to the exact number of cells necessary for transplantation and whether or not, once translated

to human trials, could be injected into the desired location (whether the spinal cord or another location). This would allow for customizable treatments that could be based on patients' needs.

This Doctoral work, although in the beginning stages of finding a DPN specific treatment, has yielded some interesting results and definitely many avenues for future research and continuing work. The questions raised throughout optimization of protocols and techniques will be the starting point for continuing independent work in the search for a viable treatment for patients suffering from diabetes and associated painful DPN.

References

Abe S, Hamada K, Miura M, Yamaguchi S. Neural crest stem cell property of apical pulp cells derived from human developing tooth. Cell Biol Int. 2012;36(10):927-36. doi: 10.1042/CBI20110506. PubMed PMID: 22731688.

Akiyama K, Chen C, Gronthos S, Shi S. Lineage differentiation of mesenchymal stem cells from dental pulp, apical papilla, and periodontal ligament. Methods Mol Biol. 2012;887:111-21. doi: 10.1007/978-1-61779-860-3_11. PubMed PMID: 22566051.

Anlar B, Sullivan KA, Feldman EL. Insulin-like growth factor-I and central nervous system development. Horm Metab Res. 1999;31(2-3):120-5. doi: 10.1055/s-2007-978708. PubMed PMID: 10226791.

Apfel SC. Introduction to diabetic neuropathy. Am J Med. 1999;107(2B):1S

Apfel SC. Neurotrophic factors in peripheral neuropathies: therapeutic implications. Brain Pathol. 1999;9(2):393-413. PubMed PMID: 10219753.

Baron R. Mechanisms of disease: neuropathic pain--a clinical perspective. Nat Clin Pract Neurol. 2006;2(2):95-106. doi: 10.1038/ncpneuro0113. PubMed PMID: 16932531.

Baron R, Binder A, Wasner G. Neuropathic pain: diagnosis, pathophysiological mechanisms, and treatment. Lancet Neurol. 2010;9(8):807-19. doi: 10.1016/S1474-4422(10)70143-5. PubMed PMID: 20650402.

Bitar MS, Pilcher CW, Khan I, Waldbillig RJ. Diabetes-induced suppression of IGF-1 and its receptor mRNA levels in rat superior cervical ganglia. Diabetes Res Clin Pract. 1997;38(2):73-80. PubMed PMID: 9483370.

Boyle J, Eriksson ME, Gribble L, Gouni R, Johnsen S, Coppini DV, et al. Randomized, placebo-controlled comparison of amitriptyline, duloxetine, and pregabalin in patients with chronic diabetic peripheral neuropathic pain: impact on pain, polysomnographic sleep, daytime functioning, and quality of life. Diabetes Care. 2012;35(12):2451-8. doi: 10.2337/dc12-0656. PubMed PMID: 22991449; PubMed Central PMCID: PMCPMC3507552.

Bueno C, Ramirez C, Rodríguez-Lozano FJ, Tabarés-Seisdedos R, Rodenas M, Moraleda JM, et al. Human adult periodontal ligament-derived cells integrate and differentiate after implantation into the adult mammalian brain. Cell Transplant. 2013;22(11):2017-28. doi: 10.3727/096368912X657305. PubMed PMID: 23043788.

Campbell CM, Kipnes MS, Stouch BC, Brady KL, Kelly M, Schmidt WK, et al. Randomized control trial of topical clonidine for treatment of painful diabetic neuropathy. Pain. 2012;153(9):1815-23. doi: 10.1016/j.pain.2012.04.014. PubMed PMID: 22683276; PubMed Central PMCID: PMCPMC3413770.

Cardozo AJ, Gómez DE, Argibay PF. Neurogenic differentiation of human adipose-derived stem cells: relevance of different signaling molecules, transcription factors, and key marker genes. Gene. 2012;511(2):427-36. doi: 10.1016/j.gene.2012.09.038. PubMed PMID: 23000064.

Chen CY, Liu YJ, Shi SG, Chen FM, Cai C, Li B, et al. Osteogenic differentiation of human periodontal ligament stem cells expressing lentiviral NEL-like protein 1. Int J Mol Med. 2012;30(4):863-9. doi: 10.3892/ijmm.2012.1053. PubMed PMID: 22767336.

Cheng Z, Zheng Q, Wang W, Guo X, Wu Y, Zheng J. Targeted induction of differentiation of human bone mesenchymal stem cells into neuron-like cells. J Huazhong Univ Sci Technolog Med Sci. 2009;29(3):296-9. doi: 10.1007/s11596-009-0306-y. PubMed PMID: 19513609.

Cheung HS, Pelaez D, Huang CY. Isolation and use of pluripotent stem cell population from adult neural crest-derived tissues. WO2013131012 (**2013**).

Chu Q, Moreland R, Yew NS, Foley J, Ziegler R, Scheule RK. Systemic Insulin-like growth factor-1 reverses hypoalgesia and improves mobility in a mouse model of diabetic peripheral neuropathy. Mol Ther. 2008;16(8):1400-8. doi: 10.1038/mt.2008.115. PubMed PMID: 18545223.

Coull JA, Boudreau D, Bachand K, Prescott SA, Nault F, Sík A, et al. Trans-synaptic shift in anion gradient in spinal lamina I neurons as a mechanism of neuropathic pain. Nature. 2003;424(6951):938-42. doi: 10.1038/nature01868. PubMed PMID: 12931188.

Coura GS, Garcez RC, de Aguiar CB, Alvarez-Silva M, Magini RS, Trentin AG. Human periodontal ligament: a niche of neural crest stem cells. J Periodontal Res. 2008;43(5):531-6. doi: 10.1111/j.1600-0765.2007.01065.x. PubMed PMID: 18624954.

Cova L, Armentero MT, Zennaro E, Calzarossa C, Bossolasco P, Busca G, et al. Multiple neurogenic and neurorescue effects of human mesenchymal stem cell after transplantation in an experimental model of Parkinson's disease. Brain Res. 2010;1311:12-27. doi: 10.1016/j.brainres.2009.11.041. PubMed PMID: 19945443.

Craner MJ, Klein JP, Black JA, Waxman SG. Preferential expression of IGF-I in small DRG neurons and down-regulation following injury. Neuroreport. 2002;13(13):1649-52. PubMed PMID: 12352620.

Crobu F, Latini V, Marongiu MF, Sogos V, Scintu F, Porcu S, et al. Differentiation of single cell derived human mesenchymal stem cells into cells with a neuronal phenotype: RNA and microRNA expression profile. Mol Biol Rep. 2012;39(4):3995-4007. doi: 10.1007/s11033-011-1180-9. PubMed PMID: 21773948.

D'Angelo F, Armentano I, Mattioli S, Crispoltoni L, Tiribuzi R, Cerulli GG, et al. Micropatterned hydrogenated amorphous carbon guides mesenchymal stem cells towards neuronal differentiation. Eur Cell Mater. 2010;20:231-44. PubMed PMID: 20925022.

Delcroix GJ, Curtis KM, Schiller PC, Montero-Menei CN. EGF and bFGF pre-treatment enhances neural specification and the response to neuronal commitment of MIAMI cells. Differentiation. 2010;80(4-5):213-27. doi: 10.1016/j.diff.2010.07.001. PubMed PMID: 20813449.

Dennis G, Sherman BT, Hosack DA, Yang J, Gao W, Lane HC, et al. DAVID: Database for Annotation, Visualization, and Integrated Discovery. Genome Biol. 2003;4(5):P3. PubMed PMID: 12734009.

Degistirici Ö, Thie M. Neural stem cells. EP1705245 (**2009**).

Dixon JW, Mood AM. A Method for Obtaining and Analyzing Sensitivity Data. Journal of the American Statistical Association. 1948(43):109-126.

Dobretsov M, Backonja MM, Romanovsky D, Stimers JR. Animal Models of Diabetic Neuropathic Pain. Springer Protocols, volume 49. 147-169, 2011.

Dupin E, Calloni G, Real C, Gonçalves-Trentin A, Le Douarin NM. Neural crest progenitors and stem cells. C R Biol. 2007;330(6-7):521-9. doi: 10.1016/j.crvi.2007.04.004. PubMed PMID: 17631447.

Dupin E, Coelho-Aguiar JM. Isolation and differentiation properties of neural crest stem cells. Cytometry A. 2013;83(1):38-47. doi: 10.1002/cyto.a.22098. PubMed PMID: 22837061.

Dupin E, Sommer L. Neural crest progenitors and stem cells: from early development to adulthood. Dev Biol. 2012;366(1):83-95. doi: 10.1016/j.ydbio.2012.02.035. PubMed PMID: 22425619.

Edalatmanesh MA, Bahrami AR, Hosseini E, Hosseini M, Khatamsaz S. Neuroprotective effects of mesenchymal stem cell transplantation in animal model of cerebellar degeneration. Neurol Res. 2011;33(9):913-20. doi: 10.1179/1743132811Y.0000000036. PubMed PMID: 22080991.

Fernandes KJ, McKenzie IA, Mill P, Smith KM, Akhavan M, Barnabé-Heider F, et al. A dermal niche for multipotent adult skin-derived precursor cells. Nat Cell Biol. 2004;6(11):1082-93. doi: 10.1038/ncb1181. PubMed PMID: 15517002.

Féron F, Perry C, Girard SD, Mackay-Sim A. Isolation of adult stem cells from the human olfactory mucosa. Methods Mol Biol. 2013;1059:107-14. doi: 10.1007/978-1-62703-574-3_10. PubMed PMID: 23934838.

Ferry RJ, Cerri RW, Cohen P. Insulin-like growth factor binding proteins: new proteins, new functions. Horm Res. 1999;51(2):53-67. doi: 23315. PubMed PMID: 10352394.

Fortino VR, Chen RS, Pelaez D, Cheung HS. Neurogenesis of neural crest-derived periodontal ligament stem cells by EGF and bFGF. J Cell Physiol. 2014;229(4):479-88. doi: 10.1002/jcp.24468. PubMed PMID: 24105823; PubMed Central PMCID: PMCPMC4292882.

Fournier BP, Larjava H, Häkkinen L. Gingiva as a source of stem cells with therapeutic potential. Stem Cells Dev. 2013;22(24):3157-77. doi: 10.1089/scd.2013.0015. PubMed PMID: 23944935.

Gammill LS, Bronner-Fraser M. Neural crest specification: migrating into genomics. Nat Rev Neurosci. 2003;4(10):795-805. doi: 10.1038/nrn1219. PubMed PMID: 14523379.

Garcez RC, Teixeira BL, Schmitt SoS, Alvarez-Silva M, Trentin AG. Epidermal growth factor (EGF) promotes the in vitro differentiation of neural crest cells to neurons and melanocytes. Cell Mol Neurobiol. 2009;29(8):1087-91. doi: 10.1007/s10571-009-9406-2. PubMed PMID: 19415484.

Geerts M, Bours G, de Wit R, Landewé S, van Haarlem A, Schaper N. Prevalence and impact of pain in diabetic neuropathy. Eur. Diab. Nursing. 2009(6):58–64. doi: 10.1002/edn.136

Godoy J, Nishimura M, Webster NJ. Gonadotropin-releasing hormone induces miR-132 and miR-212 to regulate cellular morphology and migration in immortalized LbetaT2 pituitary gonadotrope cells. Mol Endocrinol. 2011;25(5):810-20. doi: 10.1210/me.2010-0352. PubMed PMID: 21372146; PubMed Central PMCID: PMCPMC3082323.

Gögel S, Gubernator M, Minger SL. Progress and prospects: stem cells and neurological diseases. Gene Ther. 2011;18(1):1-6. doi: 10.1038/gt.2010.130. PubMed PMID: 20882052.

Gualco E, Wang JY, Del Valle L, Urbanska K, Peruzzi F, Khalili K, et al. IGF-IR in neuroprotection and brain tumors. Front Biosci (Landmark Ed). 2009;14:352-75. PubMed PMID: 19273072; PubMed Central PMCID: PMCPMC2679154.

Guo H, Yang Y, Geng Z, Zhu L, Yuan S, Zhao Y, et al. The change of insulin-like growth factor-1 in diabetic patients with neuropathy. Chin Med J (Engl). 1999;112(1):76-9. PubMed PMID: 11593647.

Hauser S, Widera D, Qunneis F, Müller J, Zander C, Greiner J, et al. Isolation of novel multipotent neural crest-derived stem cells from adult human inferior turbinate. Stem Cells Dev. 2012;21(5):742-56. doi: 10.1089/scd.2011.0419. PubMed PMID: 22128806; PubMed Central PMCID: PMCPMC3296122.

His W. Studies of the first system of the vertebrate body. The first development of the chick in the egg. Leipzig 1868. (Accessed October 8, 2013). http://www.biodiversitylibrary.org/ia/untersuchungen1868hisw

Ho KY, Huh BK, White WD, Yeh CC, Miller EJ. Topical amitriptyline versus lidocaine in the treatment of neuropathic pain. Clin J Pain. 2008;24(1):51-5. doi: 10.1097/AJP.0b013e318156db26. PubMed PMID: 18180637.

Huang CY, Pelaez D, Dominguez-Bendala J, Bendala JD, Garcia-Godoy F, Cheung HS. Plasticity of stem cells derived from adult periodontal ligament. Regen Med. 2009;4(6):809-21. doi: 10.2217/rme.09.55. PubMed PMID: 19903001.

Huang L, Liang J, Geng Y, Tsang WM, Yao X, Jhanji V, et al. Directing adult human periodontal ligament-derived stem cells to retinal fate. Invest Ophthalmol Vis Sci. 2013;54(6):3965-74. doi: 10.1167/iovs.13-11910. PubMed PMID: 23661377.

Ichim TE, Solano F, Lara F, Paris E, Ugalde F, Rodriguez JP, et al. Feasibility of combination allogeneic stem cell therapy for spinal cord injury: a case report. Int Arch Med. 2010;3:30. doi: 10.1186/1755-7682-3-30. PubMed PMID: 21070647; PubMed Central PMCID: PMCPMC2989319.

Im HI, Hollander JA, Bali P, Kenny PJ. MeCP2 controls BDNF expression and cocaine intake through homeostatic interactions with microRNA-212. Nat Neurosci. 2010;13(9):1120-7. doi: 10.1038/nn.2615. PubMed PMID: 20711185; PubMed Central PMCID: PMCPMC2928848.

Ishii DN. Implication of insulin-like growth factors in the pathogenesis of diabetic neuropathy. Brain Res Brain Res Rev. 1995;20(1):47-67. PubMed PMID: 7711767.

Ishii DN, Lupien SB. Insulin-like growth factors protect against diabetic neuropathy: effects on sensory nerve regeneration in rats. J Neurosci Res. 1995;40(1):138-44. doi: 10.1002/jnr.490400116. PubMed PMID: 7714922.

Jang S, Cho HH, Cho YB, Park JS, Jeong HS. Functional neural differentiation of human adipose tissue-derived stem cells using bFGF and forskolin. BMC Cell Biol. 2010;11:25. doi: 10.1186/1471-2121-11-25. PubMed PMID: 20398362; PubMed Central PMCID: PMCPMC2867791.

Jarmalavičiūtė A, Tunaitis V, Strainienė E, Aldonytė R, Ramanavičius A, Venalis A, et al. A New Experimental Model for Neuronal and Glial Differentiation Using Stem Cells Derived from Human Exfoliated Deciduous Teeth. J Mol Neurosci. 2013. doi: 10.1007/s12031-013-0046-0. PubMed PMID: 23797732.

Jensen TS, Madsen CS, Finnerup NB. Pharmacology and treatment of neuropathic pains. Curr Opin Neurol. 2009;22(5):467-74. doi: 10.1097/WCO.0b013e3283311e13. PubMed PMID: 19741531.

Jones JI, Clemmons DR. Insulin-like growth factors and their binding proteins: biological actions. Endocr Rev. 1995;16(1):3-34. doi: 10.1210/edrv-16-1-3. PubMed PMID: 7758431.

Kim BJ, Jin HK, Bae JS. Bone marrow-derived mesenchymal stem cells improve the functioning of neurotrophic factors in a mouse model of diabetic neuropathy. Lab Anim Res. 2011;27(2):171-6. doi: 10.5625/lar.2011.27.2.171. PubMed PMID: 21826178; PubMed Central PMCID: PMCPMC3146005.

Kim SU, de Vellis J. Stem cell-based cell therapy in neurological diseases: a review. J Neurosci Res. 2009;87(10):2183-200. doi: 10.1002/jnr.22054. PubMed PMID: 19301431.

Koh SH, Kim KS, Choi MR, Jung KH, Park KS, Chai YG, et al. Implantation of human umbilical cord-derived mesenchymal stem cells as a neuroprotective therapy for ischemic stroke in rats. Brain Res. 2008;1229:233-48. doi: 10.1016/j.brainres.2008.06.087. PubMed PMID: 18634757.

Krejčí E, Grim M. Isolation and characterization of neural crest stem cells from adult human hair follicles. Folia Biol (Praha). 2010;56(4):149-57. PubMed PMID: 20974047.

Kulkantrakorn K, Lorsuwansiri C, Meesawatsom P. 0.025% capsaicin gel for the treatment of painful diabetic neuropathy: a randomized, double-blind, crossover, placebo-controlled trial. Pain Pract. 2013;13(6):497-503. doi: 10.1111/papr.12013. PubMed PMID: 23228119.

Kuo YC, Chang YH. Differentiation of induced pluripotent stem cells toward neurons in hydrogel biomaterials. Colloids Surf B Biointerfaces. 2013;102:405-11. doi: 10.1016/j.colsurfb.2012.08.061. PubMed PMID: 23010124.

Kuo YC, Wang CT. Neuronal differentiation of induced pluripotent stem cells in hybrid polyester scaffolds with heparinized surface. Colloids Surf B Biointerfaces. 2012;100:9-15. doi: 10.1016/j.colsurfb.2012.05.014. PubMed PMID: 22750107.

Lau P, Bossers K, Janky R, Salta E, Frigerio CS, Barbash S, et al. Alteration of the microRNA network during the progression of Alzheimer's disease. EMBO Mol Med. 2013;5(10):1613-34. doi: 10.1002/emmm.201201974. PubMed PMID: 24014289; PubMed Central PMCID: PMCPMC3799583.

Le Douarin N, Kalcheim C. The neural crest. 2nd ed. ed. Cambridge: Cambridge University Press; 1999.

Lee JH, Um S, Jang JH, Seo BM. Effects of VEGF and FGF-2 on proliferation and differentiation of human periodontal ligament stem cells. Cell Tissue Res. 2012;348(3):475-84. doi: 10.1007/s00441-012-1392-x. PubMed PMID: 22437875.

Leventhal PS, Russell JW, Feldman EL, Rosenfeld R, Roberts Jr CT. IGFs and the nervous system. In: Contemporary endocrinology: the IGF system. Totowa, NJ: Humana Press. 1999;425-455.

Li G, Huang LS, Jiang MH, Wu HL, Chen J, Huang Y, et al. Implantation of bFGF-treated islet progenitor cells ameliorates streptozotocin-induced diabetes in rats. Acta Pharmacol Sin. 2010;31(11):1454-63. doi: 10.1038/aps.2010.130. PubMed PMID: 20953209; PubMed Central PMCID: PMCPMC4003334.

Li XW, Tian YH. Amplification and directional differentiation in vitro of human umbilical cord blood derived mesenchymal stem cells into neuron-like cells. J Clin Rehabil Tissue Eng Res. 2009(13):57-60.

Lynch ME, Clark AJ, Sawynok J, Sullivan MJ. Topical 2% amitriptyline and 1% ketamine in neuropathic pain syndromes: a randomized, double-blind, placebo-controlled trial. Anesthesiology. 2005;103(1):140-6. PubMed PMID: 15983466.

Magill ST, Cambronne XA, Luikart BW, Lioy DT, Leighton BH, Westbrook GL, et al. microRNA-132 regulates dendritic growth and arborization of newborn neurons in the adult hippocampus. Proc Natl Acad Sci U S A. 2010;107(47):20382-7. doi: 10.1073/pnas.1015691107. PubMed PMID: 21059906; PubMed Central PMCID: PMCPMC2996687.

Mahoney JM, Vardaxis V, Moore JL, Hall AM, Haffner KE, Peterson MC. Topical ketamine cream in the treatment of painful diabetic neuropathy: a randomized, placebo-controlled, double-blind initial study. J Am Podiatr Med Assoc. 2012;102(3):178-83. PubMed PMID: 22659759.

Martini C, Yassen A, Olofsen E, Passier P, Stoker M, Dahan A. Pharmacodynamic analysis of the analgesic effect of capsaicin 8% patch (Qutenza™) in diabetic neuropathic pain patients: detection of distinct response groups. J Pain Res. 2012;5:51-9. doi: 10.2147/JPR.S30406. PubMed PMID: 22536092; PubMed Central PMCID: PMCPMC3333798.

Mellios N, Sugihara H, Castro J, Banerjee A, Le C, Kumar A, et al. miR-132, an experience-dependent microRNA, is essential for visual cortex plasticity. Nat Neurosci. 2011;14(10):1240-2. doi: 10.1038/nn.2909. PubMed PMID: 21892155; PubMed Central PMCID: PMCPMC3183341.

Melton DA, Hemmati-Brivanlou A. Method of inducing and maintaining neuronal cells. EP0726948 (**1994**).

Moore KA, Kohno T, Karchewski LA, Scholz J, Baba H, Woolf CJ. Partial peripheral nerve injury promotes a selective loss of GABAergic inhibition in the superficial dorsal horn of the spinal cord. J Neurosci. 2002;22(15):6724-31. doi: 20026611. PubMed PMID: 12151551.

Morrison SJ, Kruger E. Postnatal gut neural crest stem cells. US8043853 (**2003**).

Mruthyunjaya S, Manchanda R, Godbole R, Pujari R, Shiras A, Shastry P. Laminin-1 induces neurite outgrowth in human mesenchymal stem cells in serum/differentiation factors-free conditions through activation of FAK-MEK/ERK signaling pathways. Biochem Biophys Res Commun. 2010;391(1):43-8. doi: 10.1016/j.bbrc.2009.10.158. PubMed PMID: 19895795.

Naruse K, Sato J, Funakubo M, Hata M, Nakamura N, Kobayashi Y, et al. Transplantation of bone marrow-derived mononuclear cells improves mechanical hyperalgesia, cold allodynia and nerve function in diabetic neuropathy. PLoS One. 2011;6(11):e27458. doi: 10.1371/journal.pone.0027458. PubMed PMID: 22125614; PubMed Central PMCID: PMCPMC3220696.

Nesti C, Pardini C, Barachini S, D'Alessandro D, Siciliano G, Murri L, et al. Human dental pulp stem cells protect mouse dopaminergic neurons against MPP+ or rotenone. Brain Res. 2011;1367:94-102. doi: 10.1016/j.brainres.2010.09.042. PubMed PMID: 20854799.

Ng TK, Carballosa CM, Pelaez D, Wong HK, Choy KW, Pang CP, et al. Nicotine alters MicroRNA expression and hinders human adult stem cell regenerative potential. Stem Cells Dev. 2013;22(5):781-90. doi: 10.1089/scd.2012.0434. PubMed PMID: 23030247.

Numakawa T, Yamamoto N, Chiba S, Richards M, Ooshima Y, Kishi S, et al. Growth factors stimulate expression of neuronal and glial miR-132. Neurosci Lett. 2011;505(3):242-7. doi: 10.1016/j.neulet.2011.10.025. PubMed PMID: 22027176.

Oltman CL, Davidson EP, Coppey LJ, Kleinschmidt TL, Lund DD, Adebara ET, et al. Vascular and neural dysfunction in Zucker diabetic fatty rats: a difficult condition to reverse. Diabetes Obes Metab. 2008;10(1):64-74. doi: 10.1111/j.1463-1326.2007.00814.x. PubMed PMID: 17970755.

Ossipov MH. Growth factors and neuropathic pain. Curr Pain Headache Rep. 2011;15(3):185-92. doi: 10.1007/s11916-011-0183-5. PubMed PMID: 21327569.

Ostrakhovitch EA, Byers JC, O'Neil KD, Semenikhin OA. Directed differentiation of embryonic P19 cells and neural stem cells into neural lineage on conducting PEDOT-PEG and ITO glass substrates. Arch Biochem Biophys. 2012;528(1):21-31. doi: 10.1016/j.abb.2012.08.006. PubMed PMID: 22944870.

Park HJ, Lee PH, Bang OY, Lee G, Ahn YH. Mesenchymal stem cells therapy exerts neuroprotection in a progressive animal model of Parkinson's disease. J Neurochem. 2008;107(1):141-51. doi: 10.1111/j.1471-4159.2008.05589.x. PubMed PMID: 18665911.

Pathania M, Torres-Reveron J, Yan L, Kimura T, Lin TV, Gordon V, et al. miR-132 enhances dendritic morphogenesis, spine density, synaptic integration, and survival of newborn olfactory bulb neurons. PLoS One. 2012;7(5):e38174. doi: 10.1371/journal.pone.0038174. PubMed PMID: 22693596; PubMed Central PMCID: PMCPMC3364964.

Pelaez D, Huang CY, Cheung HS. Isolation of pluripotent neural crest-derived stem cells from adult human tissues by connexin-43 enrichment. Stem Cells Dev. 2013;22(21):2906-14. doi: 10.1089/scd.2013.0090. PubMed PMID: 23750535.

Qian DX, Zhang HT, Ma X, Jiang XD, Xu RX. Comparison of the efficiencies of three neural induction protocols in human adipose stromal cells. Neurochem Res. 2010;35(4):572-9. doi: 10.1007/s11064-009-0101-y. PubMed PMID: 19960248.

Rauck R, Makumi CW, Schwartz S, Graff O, Meno-Tetang G, Bell CF, et al. A randomized, controlled trial of gabapentin enacarbil in subjects with neuropathic pain associated with diabetic peripheral neuropathy. Pain Pract. 2013;13(6):485-96. doi: 10.1111/papr.12014. PubMed PMID: 23186035.

Reid AJ, Sun M, Wiberg M, Downes S, Terenghi G, Kingham PJ. Nerve repair with adipose-derived stem cells protects dorsal root ganglia neurons from apoptosis. Neuroscience. 2011;199:515-22. doi: 10.1016/j.neuroscience.2011.09.064. PubMed PMID: 22020320.

Remenyi J, Hunter CJ, Cole C, Ando H, Impey S, Monk CE, et al. Regulation of the miR-212/132 locus by MSK1 and CREB in response to neurotrophins. Biochem J. 2010;428(2):281-91. doi: 10.1042/BJ20100024. PubMed PMID: 20307261.

Ribeiro D, Laguna Goya R, Ravindran G, Vuono R, Parish CL, Foldi C, et al. Efficient expansion and dopaminergic differentiation of human fetal ventral midbrain neural stem cells by midbrain morphogens. Neurobiol Dis. 2013;49:118-27. doi: 10.1016/j.nbd.2012.08.006. PubMed PMID: 22940632.

Russell JW, Feldman EL. Insulin-like growth factor-I prevents apoptosis in sympathetic neurons exposed to high glucose. Horm Metab Res. 1999;31(2-3):90-6. doi: 10.1055/s-2007-978704. PubMed PMID: 10226787.

Santiago MF, Alcami P, Striedinger KM, Spray DC, Scemes E. The carboxyl-terminal domain of connexin43 is a negative modulator of neuronal differentiation. J Biol Chem. 2010;285(16):11836-45. doi: 10.1074/jbc.M109.058750. PubMed PMID: 20164188; PubMed Central PMCID: PMCPMC2852920.

Sarnowska A, Braun H, Sauerzweig S, Reymann KG. The neuroprotective effect of bone marrow stem cells is not dependent on direct cell contact with hypoxic injured tissue. Exp Neurol. 2009;215(2):317-27. doi: 10.1016/j.expneurol.2008.10.023. PubMed PMID: 19063882.

Schmidt RE, Dorsey DA, Beaudet LN, Plurad SB, Parvin CA, Miller MS. Insulin-like growth factor I reverses experimental diabetic autonomic neuropathy. Am J Pathol. 1999;155(5):1651-60. doi: 10.1016/S0002-9440(10)65480-6. PubMed PMID: 10550321; PubMed Central PMCID: PMCPMC1866997.

Shibata T, Naruse K, Kamiya H, Kozakae M, Kondo M, Yasuda Y, et al. Transplantation of bone marrow-derived mesenchymal stem cells improves diabetic polyneuropathy in rats. Diabetes. 2008;57(11):3099-107. doi: 10.2337/db08-0031. PubMed PMID: 18728233; PubMed Central PMCID: PMCPMC2570407.

Sieber-Blum M, Grim M. Method of isolating epidermal neural crest stem cells. US8030072 (**2006**).

Singhatanadgit W, Varodomrujiranon M. Osteogenic potency of a 3-dimensional scaffold-free bonelike sphere of periodontal ligament stem cells in vitro. Oral Surg Oral Med Oral Pathol Oral Radiol. 2013;116(6):e465-72. doi: 10.1016/j.oooo.2012.02.035. PubMed PMID: 22901658.

Siniscalco D, Giordano C, Galderisi U, Luongo L, Alessio N, Di Bernardo G, et al. Intra-brain microinjection of human mesenchymal stem cells decreases allodynia in neuropathic mice. Cell Mol Life Sci. 2010;67(4):655-69. doi: 10.1007/s00018-009-0202-4. PubMed PMID: 19937263.

Siniscalco D, Giordano C, Galderisi U, Luongo L, de Novellis V, Rossi F, et al. Long-lasting effects of human mesenchymal stem cell systemic administration on pain-like behaviors, cellular, and biomolecular modifications in neuropathic mice. Front Integr Neurosci. 2011;5:79. doi: 10.3389/fnint.2011.00079. PubMed PMID: 22164136; PubMed Central PMCID: PMCPMC3230031.

Smith BH, Torrance N, Bennett MI, Lee AJ. Health and quality of life associated with chronic pain of predominantly neuropathic origin in the community. Clin J Pain. 2007;23(2):143-9. doi: 10.1097/01.ajp.0000210956.31997.89. PubMed PMID: 17237663.

Smith PY, Delay C, Girard J, Papon MA, Planel E, Sergeant N, et al. MicroRNA-132 loss is associated with tau exon 10 inclusion in progressive supranuclear palsy. Hum Mol Genet. 2011;20(20):4016-24. doi: 10.1093/hmg/ddr330. PubMed PMID: 21807765.

Song JS, Kim SO, Kim SH, Choi HJ, Son HK, Jung HS, et al. In vitro and in vivo characteristics of stem cells derived from the periodontal ligament of human deciduous and permanent teeth. Tissue Eng Part A. 2012;18(19-20):2040-51. doi: 10.1089/ten.TEA.2011.0318. PubMed PMID: 22571499.

Thrailkill KM. Insulin-like growth factor-I in diabetes mellitus: its physiology, metabolic effects, and potential clinical utility. Diabetes Technol Ther. 2000;2(1):69-80. PubMed PMID: 11467325.

Thrailkill KM, Quattrin T, Baker L, Kuntze JE, Compton PG, Martha PM. Cotherapy with recombinant human insulin-like growth factor I and insulin improves glycemic control in type 1 diabetes. RhIGF-I in IDDM Study Group. Diabetes Care. 1999;22(4):585-92. PubMed PMID: 10189536.

Trang T, Beggs S, Salter MW. Brain-derived neurotrophic factor from microglia: a molecular substrate for neuropathic pain. Neuron Glia Biol. 2011;7(1):99-108. doi: 10.1017/S1740925X12000087. PubMed PMID: 22613083; PubMed Central PMCID: PMCPMC3748035.

Treede RD, Jensen TS, Campbell JN, Cruccu G, Dostrovsky JO, Griffin JW, et al. Neuropathic pain: redefinition and a grading system for clinical and research purposes. Neurology. 2008;70(18):1630-5. doi: 10.1212/01.wnl.0000282763.29778.59. PubMed PMID: 18003941.

Urgelle´ s-Lorie´ L. Nociceptive vs. neuropathic pain: Physiological regulating medicine (PRM)/new approach for its control. Dolor, Clinica y Terapia 2008;17–22.

U.S. Department of Health and Human Services Food and Drug Administration Center for Drug Evaluation and Research (CDER). Guidance for Industry - Estimating the Maximum Safe Starting Dose in Initial Clinical Trials for Therapeutics in Adult Healthy Volunteers. Pharmacology and Toxicology. 2005.

Vinik AI. Diabetic neuropathy: pathogenesis and therapy. Am J Med. 1999;107(2B):17S-26S. PubMed PMID: 10484041.

Waddington RJ, Youde SJ, Lee CP, Sloan AJ. Isolation of distinct progenitor stem cell populations from dental pulp. Cells Tissues Organs. 2009;189(1-4):268-74. doi: 10.1159/000151447. PubMed PMID: 18701814.

Wanet A, Tacheny A, Arnould T, Renard P. miR-212/132 expression and functions: within and beyond the neuronal compartment. Nucleic Acids Res. 2012;40(11):4742-53. doi: 10.1093/nar/gks151. PubMed PMID: 22362752; PubMed Central PMCID: PMCPMC3367188.

Wang F, Yasuhara T, Shingo T, Kameda M, Tajiri N, Yuan WJ, et al. Intravenous administration of mesenchymal stem cells exerts therapeutic effects on parkinsonian model of rats: focusing on neuroprotective effects of stromal cell-derived factor-1alpha. BMC Neurosci. 2010;11:52. doi: 10.1186/1471-2202-11-52. PubMed PMID: 20420688; PubMed Central PMCID: PMCPMC2873592.

Wilkins A, Kemp K, Ginty M, Hares K, Mallam E, Scolding N. Human bone marrow-derived mesenchymal stem cells secrete brain-derived neurotrophic factor which promotes neuronal survival in vitro. Stem Cell Res. 2009;3(1):63-70. doi: 10.1016/j.scr.2009.02.006. PubMed PMID: 19411199.

Wu G, Ringkamp M, Hartke TV, Murinson BB, Campbell JN, Griffin JW, et al. Early onset of spontaneous activity in uninjured C-fiber nociceptors after injury to neighboring nerve fibers. J Neurosci. 2001;21(8):RC140. PubMed PMID: 11306646.

Wu Y, Cao H, Yang Y, Zhou Y, Gu Y, Zhao X, et al. Effects of vascular endothelial cells on osteogenic differentiation of noncontact co-cultured periodontal ligament stem cells under hypoxia. J Periodontal Res. 2013;48(1):52-65. doi: 10.1111/j.1600-0765.2012.01503.x. PubMed PMID: 22905750.

Wuarin L, Guertin DM, Ishii DN. Early reduction in insulin-like growth factor gene expression in diabetic nerve. Exp Neurol. 1994;130(1):106-14. doi: 10.1006/exnr.1994.1189. PubMed PMID: 7821385.

Yang D, Li T, Wang Y, Tang Y, Cui H, Zhang X, et al. miR-132 regulates the differentiation of dopamine neurons by directly targeting Nurr1 expression. J Cell Sci. 2012;125(Pt 7):1673-82. doi: 10.1242/jcs.086421. PubMed PMID: 22328530.

Yang R, Xu X. Isolation and culture of neural crest stem cells from human hair follicles. J Vis Exp. 2013(74). doi: 10.3791/3194. PubMed PMID: 23608752; PubMed Central PMCID: PMCPMC3644479.

Yu H, Fang D, Kumar SM, Li L, Nguyen TK, Acs G, et al. Isolation of a novel population of multipotent adult stem cells from human hair follicles. Am J Pathol. 2006;168(6):1879-88. doi: 10.2353/ajpath.2006.051170. PubMed PMID: 16723703; PubMed Central PMCID: PMCPMC1606635.

Yu H, Kumar SM, Kossenkov AV, Showe L, Xu X. Stem cells with neural crest characteristics derived from the bulge region of cultured human hair follicles. J Invest Dermatol. 2010;130(5):1227-36. doi: 10.1038/jid.2009.322. PubMed PMID: 19829300; PubMed Central PMCID: PMCPMC3050599.

Zhang C, Li J, Zhang L, Zhou Y, Hou W, Quan H, et al. Effects of mechanical vibration on proliferation and osteogenic differentiation of human periodontal ligament stem cells. Arch Oral Biol. 2012;57(10):1395-407. doi: 10.1016/j.archoralbio.2012.04.010. PubMed PMID: 22595622.

Zhang J, An Y, Gao LN, Zhang YJ, Jin Y, Chen FM. The effect of aging on the pluripotential capacity and regenerative potential of human periodontal ligament stem cells. Biomaterials. 2012;33(29):6974-86. doi: 10.1016/j.biomaterials.2012.06.032. PubMed PMID: 22789721.

Zhou Y, Chen KS, Gao JB, Han R, Lu JJ, Peng T, et al. [miR-124-1 promotes neural differentiation of rat bone marrow mesenchymal stem cells]. Zhongguo Dang Dai Er Ke Za Zhi. 2012;14(3):215-20. PubMed PMID: 22433412.

Zhuang HX, Snyder CK, Pu SF, Ishii DN. Insulin-like growth factors reverse or arrest diabetic neuropathy: effects on hyperalgesia and impaired nerve regeneration in rats. Exp Neurol. 1996;140(2):198-205. doi: 10.1006/exnr.1996.0129. PubMed PMID: 8690062.

Zhuang HX, Wuarin L, Fei ZJ, Ishii DN. Insulin-like growth factor (IGF) gene expression is reduced in neural tissues and liver from rats with non-insulin-dependent diabetes mellitus, and IGF treatment ameliorates diabetic neuropathy. J Pharmacol Exp Ther. 1997;283(1):366-74. PubMed PMID: 9336345.

Ziegler D, Wiefels K, Dannehl K, Gries FA. Effects of one year of near-normoglycemia on peripheral nerve function in type 1 (insulin-dependent) diabetic patients. Klin Wochenschr. 1988;66(9):388-96. PubMed PMID: 2839729.

Appendix 1 – miRNA Supplementary Table – Predicted target gene list for neural differentiation.

Gene	Description	MiRNA
SEPT2	septin 2	hsa-miR-195; hsa-miR-424; hsa-miR-497
AGTPBP1	ATP/GTP binding protein 1	hsa-miR-1305
WNT3A	wingless-type MMTV integration site family, member 3A	hsa-miR-195; hsa-miR-424; hsa-miR-497
STRN	striatin, calmodulin binding protein	hsa-miR-484
GJA1	**gap junction protein, alpha 1, 43kDa**	**hsa-miR-101**
GDNF	glial cell derived neurotrophic factor	hsa-miR-26a
CXCL12	chemokine (C-X-C motif) ligand 12 (stromal cell-derived factor 1)	hsa-miR-222
GLI3	GLI-Kruppel family member GLI3 (Greig cephalopolysyndactyly syndrome)	hsa-miR-7; hsa-miR-143
ZFP91	zinc finger protein 91 homolog (mouse)	hsa-miR-1305; hsa-miR-532-5p
APP	amyloid beta (A4) precursor protein (peptidase nexin-II, Alzheimer disease)	hsa-miR-101
S1PR1	sphingosine-1-phosphate receptor 1	hsa-miR-181a
POU4F1	POU class 4 homeobox 1	hsa-miR-769-5p
KIF5C	kinesin family member 5C	hsa-miR-424; hsa-miR-497
PTPRR	protein tyrosine phosphatase, receptor type, R	hsa-miR-195; hsa-miR-424; hsa-miR-497
TBR1	T-box, brain, 1	hsa-miR-542-5p
ASCL1	achaete-scute complex homolog 1 (Drosophila)	hsa-miR-374a; hsa-miR-374b
PRKCQ	protein kinase C, theta	hsa-miR-26a
SLC26A6	solute carrier family 26, member 6	hsa-miR-125a-5p; hsa-miR-125b
ADM	Adrenomedullin	hsa-miR-410
BTG4	B-cell translocation gene 4	hsa-miR-484
VEGFA	vascular endothelial growth factor A	hsa-miR-299-3p; hsa-miR-195; hsa-miR-424; hsa-miR-497

SIAH1	seven in absentia homolog 1 (Drosophila)	hsa-miR-1305
CNTN4	contactin 4	hsa-miR-181a
SMARCA1	SWI/SNF related, matrix associated, actin dependent regulator of chromatin, subfamily a, member 1	hsa-miR-101
CUX1	cut-like homeobox 1	hsa-miR-299-3p
SLITRK6	SLIT and NTRK-like family, member 6	hsa-miR-125a-5p; hsa-miR-125b
DRD1	dopamine receptor D1	hsa-miR-93
LPPR4	plasticity related gene 1	hsa-miR-30c; hsa-miR-30d; hsa-miR-30b
IRX5	iroquois homeobox 5	hsa-miR-222
SOX2	SRY (sex determining region Y)-box 2	hsa-miR-371-5p
SOX5	SRY (sex determining region Y)-box 5	hsa-miR-212; hsa-miR-132
DSCAML1	Down syndrome cell adhesion molecule like 1	hsa-miR-376a
MYCBP2	MYC binding protein 2	hsa-miR-181a; hsa-miR-484; hsa-miR-212; hsa-miR-132
ALDH1A2	aldehyde dehydrogenase 1 family, member A2	hsa-miR-23b
PVRL1	poliovirus receptor-related 1 (herpesvirus entry mediator C)	hsa-miR-1305
BCL11B	B-cell CLL/lymphoma 11B (zinc finger protein)	hsa-miR-1825
NUMB	numb homolog (Drosophila)	hsa-miR-146a; hsa-miR-410
LHX8	LIM homeobox 8	hsa-miR-30c; hsa-miR-30d; hsa-miR-30b
ETV4	ets variant gene 4 (E1A enhancer binding protein, E1AF)	hsa-miR-361-3p
NKX2-2	NK2 homeobox 2	hsa-miR-374a; hsa-miR-374b
DCLK1	doublecortin-like kinase 1	hsa-miR-195; hsa-miR-424; hsa-miR-497
PARD6B	par-6 partitioning defective 6 homolog beta (C. elegans)	hsa-miR-374a; hsa-miR-374b
KLF7	Kruppel-like factor 7 (ubiquitous)	hsa-miR-146a
CEBPB	CCAAT/enhancer binding protein (C/EBP), beta	hsa-miR-374a; hsa-miR-374b
NTF3	neurotrophin 3	hsa-miR-374a; hsa-miR-374b; hsa-miR-222
MAP2K1	mitogen-activated protein kinase kinase 1	hsa-miR-195; hsa-miR-424; hsa-miR-497
MCF2	MCF.2 cell line derived transforming sequence	hsa-miR-143

FOXA1	forkhead box A1	hsa-miR-212; hsa-miR-132
NR4A2	nuclear receptor subfamily 4, group A, member 2	hsa-miR-30c; hsa-miR-30d; hsa-miR-30b
NTNG1	netrin G1	hsa-miR-212; hsa-miR-132
NTN4	myeloid leukemia factor 2	hsa-miR-93
SMAD4	SMAD family member 4	hsa-miR-146a
NTNG2	netrin G2	hsa-miR-212; hsa-miR-132
CELSR2	cadherin, EGF LAG seven-pass G-type receptor 2 (flamingo homolog, Drosophila)	hsa-miR-432
NEUROG2	neurogenin 2	hsa-miR-374a; hsa-miR-374b
DOCK7	dedicator of cytokinesis 7	hsa-miR-30c; hsa-miR-30d; hsa-miR-30b
EN1	engrailed homeobox 1	hsa-miR-374a; hsa-miR-374b
EN2	engrailed homeobox 2	hsa-miR-376c
VSX1	visual system homeobox 1	hsa-miR-93
NTRK3	neurotrophic tyrosine kinase, receptor, type 3	hsa-miR-769-5p
SALL3	sal-like 3 (Drosophila)	hsa-miR-409-3p
EPHA4	EPH receptor A4	hsa-miR-532-5p; hsa-miR-93
EPHA7	EPH receptor A7	hsa-miR-195; hsa-miR-424; hsa-miR-497
PBX3	pre-B-cell leukemia homeobox 3	hsa-miR-93; hsa-miR-101
CACNA1A	calcium channel, voltage-dependent, P/Q type, alpha 1A subunit	hsa-miR-143
MYH10	myosin, heavy chain 10, non-muscle	hsa-miR-26a

Appendix 2 – MATLAB Code for IVIS Quantification

```
clear
clc

while true
matrix=csvread(uigetfile);
inten=matrix(:,4);
count=0;
counti=0;
for i=1:length(inten)
   if inten(i)>29
   count=count+1;
   end
   if inten(i)>50
   counti=counti+1;
   end
end

percentage=count*100/length(inten) %above 29
percentagei=counti*100/length(inten) %above 50
end
```